Journal of the Anatomical Society of India

Print ISSN: 0003-2778

GENERAL INFORMATION

About the Journal

Journal of the Anatomical Society of India (ISSN: Print 0003-2778) is peer-reviewed journal. The journal is owned and run by Anatomical Society of India. The journal publishes research articles related to all aspects of Anatomy and allied medical/surgical sciences. Pre-Publication Peer Review and Post-Publication Peer Review Online Manuscript Submission System Selection of articles on the basis of MRS system Eminent academicians across the globe as the Editorial board members Electronic Table of Contents alerts Available in both online and print form. The journal is published quarterly in the months of January, April, July and October.

Scope of the Journal

The aim of the *Journal of the Anatomical Society of India* is to enhance and upgrade the research work in the field of anatomy and allied clinical subjects. It provides an integrative forum for anatomists across the globe to exchange their knowledge and views. It also helps to promote communication among fellow academicians and researchers worldwide. The Journal is devoted to publish recent original research work and recent advances in the field of Anatomical Sciences and allied clinical subjects. It provides an opportunity to academicians to disseminate their knowledge that is directly relevant to all domains of health sciences.

The Editorial Board comprises of academicians across the globe.

JASI is indexed in Scopus, available in Science Direct.

Abstracting and Indexing Information

The journal is registered with the following abstracting partners:

Baidu Scholar, CNKI (China National Knowledge Infrastructure), EBSCO Publishing's Electronic Databases, Ex Libris – Primo Central, Google Scholar, Hinari, Infotrieve, Netherlands ISSN center, ProQuest, TdNet, Wanfang Data

The journal is indexed with, or included in, the following:

SCOPUS, Science Citation Index Expanded, IndMed, MedInd, Scimago Journal Ranking, Emerging Sources Citation Index.

Impact Factor® as reported in the 2019 Journal Citation Reports® (Clarivate Analytics, 2020): 0.227

Information for Authors

Article processing and publication charges will be communicated by the editorial office. All manuscripts must be submitted online at www.journalonweb.com/jasi.

Subscription Information

A subscription to JASI comprises 4 issues. Prices include postage. Annual Subscription Rate for non-members-		
Rates of Membership (with effect from 1.1.2019)		
	India	**International**
Ordinary membership	INR 1500	US $ 100
Couple membership	INR 2250	
Life membership	INR 8000	US $ 900
Subscription Rates (till 31st August)		
Individual	INR 4500	US $ 600
Library/Institutional Trade discount of 10% for agencies only	INR 10000	US $ 900
Subscription Rates (after 31st August)		
Individual	INR 5000	
Library/Institutional	INR 10500	
The Journal of Anatomical Society of India (ISSN: 0003-2778) is published quarterly **Subscriptions** are accepted on a prepaid basis only and are entered on a calendar year basis. Issues are sent by standard mail Priority rates are available upon request.		

Information to Members/Subscribers

All members and existing subscribers of the Anatomical Society of India are requested to send their membership/existing subscription fee for the current year to the Treasurer of the Society on the following address: Prof (Dr.) Punit Manik, Treasurer, ASI, Department of Anatomy, KGMU, Lucknow - 226003. Email: punitamanik@yahoo.co.in. All payments should be made through an account payee bank draft drawn in favor of the **Treasurer, Anatomical Society of India,** payable at **Lucknow** only, preferably for **Allahabad Bank, Medical College Branch, Lucknow.** Outstation cheques/drafts must include INR 70 extra as bank collection charges.

All complaints regarding non-receipt of journal issues should be addressed to the Editor-in-Chief, JASI at editorjasi@gmail.com. The new subscribers may, please contact wkhlrpmedknow_subscriptions@wolterskluwer.com.

Requests of any general information like travel concession forms, venue of next annual conference, etc. should be addressed to the General Secretary of the Anatomical Society of India.

For mode of payment and other details, please visit www.medknow.com/subscribe.asp

Claims for missing issues will be serviced at no charge if received within 60 days of the cover date for domestic subscribers, and 3 months for subscribers outside India. Duplicate copies cannot be sent to replace issues not delivered because of failure to notify publisher of change of address. The journal is published and distributed by Wolters Kluwer India Pvt. Ltd. Copies are sent to subscribers directly from the publisher's address. It is illegal to acquire copies from any other source. If a copy is received for personal use as a member of the association/ society, one cannot resale or give-away the copy for commercial or library use.

The copies of the journal to the subscribers are sent by ordinary post. The editorial board, association or publisher will not be responsible for non receipt of copies. If any subscriber wishes to receive the copies by registered post or courier, kindly contact the publisher's office. If a copy returns due to incomplete, incorrect or changed address of a subscriber on two consecutive occasions, the names of such subscribers will be deleted from the mailing list of the journal. Providing complete, correct and up-to-date address is the responsibility of the subscriber.

Nonmembers: Please send change of address information to subscriptions@medknow.com.

Advertising Policies

The journal accepts display and classified advertising. Frequency discounts and special positions are available. Inquiries about advertising should be sent to Wolters Kluwer India Pvt. Ltd, advertise@medknow. com.

The journal reserves the right to reject any advertisement considered unsuitable according to the set policies of the journal.

The appearance of advertising or product information in the various sections in the journal does not constitute an endorsement or approval by the journal and/or its publisher of the quality or value of the said product or of claims made for it by its manufacturer.

Addresses

Editorial Office

Dr. Vishram Singh, Editor-in-Chief, JASI
OC-5/103, 1st floor, Orange County Society,
Ahinsa Khand-I, Indirapuram, Ghaziabad,
Delhi, NCR- 201014.
Email: editorjasi@gmail.com

Published by

Wolters Kluwer India Pvt. Ltd
A-202, 2nd Floor, The Qube,
C.T.S. No.1498A/2 Village Marol, Andheri (East),
Mumbai - 400 059, India.
Phone: 91-22-66491818
Website: www.medknow.com

Printed at

Dhote Offset Tech. P. Ltd
Goregaon (E), Mumbai, India

Journal of the Anatomical Society of India

Print ISSN: 0003-2778

EDITORIAL BOARD

Journal of the Anatomical Society of India

Print ISSN: 0003-2778

EXECUTIVE COMMITTEE

Journal of the Anatomical Society of India

Volume 69 | Issue 4 | October-December 2020

CONTENTS

EDITORIAL

Implementation of Competency Based Medical Education in Anatomy with Poor Teacher-Student Ratio: The Utopia
Vishram Singh, Ashok Sahai 193

ORIGINAL ARTICLES

A Computed Tomography Angiography Study to Correlate Main Renal Artery Diameter with Presence of Accessory Renal Artery in Healthy Live Kidney Donors
Alka Nagar, Navbir Pasricha, Eti Sthapak, Deshraj Gurjar, Hira Lal 196

Morphological Side Differences of the Hemipelvis
Gloria Maria Hohenberger, Angelika Maria Schwarz, Andreas Heinrich Weiglein, Sabine Kuchling, Georg Hauer, Uldis Berzins, Magdalena Holter, Christoph Grechenig, Renate Krassnig, Axel Gänsslen 201

The Morphological Variants of Dural Venous Sinuses
Sercan Özkaçmaz, Yeliz Dadali, Muhammed Alpaslan, Ilyas Uçar 207

An Evaluation on the Morphology of the Nasal Bone, Piriform Aperture, and Choana on Dry Skulls
Anil Didem Aydin Kabakci, Duygu Akin Saygin, Şerife Alpa, Mustafa Buyukmumcu, Mehmet Tugrul Yılmaz 213

Morphological and Morphometric Study of the Acetabulum of Dry Human Hip Bone and Its Clinical Implication in Hip Arthroplasty
Archana Singh, Rakesh Gupta, Arun Singh 220

Polymorphic Study of Ataxin 3 Gene in Eastern Uttar Pradesh Population
Barkha Singh, Prasenjit Bose, S. N. Shamal, Deepika Joshi, Royana Singh 226

An Anatomical Description of the Vermian Fossa: The Reappraisal of an Overlooked Entity
Jeshika S. Luckrajh, J. Naidoo, L. Lazarus 233

Considering the Surface Area and Sagittal Angle in a Pair of Lumbosacral Facets: Determining the Structural Relevance of Asymmetric Facets at the Lumbosacral Junction
Uchenna Kenneth Ezemagu, F. Chinedu Akpuaka, Emmanuel C. Iyidobi, Chike P. Anibeze 237

***In vivo* Cross-Sectional Topographic Anatomy at Sternal Angle on Magnetic Resonance Imaging**
Rohit Aggarwal, Sreedhar Muthukrishnan Calicut, Raheem Abdul Sheik, Vijaya Sagar Theegala, Indrani Mukhopadhyay 243

CASE REPORTS

Ectopic Pelvic Kidney and its Renal Artery from the Common Iliac Artery
Sevda Lafci Fahrioglu, Musa Muhtaroglu, Selda Onderoglu, Sezgin Ilgi 249

Turner Syndrome Associated with Cerebellar Abnormalities
Tanya T. Kitova, Ekaterina H. Uchikova, Kristina P. Kilova, Veselin T. Belovejdov 252

IINSTRUCTIONS TO AUTHOR 256

Journal of the Anatomical Society of India on Web

http://www.journalonweb.com/jasi

The Journal of the Anatomical Society of India now accepts articles electronically. It is easy, convenient and fast. Check following steps:

1 Registration

- Register from http://www.journalonweb.com/jasi as a new author (Signup as author)
- Two-step self-explanatory process

2 New article submission

- Read instructions on the journal website or download the same from manuscript management site
- Prepare your files (Article file, First page file and Images, Copyright form & Other forms, if any)
- Login as an author
- Click on 'Submit new article' under 'Submissions'
- Follow the steps (guidelines provided while submitting the article)
- On successful submission you will receive an acknowledgement quoting the manuscript ID

3 Tracking the progress

- Login as an author
- The report on the main page gives status of the articles and its due date to move to next phase
- More details can be obtained by clicking on the ManuscriptID
- Comments sent by the editor and reviewer will be available from these pages

4 Submitting a revised article

- Login as an author
- On the main page click on 'Articles for Revision'
- Click on the link "Click here to revise your article" against the required manuscript ID
- Follow the steps (guidelines provided while revising the article)
- Include the reviewers' comments along with the point to point clarifications at the beginning of the revised article file.
- Do not include authors' name in the article file.
- Upload the revised article file against New Article File - Browse, choose your file and then click "Upload" OR Click "Finish"
- On completion of revision process you will be able to check the latest file uploaded from Article Cycle (In Review Articles-> Click on manuscript id -> Latest file will have a number with 'R', for example XXXX_100_15R3.docx)

Facilities

- Submission of new articles with images
- Submission of revised articles
- Checking of proofs
- Track the progress of article until published

Advantages

- Any-time, any-where access
- Faster review
- Cost saving on postage
- No need for hard-copy submission
- Ability to track the progress
- Ease of contacting the journal

Requirements for usage

- Computer and internet connection
- Web-browser (Latest versions - IE, Chrome, Safari, FireFox, Opera)
- Cookies and javascript to be enabled in web-browser

Online submission checklist

- First Page File (rtf/doc/docx file) with title page, covering letter, acknowledgement, etc.
- Article File (rtf/doc/docx file) - text of the article, beginning from Title, Abstract till References (including tables). File size limit 4 MB. Do not include images in this file.
- Images (jpg/jpeg/png/gif/tif/tiff): Submit good quality colour images. Each image should be less than 10 MB) in size
- Upload copyright form in .doc / .docx / .pdf / .jpg / .png / .gif format, duly signed by all authors, during the time mentioned in the instructions.

Help

- Check Frequently Asked Questions (FAQs) on the site
- In case of any difficulty contact the editor

Implementation of Competency Based Medical Education in Anatomy with Poor Teacher-Student Ratio: The Utopia

In recent times, there has been a paradigm shift in medical education due to the implementation of competency-based medical education (CBME) as part of the Government's Regulations on Graduate Medical Education.[1] These regulations envisaged that the Indian Medical Graduate (IMG) should develop competencies required to fulfill the patient's basic medical needs in society, i.e., they should possess the requisite knowledge, skills, attitudes, values, and responsiveness, so that he or she be able to solve basic medical problems in the community with skill and efficiency as physicians of the first contact. Simultaneously, he or she should be globally relevant.[2]

In addition to the first contact physician, he or she should also be a leader of the healthcare team, a good communicator, lifelong learner, and committed to the profession.[3]

The competencies were prepared accordingly, and the medical institutions all over India were asked to incorporate the same in their curriculum. This is a welcome step of the Medical Council of India (MCI)/National Medical Commission (NMC) and needs an appreciation. From these set objectives and goals we can draw that on passing out, a medical graduate should be a combo of (i) physician of the first contact, (ii) ability to solve basic medical problems, (iii) globally relevant, and (iv) have leadership capabilities of the healthcare team. For sure, all this sounds very rosy but needs a strong foundation of basic medical practice besides many other skills.

As we all know that anatomy is the backbone of medicine and provides anatomical basis of clinical practice.[4] Therefore, to produce competent IMGs it should be taught thoroughly with a blend of clinical application. Facts which are not clinically relevant for medical graduate should not be taught as a passing reference only because relevance of such anatomical facts comes later when a doctor specializes or super specializes and if he/she go for advanced training in India and abroad. The ideal way to teach anatomy is as under:

1. Teaching and discussion in small groups of not >20 students per teacher in demonstrations, seminars, group discussions, and not >5 or 6 per teacher in dissection, laboratory work, etc., for quick and clear understanding along with fair and free interaction between students and teacher and among students of that group. Since the knowledge and skills developed are to be applied on people in real time, very promptly and accurately in emergency management, hence shortcuts to small group teaching should be avoided
2. Introduce the topic with a story and tell them about desired outcomes
3. Students should conduct thorough dissection of cadavers by themselves under the supervision of a teacher
4. Surface marking (living anatomy) should be taught thoroughly. In clinical practice this forms the anatomical basis of likely hood of the structures involved at the site of patient's complaints/trauma, etc
5. Expose the students to the patients from time to time so that they can have real-life experience
6. Frequent and short assessments of desired outcomes throughout the course of study. To achieve this percentage of marks allotted to the patient should be 50% or more
7. Teaching staff should also have some clinical experience.

Keeping the above facts in mind the patient of anatomy was allotted maximum teaching hours as compared to physiology and biochemistry.

All this is possible only if there is a proper teacher-student ratio.

For undergraduate medical education, initially, the MCI maintained the teacher-student ratio of 1:10 up to 2009[5] though the Mudaliar Committee (1959) had recommended a teacher-student ratio of 1:5.[6] The MCI maintained teacher-student ratio of 1:10 even when there was a shortage of qualified medical teachers by allowing the appointment of nonmedical teachers with MSc., PhD, and DSc. qualification.[7]

Thereafter, the MCI gradually reduced the ratio step by step to 1:15 in 2019,[8] 1:20 in 2010[9] to present low of 1:25 in 2015[10] which has adversely affected the anatomy teaching.

As recommended by Mudaliar Committee as early as 1959 and subsequent committees later the MCI had increased the PG seats in almost all the medical colleges across the country. As a result 2013 onwards more and more medical PGs became available for faculty positions, thus there was silver lining to ease out the teacher-student ratio. However, suddenly in 2015 as a bruit-shock to the medical fraternity, the MCI took a quick "U-turn" and reduced the teachers-students ratio. Since medical teaching has practical, skill oriented teaching modules, CBME has been implemented. The MCI/NMC should restore the teacher-student ratio to at least 1:10 if not 1:5 immediately. At present, besides MD in anatomy, Diplomate of National Board (DNB), Fellowship of National Board (FNB) in anatomy, postgraduate medical specialists with equivalent degrees,

fellowships, etc., obtained from the USA, UK, Europe, and Australia are available and can be attracted to join medical institutions in India. Once we start getting the dividends the teacher-student ratio should be further reduced to 1:5 as per Mudaliar committee and to be globally competitive which is one of the aims and objectives of the health education in the country. Furthermore what already exists in AIIMS, most of the USA, UK, European, and Australian medical institutions, providing for adjunct faculty is another feasible and good option.[5] The adjunct faculty can be drawn from the retired teachers in anatomy and specialists of various disciplines in government and private setup who can give clinically relevant lectures on clinical anatomy. This will ease out the problem of teacher-student ratio not only in anatomy but in other subjects too.

So far the CBME has been experimented only in few medical institutions that too in postgraduation with a good result because teacher-student ratio is good in postgraduation, i.e., 1:1 to a maximum of 1:3 but to have a near similar teaching comfort for undergraduates (IMGs) a systemic planning and changes in the "UG regulations" and "Recommendations on appointment of teachers in the medical colleges," as envisaged, is necessary and should be urgently taken.

Conclusion

In our opinion, the following steps should be taken as early as possible to produce good IMGs.

1. Teacher-student ratio should be increased to 1:5 as recommended by the Mudaliar committee.[6] If not as an emergency measure, it should be restored to 1:10 with immediate effect
2. As per the existing rule book of MCI,[7] since the demonstrators or postgraduates are not recognized as teachers they should not be included while calculating the teacher-student ratio
3. The present overlap of 2 months (August and September) needs to be addressed immediately. As the session should begin on ^{t} August, 1 of every year but last admissions are allowed up to September, 30 in accordance with the Hon'ble apex court. Therefore, practically the session starts from October 1st every year
4. The anatomy faculty for MBBS students should not be used to take anatomy classes for other courses such as dental, paramedical (viz. Occupational Therapy (OT), Bachelor in Medical Laboratory Technology (BMLT), Bachelor of Medical Radio Diagnosis and Imaging Technology (BMRIT), etc.), and nursing students. For these courses, extra faculty should be appointed as per requirement of respective councils. This adversely affects the research work which is expected of them as per "Recommendations on appointment of teachers in the medical colleges"
5. It is the sacrosanct for any government or management (private medical institution) to provide good quality infrastructure and research laboratory in the anatomy and other departments for quality, meaningful, and globally competitive research. In the existing scenario, the teachers are being forced to do research without proper research facilities. This is unnecessarily killing their time in producing false-positive results which are published in predatory journals. As a corollary, a large number of International Journals have come into existence abroad publishing research papers without peer review in shortest possible time after charging money. The selection committee members should be very careful about it
6. Publication of research article should not be the only criteria for promotion. According to Sahai's Dogma[5] for teachers, to impart knowledge is at a higher pedestal than creation of knowledge. Therefore during the selection process for appointment and promotion, how much time did a person spent in teaching (prepared with a properly structured format duly certified by the institution) should be given more weightage than research publication. Similarly his/her depth of knowledge and the way it is expressed should be assessed
7. A good teacher-student ratio will also be essential to start new postgraduate/super-specialty courses in anatomy such as clinical embryology and reproductive anatomy, imaging anatomy, musculoskeletal anatomy, hepatopancreaticobiliary anatomy, endocrine anatomy, ocular anatomy, neuroanatomy, pediatric anatomy, cardiovascular and pulmonary anatomy, etc., similar to advanced countries[6]
8. Duration of first professional MBBS course should be restored to 18 months for countless reasons.

Vishram Singh[1], Ashok Sahai[2]

[1]Department of Anatomy, KMC, Mangalore, MAHE, Manipal, Karnataka, [2]Department of Anatomy, Dayalbagh Educational Institution, Deemed University, Dayalbagh, Agra, Uttar Pradesh, India

Address for correspondence: *Prof. Vishram Singh, OC-5/103, 1st Floor, Orange County Society, Ahinsa Khand-I, Indirapuram, Ghaziabad, Uttar Pradesh - 201 014, India. E-mail: drvishramsingh@gmail.com*

References

1. Graduate Medical Education Regulations. Published in Part III, Section-4 of the Gazette of India, Dated 17 May, 1997 Amended up to 08 October, 2016; 1997.
2. Frank JR, Mungroo R, Ahmad Y, Wang M, De Rossi S, Horsley T. Toward a definition of competency-based education in medicine: A systematic review of published definitions. Med Teach 2010;32:631-7.
3. Mahajan R, Aruldhas BW, Sharma M, Badyal DK, Singh T. Professionalism and ethics: A proposed curriculum for undergraduates. Int J Appl Basic Res 2016;6:157-63.
4. Standring S. Gray's Anatomy: The Anatomical Basis of Clinical Practice. 41st ed. Canada: Elsevier; 2016. [Last accessed on 2020 Oct 27].

5. Ashok S. Medical education in India: Challenges, introspection and reforms-A revision. J Anat Soc India 2016;65:167-74.
6. Mudaliar Committee. Professional education. In: Health Survey and Planning Committee Report. Vol. 1. Ch. 8.Ministry of Health and Family Welfare (MoHFW), Government of India: National Health Protocol; 1962. p. 303-7.
7. Postgraduate Medical Education Regulations. Medical Council of India; 2000.
8. Minimum Standard Requirements for the Medical College for 250 Admissions Annually Regulations, (Amended vide Gazette of India, Part III, section 4, Dated 15 July, 2009); 1999.
9. Minimum Standard Requirement for the Medical College for 250 Admissions Annually Regulations. (Amended by Gazette of India, Part III, section 4, Dated 04 November, 2010); 1999.
10. Minimum Standard Requirement for the Medical College for 250 Admissions Annually Regulations. (Amended by Gazette of India, Part III, Section 4, Dated July 2015); 1999.

Article Info

Received: 09 November 2020
Accepted: 10 November 2020
Available online: ***

Access this article online

Quick Response Code:

Website: www.jasi.org.in

DOI: 10.4103/JASI.JASI_246_20

How to cite this article: Singh V, Sahai A. Implementation of competency based medical education in anatomy with poor teacher-student ratio: The utopia. J Anat Soc India 2020;XX:XX-XX.

Original Article

A Computed Tomography Angiography Study to Correlate Main Renal Artery Diameter with Presence of Accessory Renal Artery in Healthy Live Kidney Donors

Alka Nagar, Navbir Pasricha[1], Eti Sthapak[1], Deshraj Gurjar[2], Hira Lal[3]

Department of Anatomy, GSVM Medical College, Kanpur, [1]Department of Anatomy, Dr. RML Institute of Medical Sciences, Departments of [2]Nephrology and [3]Radiology, Sanjay Gandhi Post Graduate Institute of Medical Sciences, Lucknow, Uttar Pradesh, India

Abstract

Introduction: The chosen technique of surgery during nephrectomy can be influenced by the sudden discovery of an aberrant source of blood supply to the kidney. Thus, a prospective study was undertaken to investigate the relationship between the diameter of the main renal artery and the presence of an accessory renal artery by computed tomography (CT)-angiography. **Material and Methods:** The study was conducted on 115 healthy kidney donors who presented to the department of nephrology and radiology for voluntary kidney donation. All CT examinations were performed on a 64-slice CT scanner in the arterial phase. The number of the renal arteries supplying each kidney was evaluated and their diameters were measured. **Results:** Eighty-six of the right side and 88 of the left side of the 115 kidneys donors had a single renal artery whereas 29 had one or more accessory renal artery (aRA) on the right side and 27 had one or more aRA on the left side. The mean diameter of mRA was 5.4 ± 1.0 mm in kidneys without aRA and 4.6 ± 10 mm in kidneys with aRA on the right side and on the left side the mean diameter of mRA was 5.59 ± 1.12 mm in kidneys without aRA and 4.7 ± 1.2 mm in kidneys with aRA. **Discussion and Conclusion:** The presence of additional renal arteries is very probable when the main renal artery has a diameter of < 4.15 mm. Kidneys presenting a main renal artery > 5.5 mm very probably do not present additional renal arteries. Hence, the renal artery diameter is a factor which should be considered for predicting the presence of additional renal arteries.

Keywords: *Accessory renal artery, renal artery, renal artery diameter*

Introduction

Renal artery variations are common in the general population and the frequency of variations shows social and racial differences.[1,2] Variations are more common in Africans and Caucasians and seen less common in Indians. The frequency of extrarenal arteries shows variability from 9% to 76% and is generally between 28% and 30% in anatomic and cadaveric studies.[1,3,4] The renal arteries have been conventionally described as the lateral branches of the abdominal aorta arising inferior to the origin of the superior mesenteric artery.

Variation in the pattern of renal arteries has been reported more frequently than other large vessels in the literature and alternative nomenclatures have been used to describe the same, these include aberrant artery, supernumerary artery, etc., Graves (1956) states that any artery arising from the aorta in addition to the main renal artery should be named accessory and the arteries arising from sources other than the aorta should be called "aberrant." According to the law of poiseuille, the most important factor determining the volume of blood flow in a vessel is the diameter of the vessel and the flow is directly proportional to the fourth power of vessel diameter It is imperative that artery supplying the kidney should have a sufficient caliber to supply the organ with the amount of blood it needs.[5] The diameter of a renal artery in a kidney supplied by >1 artery can be expected to be smaller than that of the renal artery in a kidney supplied by that single artery. Thus, it can be safely derived that the blood supply to a kidney is dependent on both the number of vessels supplying the kidney and their diameters.

Since renal transplantation is the treatment of choice for patients with end-stage renal

How to cite this article: Nagar A, Pasricha N, Sthapak E, Gurjar D, Lal H. A Computed tomography angiography study to correlate main renal artery diameter with presence of accessory renal artery in healthy live kidney donors. J Anat Soc India 2020;XX:XX-XX.

Article Info

Received: 13 March 2020
Accepted: 19 October 2020
Available online: ***

Address for correspondence:
Dr. Navbir Pasricha, Flat No. 705, Faculty Residential Apartments, Dr. RML Institute of Medical, Sciences, Lucknow, Uttar Pradesh, India.
E-mail: nivibedi@gmail.com

Access this article online

Website: www.jasi.org.in
DOI: 10.4103/JASI.JASI_48_20
Quick Response Code:

failure and kidney transplantation with accessory renal arteries pose a challenge to the surgeon due to higher risks of complications, both vascular and urological it is of utmost importance that the surgeon enters the operative field armed with the most accurate information about the vascular supply of the kidney.

In the past, extensive research has been undertaken on the renal arteries, both cadaveric and using imaging techniques such as ultrasonography, angiography, computed tomography (CT), and magnetic resonance imaging.[6-9] Digital angiography is considered to be the gold standard for studying the renal arterial anatomy, but CT angiography carries fewer risks and is more accurate with better detailing of the vessel wall and lumen.[10,11] Thus, whenever surgical procedures such as partial nephrectomies, pyeloplasty for uretropelvic junction stenosis, and kidney transplantation are planned, the correct anatomical information, especially regarding to vascular supply can affect the chosen surgical technique.[11-13] Thus, a prospective study was undertaken to investigate the relationship between the diameter of the main renal artery and the presence of an accessory renal artery by CT-angiography.

Aims and objectives

To find out the relationship between diameter of the main renal artery with the presence of an accessory renal artery.

Material and Methods

The study was conceptualized in the department of anatomy and was done in collaboration with the department of nephrology and radiology of an institute running a regular kidney transplant program. Prior approval from the Institutional Ethical Committee of the institute was obtained.

The study group consisted of 115 healthy kidney donors (92 women and 23 men with mean age 45.46 years) who presented to the nephrology and radiology department for voluntary kidney donation. All CT examinations were performed on a 64-slice CT scanner in the arterial phase. The number of renal arteries supplying each kidney was evaluated and their diameters were measured.

A total of 80–100 ml of 300 mg/ml intravenous contrast material plus a 20-ml chaser bolus was injected through an 18-gauge cannula positioned in an antecubital vein at a flow rate of 4 ml/s by a dual-head power injector. An automatic triggering system provided the scanning delay time to obtain an arterial phase image. For this purpose, a single unenhanced low-dose scan was first obtained. Based on this image, a region of interest (ROI) with an area of 1 mm^2 was then established by CT technologist in the lumen of the aorta at the level of the superior mesenteric artery. The patient was instructed to hold his breath as soon as the signal density in this ROI reached a threshold of 180 Hounsfield units, and the scan was initiated. The scanning delay time was 18–24 s after the start of the injection.

In our study, the main renal artery was taken as the artery with the largest caliber and originating at the expected level in case of >1 artery supplying the kidney.

The measurement of the RA diameter was performed in the proximal segment of the renal artery at a distance of 1–1.5 cm from the ostium, where the renal artery reaches a uniform width. The data of each patient with the number of arteries supplying the kidney and their diameter were tabulated.

Statistical analysis

The results were expressed as the ± standard deviation. The mean differences among the groups with and without accessory renal artery (aRA) were evaluated using the Student's *t*-test, and the correlations with mRA diameter were evaluated by Pearson's correlation analysis.

Results

The data for 115 healthy kidney donors were analyzed, 23 (20%) of whom were male and 92 (82%) were female. The mean age of the female kidney donors was 45.52 years and the mean age of the male kidney donors was 44.26 years (total mean age of male and female was 45.26 years) [Table 1].

Eighty-six (75%) of the 115 kidneys of the right side and 88 (76.52%) of the 115 kidneys of the left side had a single RA (with no aRA) [Figures 1 and 2], whereas 29 (25%) had one or more aRA on the right side [Figures 3 and 4] and 27 (23.48%) had one or more aRA on the

Table 1 : Distribution of Subjects according to the Gender & Age

Gender	No. (%)	Age	
		Mean	SD
Female	88 (79)	45.52	10.46
Male	23 (21)	44.26	13.15
Total	111 (100)	45.26	11.02

Table 2 : Comparison of mRA between the Subjects having/not having aRA in Right Side

aRA (Rt)	*n*	Diameter of mRA (Rt)		*t*	*p*
		Mean	SD		
absent	86	5.40	1.05	3.579	0.001
present	29	4.60	1.00		

Table 3 : Comparison of mRA between the Subjects having/not having aRA in Left Side

aRA (Lt)	*n*	Diameter of mRA (Lt)		*t*	*p*
		Mean	SD		
absent	88	5.60	1.12	3.639	<0.001

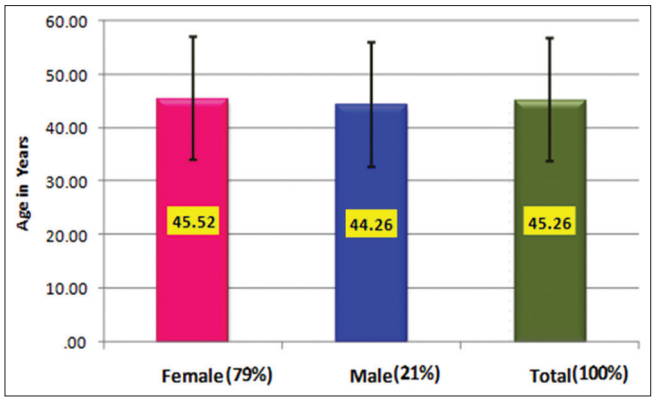

Figure 1: Distribution of subjects according to gender and age

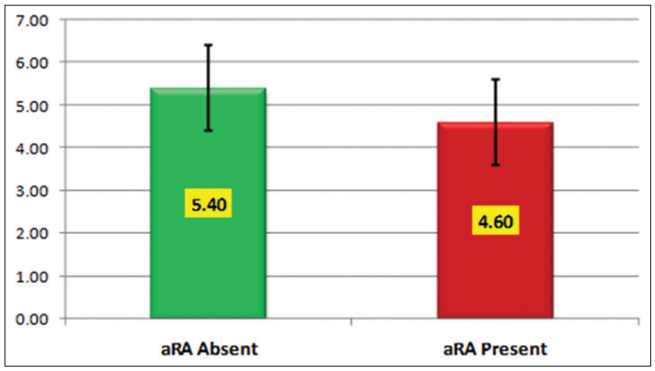

Figure 3: The mRA diameter of a kidney without an aRA and with aRA in the right kidney

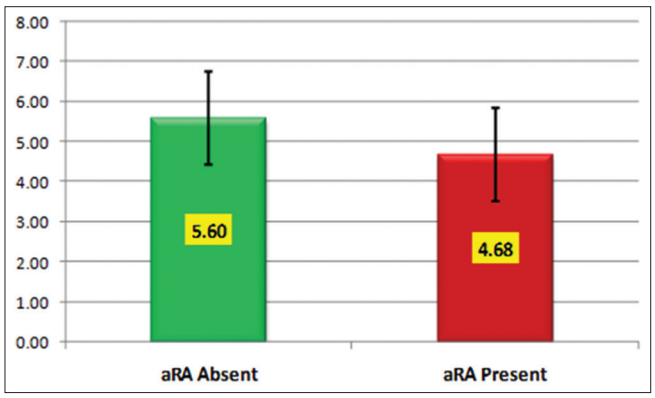

Figure 5: Comparison of mRA between the subjects having/not having aRA in left side

left side [Figures 5 and 6]. Fifty-six of the 230 kidneys had aRA. No aberrant renal artery was found.

The mean diameter of mRA was 5.4 ± 1.0 mm in kidneys without aRA and 4.6 ± 1.0 mm in kidneys with aRA on the right side and on the left side the mean diameter of mRA was 5.59 ± 1.12 mm in kidneys without aRA and 4.7 ± 1.2 mm in kidneys with aRA [Tables 2 and 3].

The mRA diameter was smaller in kidneys with aRA than in those without aRAs ($P < 0.001$ on the right side and $P < 0.0001$ on the left side).

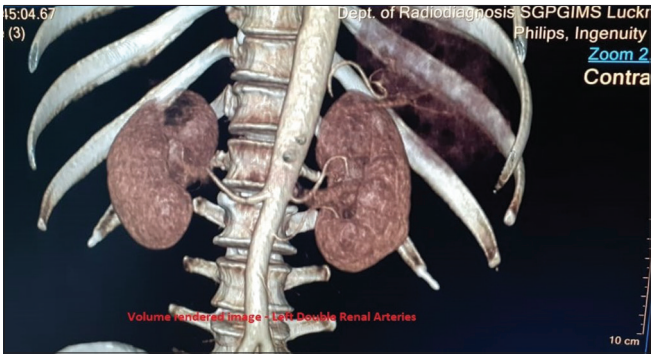

figure 2: CT Angiography showing single renal artery on both sides

Figure 4: CT Angiography showing double renal arteries on right side

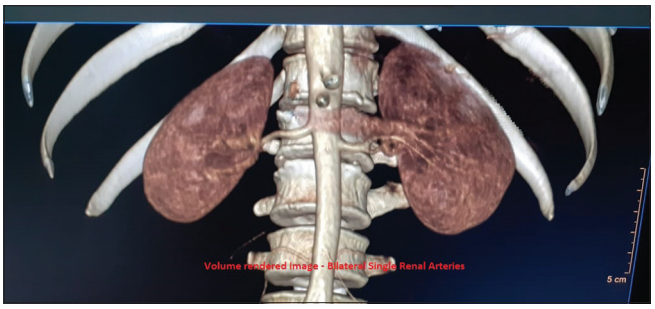

Figure 6: CT Angiography showing double renal arteries on left side

The absence or presence of an aRA was predicted by applying a Binary Regression Analysis [Table 4]. After including the parameter Side and Diameter of mRA in the Binary Logistic Regression Analysis to Predict Absence/Presence of aRA the regression equation of prediction was found to be:

Pr = 2.717–0.007 × Side – 0.760× mRA

In the above equation Side = 1 if there is right side else Side = 0

mRA represents the diameter of mRA.

The presence of aRA predicted if $Pr > 0.5$.

The above model has predictive accuracy of 77.4%.

Binary Logistic Regression Analysis to Predict Absence/ Presence of aRA by the Side and Diameter of mRA.

Table 4: Validity Parameters of the Logistic Regression Predictive Model to Predict Absence/Presence of aRA

Validity Parameter	Estimated Value	95% Confidence Interval	
		Lower	Upper
Sensitivity (Presence of aRA accurately Predicted)	14.3	9.8	18.8
Specificity (absence of aRA accurately Predicted)	97.7	95.8	99.6
PPV (Prob. Of aRA presence)	66.7	60.6	72.8
NPV (Prob. Of aRA absence)	78.0	72.6	83.3
Accuracy	77.4	72.0	82.8

Parameter	*B*	S.E.	*p*
Side Rt	-.007	.327	.982
Dia. of mRA	-.760	.167	<0.001
Constant	2.717	.856	.002

A poor sensitivity (only 14.3%) was found for the fitted logistic regression model. However, the model has a good specificity of 97.7% and accuracy (77.4%). To predict the presence of aRA on the basis of side and diameter of mRA then a positive value of Predictive value (Pr) meant aRA present, but in that case, only among 14.3% cases we actually found the presence of aRA. On the other hand, a negative value of Pr meant aRA is absent, and in that case, prediction will be accurate in 97.7% cases that is we actually found the absence of aRA. Hence, the overall accuracy of model is 77.4%.

Discussion

Embryologically kidney develops from pronephros, mesonephros, and metanephros. The former two regresses but the arterial network to these segments may remain and lead to supernumerary renal arteries. Knowledge of the arterial anatomy of the kidney is important in partial and complete nephrectomies. If there is a single renal artery it is considered as favorable factor with a lower incidence of complications. Bleeding due to an invasive procedure performed on an aRA may result in open laparotomy. Missed case of an aRA may cause infarct in a transplanted kidney and associated hypertension in the recipient. It has been documented that the presence of variations increases the likelihood of warm ischemia time, vascular thrombosis, hemorrhage, difficulty in carrying out anastomosis, and greater risk of urinary fistulas and urethral lesions.[14,15]

Accessory renal arteries constitute the most common, clinically important renal vascular variant. The prevalence of an aRA has been generally accepted to be approximately 25%–30% in different study series.[1-4,7] The prevalence of aRA in our study group (24%) was similar to that described in the literature. Cadaveric studies have also found >1 aRA in different studies with the incidence of 2%–3%[16,17] but we could not find a 3rd renal artery supplying the kidney in our study.

Not only the number of arteries supplying the kidney but also the orthogonal diameter of each artery is important information for the radiologists and surgeons before any intended instrumentation. According to a study carried out by Aytac *et al*. using sonography and digital subtraction angiography,[6] it was derived that if the renal arterial diameter is 4.65 mm or less there is quite probability of an accessory renal artery, and if it is <4.15 mm the probability of an accessory increases with 98% specificity. They also concluded that if they encountered mRA diameter 5.5 mm or more, they could not find an accessory renal artery. In our study too we found out that the mRA diameter was smaller in kidneys with aRA than in those without aRAs. In our study, the mean renal artery diameter in case of absent aRA was 5.40 mm (right side) and 5.59 mm (left) which was significantly more as compared to cases with present aRA, 4.6 mm (right), and 4.7 mm (left) ($P < 0.001$ in the right side and $P < 0.0001$ in left side).

Our study suggests that the diameter of the main renal artery supplying the kidney is a key factor to be investigated and documented before proceeding with any interventions such as transplant or nephrectomies.

Conclusion

In light of the fact that there is limited surgical visibility and exposure in laparoscopic nephrectomies and complications associate with accessory renal arteries, it is imperative to have a thorough knowledge about renal vasculature before any intervention is planned. The statistically significant difference in diameter of mRA in kidneys without aRA and in kidneys with aRA shows that the renal artery diameter is a factor which should be considered preoperatively for predicting the presence of additional renal arteries.

Financial support and sponsorship

Nil.

Conflicts of interest

There are no conflicts of interest.

References

1. Kadir S. Kidneys. In: Kadir S, ed. Atlas of normal and variant angiographic anatomy. Philadelphia: W.B. Saunders Company, 1991;387-429.
2. Boijsen E. Abrams' angiography. 4th ed. Philadelphia: Little, Brown and Company; 1997. Renal angiography: Techniquesand hazards; anatomic and physiologicconsiderations. In: Baum S, ed; pp. 1101–31.
3. Khamanarong K, Prachaney P, Utraravichien A, Tong-Un T,

Sripaoraya K. Anatomy of renal arterial supply. Clin Anat 2004;17:334-6.

4. Satyapal KS, Haffejee AA, Singh B, Ramsaroop L, Robbs JV, Kalideen JM. Additional renal arteries: Incidence and morphometry. Surg Radiol Anat 2001;23:33-8.
5. Guyton AC, Hall JE. Overview of the circulation, medical physics of pressure, flow, and resistance. In: Guyton AC, Hall JE, editors. Textbook of Medical Physiology. 12th ed.. Philadelphia: Elsevier Saunders; 2011. p. 163-70.
6. Aytac SK, Yigit H, Sancak T, Ozcan H. Correlation between the diameter of the main renal artery and the presence of an accessory renal artery: Sonographic and angiographic evaluation. J Ultrasound Med 2003;22:433-9.
7. Çınar C, Türkvatan A. Prevalence of renal vascular variations: Evaluation with MDCT angiography. Diagn Interv Imaging 2016;97:891-7.
8. Klatte T, Ficarra V, Gratzke C, Kaouk J, Kutikov A, Macchi V, *et al*. A literature review of renal surgical anatomy and surgical strategies for partial nephrectomy. Eur Urol 2015;68:980-92.
9. Kock MCJM, Ijzermans JNM, Visser K, Hussain SM, Weimar W, Peter Pattynama MT, *et al*. Contrast-enhanced MR angiography and digital subtraction angiography in living renal donors: diagnostic agreement, impact on decision making, and costs. AJR Am J Roentgenol. 2005;185:448-56.
10. European Association of Urology. EAU guidelines. Edition Presented at the 25th EAU Annual Congress, Barcelona; 2010.
11. American College of Radiology. ACR-SIR-SPR Practice Parameter for Performance of Arteriography. Res. 5-2012, Amended; 2014.
12. Arévalo Pérez J, Gragera Torres F, Marín Toribio A, Koren Fernández L, Hayoun C, Daimiel Naranjo I. Angio CT assessment of anatomical variants in renal vasculature: Its importance in the living donor. Insights Imaging 2013;4:199-211.
13. Urban BA, Ratner LE, Fishman EK. Three-dimensional volume-rendered CT angiography of the renal arteries and veins: Normal anatomy, variants, and clinical applications. Radiographics 2001;21:373-86.
14. Sampaio FJ, Passos MA. Renal arteries: Anatomic study for surgical and radiological practice. Surg Radiol Anat 1992;14:113-7.
15. Kok NF, Dols LF, Hunink MG, Alwayn IP, Tran KT, Weimar W, *et al*. Complex vascular anatomy in live kidney donation: Imaging and consequences for clinical outcome. Transplantation 2008;85:1760-5.
16. Neri E, Caramella D, Bisogni C, Laiolo E, Trincavelli F, Viviani A, *et al*. Detection of accessory renal arteries with virtual vascular endoscopy of the aorta. Cardiovasc Intervent Radiol 1999;22:1-6.
17. Merklin RJ, Michels NA. The variant renal and suprarenal blood supply with data on the inferior phrenic, ureteral and gonadal arteries: A statistical analysis based on 185 dissections and review of the literature. J Int Coll Surg 1958;29:41-76.

Original Article

Morphological Side Differences of the Hemipelvis

Gloria Maria Hohenberger, Angelika Maria Schwarz[1], Andreas Heinrich Weiglein[2], Sabine Kuchling[3], Georg Hauer, Uldis Berzins, Magdalena Holter[4], Christoph Grechenig[5], Renate Krassnig, Axel Gänsslen[6]

Department of Orthopaedics and Trauma, Medical University of Graz, Auenbruggerplatz 5, [1]Department of Orthopaedics and Trauma, AUVA Trauma Hospital Styria | Graz, Göstinger Straße 24, [2]Division of Macroscopic and Clinical Anatomy, Medical University of Graz, Harrachgasse 21, [4]Institute for Medical Informatics, Statistics and Documentation, Medical University of Graz, Auenbruggerplatz 2, Graz, [3]Department of Trauma Surgery, General Hospital Wolfsberg, Paul-Hackhofer-Straße 9, Wolfsberg, [5]Department of Ophthalmology and Optometry, Medical University of Vienna, Währinger Gürtel 18-20, Vienna, Austria, [6]Department of Trauma, Clinical Centre Wolfsburg, Sauerbruchstraße 7, Wolfsburg, Germany

Abstract

Introduction: Differences of anatomical characteristics regarding side and gender have been the topic of interest in various recent studies. Studies have reported either significant or insignificant differences of the bony pelvis. The aim of this study was to evaluate possible gender and side differences of the pelvis in a cadaveric model. **Material and Methods:** Fifty human cadaver pelves, preserved by the use of Thiel's method, underwent measurement during this study. Diverse parameters were measured on both hemipelves by three surgeons. Analysis of the morphology of the acetabular cavity was performed by measuring its longitudinal, horizontal, and maximal diameters. **Results:** The distance between the anterior superior iliac spine and the posterior superior iliac spine (females: mean of 15.9 cm; males: mean of 16.9 cm) and the horizontal diameter of the acetabular cavity (females: mean of 4.5 cm; males: mean of 4.9 cm) were statistically significantly shorter in females than in males. The subpubic angle was significantly ($P < 0.001$) larger in females (mean 61.4°; standard deviation [SD] 11.02°; range 37°–82°) when compared to males (mean 45.5°; SD 7.48°; range 35°–60°). The vertical diameter of the obturator foramen was significantly ($P = 0.002$) smaller for the right (mean 3.1; SD 0.56; range 1.9–4.6) in comparison to the left side (mean 3.4; SD 0.57; range 2.5–5.2). **Discussion and Conclusion:** Overall, a clear gender difference was observed for typical gender-specific parameters, whereas the anatomy of the hemipelves showed no relevant side differences.

Keywords: *Gender differences, hemipelvis, morphologic differences, pelvis, side differences*

Introduction

Differences of anatomical characteristics regarding side and gender have been the topic of interest in various recent studies.

Macedo and Magee,[1] as well as Moromizato *et al*.[2] found statistically significant differences regarding the passive range of motion between dominant and nondominant sides in several joints. Bonneau *et al*.[3] examined 91 adult femora and evaluated an increased anteversion of the femoral neck in women compared to men. In Rouleau *et al*.'s[4] radiologic study concerning the proximal ulna dorsal angulation, this was significantly decreased on left female extremities compared to male elbow joints. Chanplakorn *et al*.[5] conducted a computed tomographic (CT) analysis of 740 pedicles concerning the cervical vertebral segments three to seven. The authors did not find significant differences during side comparison; however, male cervical pedicles showed larger dimensions of some studied parameters compared to females in their sample. Yu *et al*.[6] found an increased pedicle height and width in the thoracic vertebral segments 1–6 in 503 specimens, whereas Chawla *et al*.[7] stated no significant side differences regarding the third lumbar vertebra.

Some studies have also reported either significant or insignificant differences of the bony pelvis.[8-10] The aim of this study was to evaluate possible gender and side differences of the pelvis in a cadaveric model.

Materials and Methods

Dissection and measurement

A total of 50 pelves from adult human cadavers donated to science, embalmed with Thielxs method,[11] were evaluated. All investigated cadavers were donated to the Department of Macroscopic and Clinical Anatomy of the Medical University of Graz under the approval of the Anatomical Donation Program of the University of Graz and according to the Austrian law for donations. Twenty-eight were from male and 22 from female body donors. None of the specimens had signs of

How to cite this article: Hohenberger GM, Schwarz AM, Weiglein AH, Kuchling S, Hauer G, Berzins U, *et al.* Morphological side differences of the hemipelvis. J Anat Soc India 2020;69:XX-XX.

Article Info

Received: 23 July 2020
Accepted: 12 October 2020
Available online: ***

Address for correspondence:
Dr. Gloria Maria Hohenberger, Department of Orthopaedics and Trauma, Medical University of Graz, Auenbruggerplatz 5, 8036 Graz, Austria.
E-mail: hohenberger.gloria@gmail.com

Access this article online

Website: www.jasi.org.in
DOI: 10.4103/JASI.JASI_97_19
Quick Response Code:

previous fractures or malformations. After removal of the surrounding soft tissues and bilateral enucleation of the hip joints, measurements in centimeters were conducted on both hemipelves using a digital caliper. Three surgeons individually measured several parameters [Figures 1 and 2], and the mean of their results was assessed.

Detailed analysis of the morphology of the acetabular cavity was performed by measuring its long, horizontal, and maximal diameters [Figure 2].

In addition, the thickness of the acetabular fossa, was measured (in millimeters), and the anterior acetabular ridge shape was morphologically classified as either straight, curved, or irregular [Figure 3]. The acetabular depth was evaluated by the placement of a ruler across its diameter and measurement of the distance between the deepest part of the acetabular cavity and the ruler.

Statistical analysis

All measurements were exported into Microsoft Excel sheets (Microsoft Excel 2010; Microsoft, Redmond, WA, USA). Statistical analysis was performed using SPSS statistical software (version 22.0; IBM Corp, Armonk, NY, USA). For descriptive statistic mean ± standard deviation (SD), median, minimum, and maximum were calculated. For side comparison, dependent *t*-tests were conducted and for gender comparison, a repeated ANOVA measurement was conducted, including gender as within-subject effect. By the use of Bonferroni correction, a value of $P < 0.002$ for side and gender differences was regarded as statistically significant.

1	Anterior superior iliac spine-posterior superior iliac spine
2	Anterior inferior iliac spine-posterior inferior iliac spine
3	Anterior superior iliac spine–proximal part of ischial tuberosity
4	Anterior superior iliac spine-iliopectineal eminence
5	Anterior inferior iliac spine-iliopectineal eminence
6	Anterior superior iliac spine-anterior inferior iliac spine
7	Posterior superior iliac spine-posterior inferior iliac spine
8	Iliopectineal eminence-pubic tubercle
9	Pubic tubercle-pubic symphysis
10	Height of pubic symphysis
11	Anterior superior iliac spine-iliac eminence
12	Anterior superior iliac spine-thinning out of iliac eminence
13	Posterior wall of acetabulum proximal
14	Posterior wall of acetabulum distal
15	Distance between 13 and 14
16	Subpubic angle
17	Obturator foramen oblique diameter
18	Obturator foramen vertical diameter
19	Ischial tuberosity height
20	Ischial tuberosity breadth

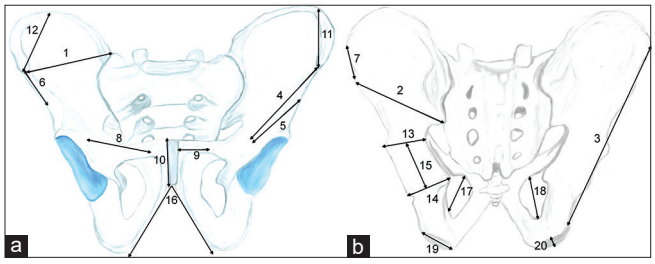

Figure 1: Measurement pattern. The pelvis is depicted from the ventral (a) and dorsal sides (b)

Results

The distance between the anterior superior iliac spine (ASIS) and the posterior superior iliac spine (PSIS) showed a mean of 16.9 cm in males (SD 1.10; range 14.3–19.4) and 15.9 cm in females (SD 0.99; range 13.50–17.40, respectively. Repeated measurement ANOVA revealed a statistically significant difference between sexes ($P = 0.001$). The horizontal diameter of the acetabular cavity was significantly ($P = 0.002$) shorter in females (mean 4.5; SD 0.38; range 3.1–5.3) than in males (mean 4.9; SD 0.42; range 4.1–5.9). In addition, the subpubic angle was significantly larger in females (mean 61.4°; SD 11.02°; range 37°–82°) compared to males (mean 45.5°; SD 7.48°; range 35°–60°), ($P < 0.001$), [Figure 4].

Regarding side differences, the vertical diameter of the obturator foramen was significantly ($P = 0.002$) smaller for the right (mean 3.1; SD 0.56; range 1.9–4.6) in comparison to the left side (mean 3.4; SD 0.57; range 2.5–5.2).

Statistically insignificant differences regarding gender and sides are presented in Tables 1 and 2.

The anterior acetabular ridge's shape was straight in 57 hemipelves, curved in 36 and irregular in seven specimens. In 14 pelves, their hemipelves showed different patterns,

1	Longitudinal diameter
2	Horizontal diameter
3	Maximal diameter

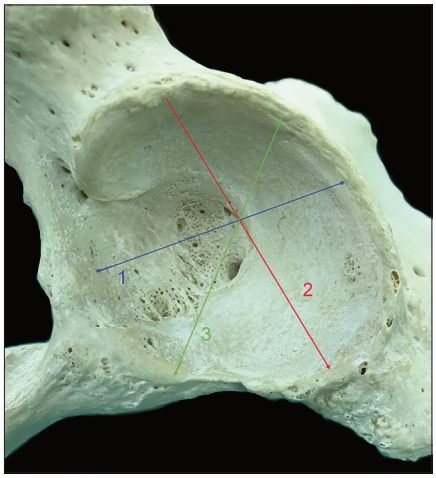

Figure 2: Evaluation of the acetabulum

Table 1a: Measurements of the pelvic rings with regard to gender differences

n	Sex	*n*	Mean	SD	Median	Minimum	Maximum	*P*
1	Male	56	16.87	1.10	17.05	14.30	19.40	0.001
	Female	44	15.87	0.99	16.00	13.50	17.40	
2	Male	56	15.26	1.67	15.30	10.10	17.70	0.096
	Female	44	14.45	1.77	15.01	10.30	17.00	
3	Male	56	14.29	1.11	14.26	12.36	16.54	0.025
	Female	44	13.48	1.41	13.30	9.70	17.29	
4	Male	56	8.20	1.22	8.38	3.90	10.30	0.705
	Female	44	8.31	1.17	8.53	3.90	10.40	
5	Male	56	5.34	1.27	5.11	3.68	10.50	0.030
	Female	44	4.79	0.96	4.60	3.50	8.80	
6	Male	56	4.54	0.74	4.50	2.95	7.90	0.900
	Female	44	4.56	0.44	4.50	3.53	5.62	
7	Male	56	4.07	0.93	3.92	2.23	6.54	0.932
	Female	44	4.09	0.97	3.93	2.10	6.87	
8	Male	56	5.92	0.97	6.00	3.65	7.89	0.951
	Female	44	5.90	1.07	5.98	3.10	7.90	
9	Male	56	7.56	1.12	7.74	2.51	9.60	0.490
	Female	44	7.73	1.09	7.90	5.20	9.60	
10	Male	56	5.19	0.49	5.20	4.02	6.46	0.142
	Female	44	4.93	0.78	4.89	3.32	7.40	
11	Male	56	7.40	1.63	7.77	3.54	10.00	0.537
	Female	44	7.14	1.33	7.46	2.93	8.80	
12	Male	56	5.55	1.64	5.33	2.60	8.81	0.330
	Female	44	5.15	1.51	4.91	2.30	8.17	
13	Male	56	5.33	0.61	5.26	3.94	7.43	0.091
	Female	44	5.07	0.59	5.04	3.87	6.42	
14	Male	56	5.07	0.63	5.10	3.10	7.32	0.064
	Female	44	4.78	0.57	4.73	3.40	6.35	
15	Male	56	4.41	0.78	4.25	2.80	6.40	0.399
	Female	44	4.24	0.83	4.08	2.80	6.40	
16	Male	56	45.50	7.48	45.00	35	60	<0.001
	Female	44	61.41	11.02	59.00	37	82	
17	Male	56	4.92	0.68	5.07	3.00	6.26	0.039
	Female	44	4.56	0.83	4.64	2.60	6.00	
18	Male	56	3.19	0.53	3.09	2.00	4.60	0.570
	Female	44	3.27	0.64	3.25	1.90	5.15	
19	Male	56	6.02	1.02	5.89	4.23	9.20	0.504
	Female	44	5.79	1.44	5.41	3.80	9.50	
20	Male	56	3.23	0.45	3.24	2.25	4.31	0.180
	Female	44	3.07	0.50	3.07	1.80	3.90	

SD: Standard deviation

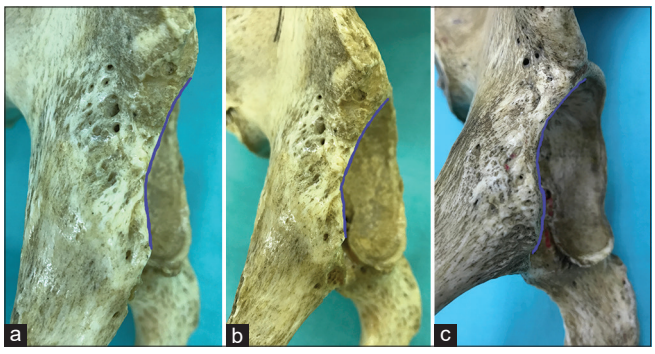

Figure 3: Variations of the anterior acetabular ridge's shape (a) straight, (b) curved, (c) irregular

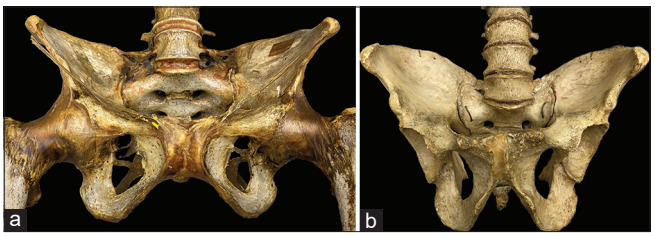

Figure 4: Difference of subpubic angle in a female (a) and male (b) pelvis

whereas eleven of these had a combination of a curved and straight ridge and further three pelves had an irregular and a curved form.

Table 1b: Measurements of the pelvic rings with regard to side differences

n	Side	*n*	Mean	SD	Median	Minimum	Maximum	*P*
1	Left	50	16.47	1.15	16.70	13.50	19.00	0.346
	Right	50	16.38	1.18	16.55	13.80	19.40	
2	Left	50	14.92	1.77	15.30	10.10	17.50	0.798
	Right	50	14.89	1.76	15.06	10.30	17.70	
3	Left	50	14.00	1.35	13.85	9.70	17.29	0.085
	Right	50	13.87	1.28	13.90	10.20	16.79	
4	Left	50	8.20	1.09	8.40	3.90	10.30	0.586
	Right	50	8.30	1.30	8.38	3.90	10.40	
5	Left	50	4.85	0.78	4.81	3.50	7.80	0.020
	Right	50	5.34	1.43	5.02	3.60	10.50	
6	Left	50	4.52	0.56	4.51	2.95	5.72	0.518
	Right	50	4.57	0.68	4.47	3.53	7.90	
7	Left	50	4.19	1.07	4.03	2.10	6.87	0.085
	Right	50	3.97	0.80	3.85	2.23	6.06	
8	Left	50	5.97	0.95	6.00	3.65	7.90	0.496
	Right	50	5.85	1.07	5.98	3.10	7.89	
9	Left	50	7.66	1.22	7.81	2.51	9.60	0.761
	Right	50	7.60	0.99	7.82	5.20	9.60	
10	Left	50	5.07	0.61	5.10	3.39	6.90	0.902
	Right	50	5.08	0.69	5.10	3.32	7.40	
11	Left	50	7.39	1.38	7.80	3.54	9.80	0.119
	Right	50	7.18	1.63	7.61	2.93	10.00	
12	Left	50	5.17	1.48	5.14	2.60	8.69	0.023
	Right	50	5.58	1.68	5.41	2.30	8.81	
13	Left	50	5.20	0.66	5.20	3.87	7.43	0.687
	Right	50	5.24	0.57	5.19	3.96	6.70	
14	Left	50	4.97	0.55	4.95	3.89	6.35	0.410
	Right	50	4.91	0.68	4.85	3.10	7.32	
15	Left	50	4.32	0.78	4.20	2.80	6.40	0.834
	Right	50	4.35	0.83	4.09	3.13	6.40	
17	Left	50	4.79	0.69	4.80	3.00	5.81	0.668
	Right	50	4.73	0.84	4.80	2.60	6.26	
18	Left	50	3.37	0.57	3.35	2.50	5.15	0.002
	Right	50	3.09	0.56	3.03	1.90	4.60	
19	Left	50	5.95	1.21	5.80	4.18	9.50	0.441
	Right	50	5.88	1.25	5.69	3.80	9.20	
20	Left	50	3.15	0.51	3.13	1.80	4.30	0.746
	Right	50	3.17	0.45	3.19	1.90	4.31	

SD: Standard deviation

Table 2a: Evaluated characteristics of the acetabulum concerning gender differences

	Sex	*n*	Mean	SD	Median	Minimum	Maximum	*P*
1	Male	56	5.11	0.44	5.10	4.20	6.05	0.050
	Female	44	4.86	0.49	4.79	4.10	5.81	
2	Male	56	4.88	0.42	4.90	4.12	5.93	0.002
	Female	44	4.54	0.38	4.50	3.12	5.34	
3	Male	56	5.12	0.37	5.09	4.30	6.08	0.010
	Female	44	4.86	0.36	4.80	4.24	5.63	
Depth acetabular cavity	Male	56	3.39	0.51	3.34	2.40	5.10	0.038
	Female	44	3.11	0.55	3.09	1.80	4.80	
Thickness acetabular fossa (mm)	Male	56	6.64	4.33	6.75	0.60	16.00	0.104
	Female	44	4.79	3.41	5.00	0.50	13.00	

SD: Standard deviation

Table 2b: Evaluated characteristics of the acetabulum with sides differences

	Side	*n*	Mean	SD	Median	Minimum	Maximum	*P*
1	Left	50	5.00	0.48	4.96	4.16	6.03	0.836
	Right	50	5.00	0.48	5.00	4.10	6.05	
2	Left	50	4.71	0.48	4.67	3.12	5.68	0.414
	Right	50	4.75	0.40	4.73	4.01	5.93	
3	Left	50	4.98	0.38	4.94	4.24	6.00	0.272
	Right	50	5.03	0.40	5.00	4.30	6.08	
Depth acetabular cavity	Left	50	3.27	0.49	3.29	1.90	4.40	0.924
	Right	50	3.27	0.60	3.20	1.80	5.10	
Thickness acetabular fossa(mm)	Left	50	5.74	3.91	5.81	0.70	16.00	0.448
	Right	50	5.91	4.21	5.61	0.50	16.00	

SD: Standard deviation

Discussion

Possible side and gender differences have been under discussion in various articles.

Boulay *et al*.[8] performed measurements by the use of an electromagnetic device which provided three-dimensional spatial coordinate measurements in twelve anatomical specimens. During this analysis, 349 different targets, including angles and distances, were checked in detail for side differences. On the right side, the main axis of the obturator foramen was significantly larger compared to the left side. This was comparable to the presented sample with a significantly smaller vertical diameter ($P = 0.002$) on the right (mean 3.1 cm) compared to the left side (mean 3.4 cm).

The distance between the ASIS and the PSIS showed no side differences which was also observed by Boulay *et al*.[8] However, a statistically significant difference ($P = 0.001$) between the sexes was observed in the present study between ASIS and PSIS (males: 16.9 cm; females: 15.9 cm).

Among other characteristics, Ma *et al*.[12] evaluated the acetabular depth in 100 patients by routine CT scans. They found a significant difference between male and female specimens in both coronal (2.1 vs. 1.8 cm) and axial (2.5/2.6 vs. 2.3 cm) planes but no differences regarding side.

Zeng *et al*.[10] in a CT analysis reported that the acetabular depth was significantly smaller in women (left: 1.74 cm; right: 1.73 cm) than in men (left: 1.94 cm; right: 1.93 cm). However, further statistical tests did not reveal significant differences when the acetabular depth was adjusted for individual body height.

Chauhan *et al*.[13] found a significant gender difference between both acetabular depths (males: left: 28.18 mm, right: 27.49 mm; females: left: 25.70 mm, right: 24.68 mm). In contrast, our results only showed a tendency of a larger acetabular depth compared to previous studies. No gender difference (female: 3.11 cm; male: 3.39 cm) or side difference (left: 3.27 cm; right: 3.27 cm) was observed.

However, the horizontal diameter of the acetabular cavity was significantly shorter in females (mean 4.5 cm) than in males (mean 4.9 cm). Chauhan *et al*.[13] observed a slight significant difference between sexes on the right side (males: right: 4.71 cm, left: 4.75 cm; females: right: 4.44 cm, left: 4.60 cm). These results were comparable to the presented values.

In a noncomparable analysis of the morphology of the anterior acetabular ridge's shape in 154 hip joints by Taştekın Aksu *et al*.,[14] the shape was found to be curved in 46.1%, straight in 23.3%, angular in 16.8%, and irregular in 13.6%. Thoudam and Chandra.[15] and Vyas *et al*.[16] found the curved form to be most common with 60%. In our sample, the straight form was most present in even 57%, although the occurrence of this form has been reported in a low range of 4%–4.5%[15] up to 31.6%.[16] However, these highly varying results may be due to interobserver variability.

Not surprisingly, we also observed a significantly larger subpubic angle in females (mean 61.4°; SD 11.02°; range 37°–82°) in comparison to males (mean 45.5°; SD 7.48°; range 35°–60°). Igbigbi and Nanono-Igbigbi[17] observed higher values for their Ugandan collective with a mean of 116.1° (range: 75–155) for females and 93.9° (range: 50–140) in males in a radiologic study. Small *et al*.[18] reported an average angle of 84.1° (range: 52.5–100.2) in females and of 63.9° in males (45.3–93.2) black South Africans. Since our sample consisted of Caucasian specimens, varying values may be the result of racial differences.

Conclusion

Overall, a clear gender difference was observed for typical gender-specific parameters, whereas the anatomy of the hemipelves showed no relevant side differences. In contrast, Boulay *et al*.[8] found some differences, which were clinically unimportant due to their large sample size. The results in the present study indicate that gender and side differences may be neglected during preoperative planning of the acetabular component for total hip arthroplasty

or during the use of prebended plates during acetabular osteosynthesis.

Financial support and sponsorship

Nil.

Conflicts of interest

There are no conflicts of interest.

References

1. Macedo LG, Magee DJ. Differences in range of motion between dominant and nondominant sides of upper and lower extremities. J Manipulative Physiol Ther 2008;31:577-82.
2. Moromizato K, Kimura R, Fukase H, Yamaguchi K, Ishida H. Whole-body patterns of the range of joint motion in young adults: Masculine type and feminine type. J Physiol Anthropol 2016;35:23.
3. Bonneau N, Libourel PA, Simonis C, Puymerail L, Baylac M, Tardieu C, *et al*. A three-dimensional axis for the study of femoral neck orientation. J Anat 2012;221:465-76.
4. Rouleau DM, Faber KJ, Athwal GS. The proximal ulna dorsal angulation: a radiographic study. J Shoulder Elbow Surg 2010;19:26-30.
5. Chanplakorn P, Kraiwattanapong C, Aroonjarattham K, Leelapattana P, Keorochana G, Jaovisidha S, *et al*. Morphometric evaluation of subaxial cervical spine using multi-detector computerized tomography (MD-CT) scan: The consideration for cervical pedicle screws fixation. BMC Musculoskelet Disord 2014;15:125.
6. Yu CC, Bajwa NS, Toy JO, Ahn UM, Ahn NU. Pedicle morphometry of upper thoracic vertebrae: An anatomic study of 503 cadaveric specimens. Spine (Phila Pa 1976) 2014;39:E1201-9.
7. Chawla K, Sharma M, Abhaya A, Kochhar S. Morphometry of the lumbar pedicle in North West India. Eur J Anat 2011;15:155-61.
8. Boulay C, Tardieu C, Bénaim C, Hecquet J, Marty C, Prat-Pradal D, *et al*. Three-dimensional study of pelvic asymmetry on anatomical specimens and its clinical perspectives. J Anat 2006;208:21-33.
9. Buller LT, Rosneck J, Monaco FM, Butler R, Smith T, Barsoum WK. Relationship between proximal femoral and acetabular alignment in normal hip joints using 3-dimensional computed tomography. Am J Sports Med 2012;40:367-75.
10. Zeng Y, Wang Y, Zhu Z, Tang T, Dai K, Qiu S. Differences in acetabular morphology related to side and sex in a Chinese population. J Anat 2012;220:256-62.
11. Thiel W. The presentation of the whole corpse with natural color. Ann Anat 1992;174:185-95.
12. Ma H, Han Y, Yang Q, Gong Y, Hao S, Li Y, *et al*. Three-dimensional computed tomography reconstruction measurements of acetabulum in Chinese adults. Anat Rec (Hoboken) 2014;297:643-9.
13. Chauhan R, Paul S, Dhaon BK. Anatomical parameters of north Indian hip joints – Cadaveric study. J Anat Soc India 2002;51:39-42.
14. Taştekın Aksu F, Gülrız Çerı N, Arman C, Tetık S. Morphology and morphometry of the acetabulum. CİLT 20.2006; SAYI 3:143-8.
15. Thoudam B, Chandra P. Acetabulum-morphological and morphometrical study. Res J Pharm Biol Chem Sci 2014;5:793-9.
16. Vyas K, Shroff B, Zanzrukiya K. An osseous study of morphological aspect of acetabulum of hip bone. Int J Res Med 2013;2:78-82.
17. Igbigbi PS, Nanono-Igbigbi AM. Determination of sex and race from the subpubic angle in Ugandan subjects. Am J Forensic Med Pathol 2003;24:168-72.
18. Small C, Brits DM, Hemingway J. Quantification of the subpubic angle in South Africans. Forensic Sci Int 2012;222:395.e1-6.

Original Article

The Morphological Variants of Dural Venous Sinuses

Sercan Özkaçmaz, Yeliz Dadali[1], Muhammed Alpaslan[1], Ilyas Uçar[2]

Department of Radiology, Faculty of Medicine, Yuzuncu Yil University, Van, [1]Department of Radiology, Faculty of Medicine, Kırşehir Ahi Evran University, [2]Department of Physical Therapy and Rehabilitation, Institute of Physical Therapy and Rehabilitation, Kırşehir Ahi Evran University, Kırşehir, Turkey

Abstract

Introduction: In this study, we aimed to analyze the dural venous system variations in Turkey by magnetic resonance imaging examinations. **Material and Methods:** Images of a total of 200 patients (65 males, 135 females M/F: 0.48) who underwent a magnetic resonance venography examination were retrospectively screened. **Results:** Variation was detected in 101 patients (53.85% of males [35/65] and 48.89% of females [66/135]). In 16.5% of the patients, only one variation of dural venous system was detected, while the most common variation was left transverse hypoplasia in this group. Twenty-six percent of the patients had two variations of the dural venous system since the most common dual variations were left transverse hypoplasia + left sigmoid hypoplasia in this group. In 8% of the patients, three or more variations of the dural venous system were observed as the most common variations were right transverse hypoplasia + right sigmoid hypoplasia + presence of occipital sinus in this group. **Discussion and Conclusion:** It is essential to know the anatomical variations of the dural venous system for the discrimination between pathological processes such as thrombosis and physiologic conditions. Furthermore, the association of these variations with each other must be kept in mind for the explanation of the presence of multiple variations in the same individuals.

Keywords: *Anatomy, dural venous sinuses, magnetic resonance venography, variation*

Introduction

The dural venous system, comprised widespread venous structures including superior sagittal (unpaired), inferior sagittal (unpaired), transverse, sigmoid, straight (unpaired), superior-inferior petrosal, tentorial, occipital (unpaired), cavernous, sphenoparietal, petrosquamous, anterior-posterior intercavernous sinuses (unpaired), torcular herophili (unpaired), basilar and falcine venous plexuses. Because of this complex texture, various variations may be seen in the dural venous system.[1]

Thrombosis and septic thrombophlebitis are the main pathological conditions of the dural venous system, which leads to severe neurological consequences and even death.[2] For the differentiation of anatomic variations and pathological conditions such as dural venous thrombosis-thrombophlebitis, anatomy and the variations of the dural venous system must be well-known to prevent misdiagnosis.[1] Advances in imaging techniques provide a better examination of main dural venous structures. Especially Computed Tomography Venography and magnetic resonance venography (MRV) are very useful for the discrimination of variations and thrombosis.[3]

In this study, we examined the frequency and associations of anatomical variations of the dural venous system in our patients by MRV.

Material and Methods

Medical records of 206 patients (41 ± 19 years old [18–78]) who underwent MRV with complaints of headache, nausea, vomiting, vertigo, seizure or neurological deficits between June 2017 and June 2019 were screened in the hospital database. Six patients were excluded from the study in whom a dural venous sinus thrombosis was detected. Among these 6 ones, thrombosis was seen in only right transverse sinus in two patients, in only superior sagittal sinus (SSS) in one patient. In two patients, left transverse + left sigmoid sinus thrombosis was detected. SSS + left transverse sinus thrombosis was observed in remained one patient. Finally, 200 patients were included in this study.

MRV examinations were performed by using a two-dimensional TOF MRV

How to cite this article: Özkaçmaz S, Dadali Y, Alpaslan M, Uçar I. The morphological variants of dural venous sinuses. J Anat Soc India 2020;69:XX-XX.

Article Info

Received: 23 August 2019
Accepted: 13 September 2020
Available online: ***

Address for correspondence:
Dr. Sercan Özkaçmaz, Department of Radiology, Faculty of Medicine, Yuzuncu Yil University, Bardakçı, Van 65100, Turkey. E-mail: sercanozkacmaz@hotmail.com

Access this article online

Website: www.jasi.org.in
DOI: 10.4103/JASI.JASI_112_19
Quick Response Code:

technique on GE Signa Excite 1.5 Tesla Magnetic Resonance Imaging system (Signa Excite HD; GE Medical Systems, Milwaukee, WI, USA) with a standard head coil. Time of repetition/time of echo (TR/TE) was 28/10.8, and a Flip angle of 60° was used. The field of view was 240 mm, with a matrix size of 256 × 160. Images were acquired in coronal planes with a slice thickness of 1.5 mm. Maximum pixel intensity projection images were obtained, and the images were interpreted by two radiologists. The sinuses, except occipital and falcine sinuses, were reported as normal, hypoplastic, or agenetic. Occipital and falcine sinuses were reported as absent or present.

Patients were classified into four groups as having no dural venous variation (Group C), only one variation (Group O), two variations (Group D), and three or more variations (Group T+).

The study was approved by a local ethics committee on August 06, 2019, with a number of 2019-14/142

Results

Among these 200 patients, variation was observed in 101 ones. The overall variation rate was 50.5%. The incidence of dural venous system variation was found to be as 53.85% (35/65) in males and 48.89% (66/135) in females. The variation rate was found higher in males than in females [Table 1]. These variations are believed to be occurring as a consequence of a congenital condition with no association with aging and other pathological processes as they may be seen in childhood and do not exhibit an alteration at the subsequent imaging examinations.[4]

Groups

In 99 patients (49.5%) (control Group 1 [C]) there was no dural venous system variation. Only one variation was detected in 33 patients (16.5%) (Group 2 [O]) [Table 2]. Two variations were observed in 52 patients (26%) (Group 3 [D]) [Table 3]. Three or more variations were seen in 16 patients (8%) (Group 4 [T+]) [Table 4].

The most common single variation was left transverse hypoplasia, which was detected in 17 patients (8.5%) [Figure 1]. Left transverse hypoplasia + left sigmoid hypoplasia was the most common dual variation that was detected in 25 patients (12.5%) [Figure 2]. The most common triple or more variations was right transverse hypoplasia + right sigmoid hypoplasia + presence of occipital sinus, which was observed in 4 patients (2%) [Figure 3].

There was no significant difference for the presence of complaints between the groups as the symptoms were observed with similar rates in these four groups.

Transverse sinuses

A total of 33 variations were detected in the right transverse sinus. The frequency of variation of the right transverse sinus was found to be 16.5%. Hypoplasia was observed in 30 patients while aplasia in remained three ones.

A total of 59 variations were detected in the left transverse sinus. The frequency of variation of the left transverse sinus was found to be 29.5%. Hypoplasia was observed in 56 patients, while aplasia remained three ones [Figure 4].

Sigmoid sinuses

A total of 23 variations were detected in the right sigmoid sinus. The frequency of variation of the right sigmoid sinus was found to be 11.5%. Twenty-two of the variations of right sigmoid sinus were hypoplasia while one aplasia detected.

A total of 37 variations were detected in the left sigmoid sinus. The frequency of variation of the left sigmoid sinus was found to be 18.5%. Thirty-six of the variations of left sigmoid sinus were hypoplasia, while aplasia was detected in one patient.

Superior sagittal sinus

A total of two variations of the SSS were observed, while all of them were hypoplasia. No aplasia of SSS was detected. The frequency of variation of SSS was found to be 1%.

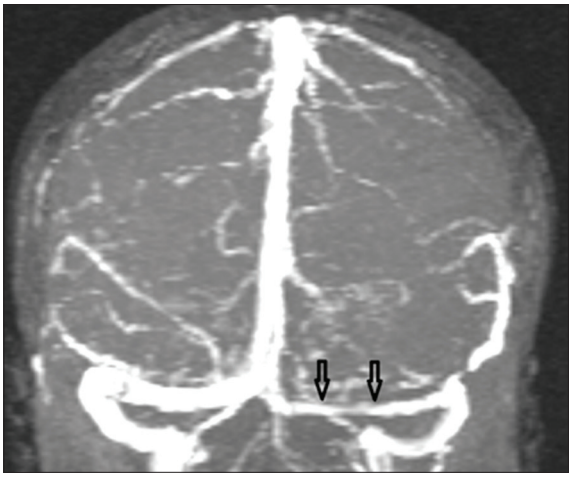

Figure 1: Left transverse sinus hypoplasia (arrows)

Table 1: Distribution of the patients to the groups according to the number of variations

	n (rate%)			
	Group 1 (C) No variation	**Group 2 (O) One variation**	**Group 3 (D) Two variations**	**Group 4 (T+) ≥3 variations**
Female	69 (51.1)	22 (16.3)	34 (25.2)	10 (7.4)
Male	30 (46.2)	11 (16.9)	18 (27.7)	6 (9.2)
Total	99 (49.5)	33 (16.5)	52 (26)	16 (8)

Straight sinus

A total of four variations were detected in the straight sinus. The frequency of variation of the straight sinus was found to be 2%. Three hypoplasia and one aplasia of straight sinus were observed.

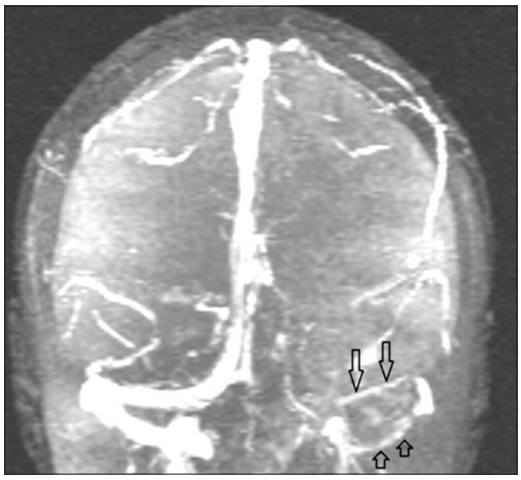

Figure 2: Left transverse sinus hypoplasia (long arrows) +left sigmoid sinus hypoplasia (short arrows)

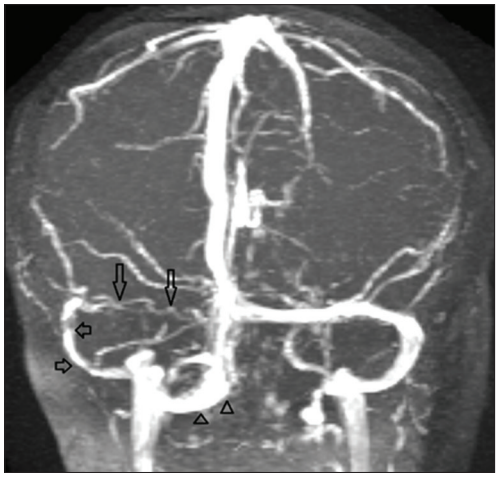

Figure 3: Right transverse sinus hypoplasia (long arrows) + right sigmoid sinus hypoplasia (short arrows) + occipital sinus (arrowheads)

Figure 4: Left transverse sinus aplasia

Inferior sagittal sinus

A total of 11 variations were detected in the inferior sagittal sinus. The frequency of variation of the inferior sagittal sinus was found to be 5.5%. Six of the variations of inferior sagittal sinus were hypoplasia, while 5 ones were aplasia.

Occipital and falcine sinus

In 19 patients (9.5%), occipital sinus was detected. The most common variations which accompanied the presence of occipital sinus were right transverse hypoplasia + right sigmoid hypoplasia [Table 5].

We did not observe falcine sinus in this study.

Discussion

As the dural venous system includes various superficial and deep structures, various pathological conditions and anatomical variations can affect this system. For accurate differentiation of these physiological and pathological conditions, the variations and their association must be well known.[5] In this study, we examined the frequency and types of variations. Furthermore, we investigated the associations of these variations with each other.

We identified thirty hypoplasia and three aplasias in the right transverse sinus while the overall variation frequency of right transverse sinus was 16.5%. In 56 patients, hypoplasia and in 3 ones aplasia of the left transverse sinus was detected with a total variation frequency of 29.5%. In a study by Surendrababu *et al*.[6] they detected right transverse sinus hypoplasia in 13%, left transverse sinus hypoplasia in 35%, and left transverse sinus aplasia in 1% of their patients. Our results were compatible with this study regarding variation rates of right and left transverse sinuses. Goyal *et al*.[7] observed variation of the right transverse sinus in 6.2% of their patients (hypoplasia in 5.5% and aplasia in 0.7%). They detected hypoplasia of the left transverse sinus in 21.3% and aplasia of

Table 2: Distribution of the patients with one variation (Group 2) according to their variation types

	n (rate%)		
	Female	Male	Total
Left transverse hypoplasia	11 (8.1)	6 (9.2)	17 (8.5)
Inferior sagittal hypoplasia	1 (0.7)	2 (3.1)	3 (1.5)
Right transverse hypoplasia	2 (1.5)	-	2 (1.0)
Straight sinus hypoplasia	2 (1.5)	-	2 (1.0)
Inferior sagittal aplasia	1 (0.7)	2 (3.1)	3 (1.5)
Occipital sinus	2 (1.5)	1 (1.5)	3 (1.5)
Left sigmoid hypoplasia	2 (1.5)	-	2 (1.0)
Straight sinus aplasia	1 (0.7)	-	1 (0.5)
Total	22 (16.3)	11 (16.9)	33 (16.5)

Table 3: Distribution of the patients with two variations (Group 3) according to their variation types

Double variations	*n* (rate%)		
	Female	Male	Total
Left transverse hypoplasia + left sigmoid hypoplasia	18 (13.3)	7 (10.8)	25 (12.5)
Right transverse hypoplasia + right sigmoid hypoplasia	5 (3.7)	8 (12.3)	13 (6.5)
Left sigmoid hypoplasia + left transverse aplasia	1 (0.7)	1 (1.5)	2 (1.0)
Right transverse hypoplasia + left transverse hypoplasia	2 (1.5)	-	2 (1.0)
Right transverse hypoplasia + inferior sagittal aplasia	-	1 (1.5)	1 (0.5)
Left transverse hypoplasia + occipital sinus	1 (0.7)	-	1 (0.5)
Right transverse hypoplasia + occipital sinus	1 (0.7)	-	1 (0.5)
Left sigmoid hypoplasia + inferior sagittal aplasia	1 (0.7)	-	1 (0.5)
Right sigmoid hypoplasia+ occipital sinus	1 (0.7)	-	1 (0.5)
Right transverse hypoplasia + superior sagittal hypoplasia	-	1 (1.5)	1 (0.5)
Left transverse hypoplasia + inferior sagittal hypoplasia	1 (0.7)	-	1 (0.5)
Left transverse hypoplasia + left sigmoid aplasia	1 (0.7)	-	1 (0.5)
Right transverse aplasia + occipital sinus	1 (0.7)	-	1 (0.5)
Right tranverse aplasia + right sigmoid hypoplasia	1 (0.7)	-	1 (0.5)
Total	34 (25.2)	18 (27.7)	52 (26.0)

Table 4: Distribution of the patients with three or more variations (Group 4) according to their variation types

Three or more variations	*n* (rate%)		
	Female	Male	Total
Right transverse hypoplasia + right sigmoid hypoplasia + occipital sinus	3 (2.2)	1 (1.5)	4 (2)
Left transverse hypoplasia + left sigmoid hypoplasia + occipital sinus	-	2 (3.1)	2 (1)
Right transverse hypoplasia + Left transverse hypoplasia + occipital sinus	2 (1.5)	-	2 (1)
Right transverse aplasia + Left transverse hypoplasia + right sigmoid hypoplasia	-	1 (1.5)	1 (0.5)
Right transverse hypoplasia + left transverse hypoplasia + inferior sagittal hypoplasia	1 (0.7)	-	1 (0.5)
Right transverse hypoplasia + right sigmoid hypoplasia + straight hypoplasia	-	1 (1.5)	1 (0.5)
Left transverse aplasia + left sigmoid hypoplasia + occipital sinus	1 (0.7)	-	1 (0.5)
Left transverse hypoplasia + Left sigmoid hypoplasia + superior sagittal hypoplasia	1 (0.7)	-	1 (0.5)
Left transverse hypoplasia + left sigmoid hypoplasia + occipital sinus + inferior sagittal hypoplasia	-	1 (1.5)	1 (0.5)
Right transverse hypoplasia + left transverse hypoplasia + right sigmoid hypoplasia + right sigmoid hypoplasia + occipital sinus	1 (0.7)	-	1 (0.5)
Right transverse hypoplasia + right sigmoid aplasia + occipital sinus	1 (0.7)	-	1 (0.5)
Total	10 (7.4)	6 (9.2)	16 (8)

Table 5: The association of presence of occipital sinus with other variations

Variations	*n* (rate%)		
	Female	Male	Total
Occipital sinus (one variation)	2 (1.5)	1 (1.5)	3 (1.5)
Left transverse hypoplasia + occipital sinus	1 (0.7)	-	1 (0.5)
Right transverse hypoplasia + occipital sinus	1 (0.7)	-	1 (0.5)
Right sigmoid hypoplasia + occipital sinus	1 (0.7)	-	1 (0.5)
Right transverse aplasia + occipital sinus	1 (0.7)	-	1 (0.5)
Right transverse hypoplasia + right sigmoid hypoplasia + occipital sinus	3 (2.2)	1 (1.5)	4 (2.0)
Left transverse hypoplasia + left sigmoid hypoplasia + occipital sinus	-	2 (3.1)	2 (1.0)
Right transverse hypoplasia + left transverse hypoplasia + occipital sinus	2 (1.5)	-	2 (1.0)
Left transverse aplasia + left sigmoid hypoplasia + occipital sinus	1 (0.7)	-	1 (0.5)
Left transverse hypoplasia + left sigmoid hypoplasia + occipital sinus + inferior sagittal hypoplasia	-	1 (1.5)	1 (0.5)
Right transverse hypoplasia + left transverse hypoplasia + right sigmoid hypoplasia + right sigmoid hypoplasia + occipital sinus	1 (0.7)	-	1 (0.5)
Right transverse hypoplasia + right sigmoid aplasia + occipital sinus	1 (0.7)	-	1 (0.5)
Total	14 (10.4)	5 (7.7)	19 (9.5)

the left transverse sinus in 4.1% of their patients (total variation rate was 25.4%). While our left transverse sinus variation rate was similar to their results, but our right transverse sinus variation rate was markedly higher. Their bilateral transverse sinus hypoplasia rate was 1.5%. We found bilateral transverse sinus hypoplasia in our 6 patients (3%). Our bilateral transverse sinus hypoplasia rate was compatible with their study. Alper *et al*.[8] detected left transverse sinus hypoplasia in 39%, aplasia in 20%, right transverse sinus hypoplasia in 6%, and aplasia in 4% of their patients. When compared with their study, our left transverse sinus variation rate was lower and right transverse sinus variation rate was higher. Tantawy *et al*.[9] reported left transverse sinus hypoplasia in 22%, aplasia in 3.6%, right transverse sinus hypoplasia in 8%, and aplasia in 1.7% of their 363 patients. When compared with their results, our transverse sinus variation rate was higher on both sides (right and left).

We observed 23 variations in the right sigmoid sinus, while 22 of them were hypoplasia and one was aplasia. The variation rate of the right sigmoid sinus was 11.5%. There were 36 hypoplasia and one aplasia in the left sigmoid sinus with a variation rate of 18.5%. The variation rate of the left sigmoid sinus was higher than the right sigmoid sinus variation rate. In a study by Ahmed *et al*.[5] they detected right sigmoid sinus hypoplasia in 2.9% (n = 6) of their patients, but they did not observe right sigmoid sinus aplasia. The variation rate of left sigmoid sinus was 23.3% while they found left transverse sinus hypoplasia in 22.05% (n = 45) and aplasia in 0.98% (n = 2) of their patients. Our variation rate of the left transverse sinus was mildly lower than their results (18.5% vs. 23.3%), but we observed higher variation rates of the right sigmoid sinus (11.5% vs. 2.9%). Shirodkar *et al*.[10] reported right transverse sinus variations in 6% (hypoplasia in 5% and aplasia in 1%) and left transverse sinus variations in 13% (hypoplasia in 7% and aplasia in 6%) of their patients. Our results were similar to their results, but the rate of aplasia of the left transverse sinus was lower in our patients (1.5% vs. 6%).

A total of 2 variations of the SSS were observed in our study, while all of them were hypoplasia of 1/3rd of the SSS. No aplasia of SSS was detected. The rate of variation of SSS was found to be 1%. Goyal *et al*.[7] reported a 2.3% variation rate (0.4% (n = 6) was hypoplasia of anterior 1/3rd part) of SSS. Ahmed *et al*.[5] did not observe any SSS variations in their 204 patients. Our variation rate results of SSS was compatible with previous studies.

Three hypoplasia and one aplasia (2% n = 4) of straight sinus were detected in our study. Ahmed *et al*.[5] reported no variation of the straight sinus in their patients. Goyal *et al*.[7] identified 4 hypoplasia (0.2%) in their patients. We found higher variation rates of straight sinus when compared with previous studies.

Among 11 variations (5.5%) of inferior sagittal sinus variations, 6 ones were hypoplasia, and 5 ones were aplasia in our study. Ahmed *et al*.[5] reported a 13.95% variation rate of the inferior sigmoid sinus. Ayanzen *et al*.[11] detected inferior sagittal sinus in only 52% of their patients. The variation rate of the inferior sagittal sinus in our study was lower than the results of previous studies.

We detected occipital sinus in 19 patients (9.5%). Goyal *et al*.[7] reported occipital sinus in 1.4% of their patients. However, in literature, some studies suggested that occipital sinus was found in 4%–10%[11,12] of individuals. Our occipital sinus results were similar to previous studies.

Falcine sinus is a dural venous sinus variation with an incidence of 5.3%, which may be associated with straight sinus variations.[13] We did not observe any falcine sinus in especially our patients with hypoplastic/agenetic straight sinus.

We detected dual venous sinus variations in 51 patients (25.5%). The most common dual variations were left transverse hypoplasia + left sigmoid hypoplasia (n = 25, 12.5%), right transverse hypoplasia + right sigmoid hypoplasia (n = 13, 6.5%), left transverse aplasia + left sigmoid hypoplasia (n = 2, 1%), and right transverse hypoplasia + left transverse hypoplasia (n = 2, 1%).

We observed three or more variations in 16 patients (8%). The most common three or more variations were right transverse hypoplasia + right sigmoid hypoplasia + occipital sinus (n = 4 2%), left transverse hypoplasia + left sigmoid hypoplasia + occipital sinus (n = 2 1%) and right transverse hypoplasia + left transverse hypoplasia + occipital sinus (n = 2 1%).

We observed that in the patients with multiple dural venous variations, ipsilateral transverse and sigmoid variations usually accompany each other, and also frequently an occipital sinus presents with such conditions. This is probably due to provide the drainage via the occipital sinus.

Conclusion

Multiple dural venous sinus variations may be misdiagnosed as thrombosis especially in the patients with neurological complaints as dural venous thrombosis usually involves two or more different dural sinuses. The frequency and the association of multiple variations must be well known because accurate discrimination between these variations and pathological conditions such as thrombosis is essential to prevent misdiagnosis.

Acknowledgements

We declare that there are no conflicts of interest and no funding in this study.

Financial support and sponsorship

Nil.

Conflicts of interest

There are no conflicts of interest.

References

1. Joseph SC, Elias R, Tubbs RS. Variations of the ıntracranial dural venous sinuses. In: Tubbs RS, Iwanaga J, Oskouian R, Loukas M, Shoja M, Monteith S, editors. Anatomy, Imaging and Surgery of the Intracranial Dural Venous Sinuses. St. Louis, Missouri, USA: Elsevier; 2019. p. 205-20.
2. Shen X, Morón FE, Gao B. Imaging of cerebral venous complications in patients with infections. Radiol Infect Dis 2017;4:131-5.
3. Kouzmitcheva E, Andrade A, Muthusami P, Shroff M, MacGregor DL, deVeber G, *et al*. Anatomical venous variants in children with cerebral sinovenous thrombosis. Stroke 2019;50:178-80.
4. Mankad K, Biswas A, Espagnet MC, Dixon L, Reddy N, Tan AP, *et al.* Venous pathologies in paediatric neuroradiology: from foetal to adolescent life. Neuroradiology 2020;62:15-37.
5. Ahmed MS, Imtiaz S, Shazlee MK, Ali M, Iqbal J, Usman R. Normal variations in cerebral venous anatomy and their potential pitfalls on 2D TOF MRV examination: Results from a private tertiary care hospital in Karachi. J Pak Med Assoc 2018;68:1009-13.
6. Surendrababu NRS, Livingstone RS. Variations in the cerebral venous anatomy and pitfalls in the diagnosis of cerebral venous sinus thrombosis: Low field MR experience. Indian J Med Sci 2006;60:135-42.
7. Goyal G, Singh R, Bansal N, Paliwal VK. Anatomical variations of cerebral MR venography: Is gender matter? Neurointervention 2016;11:92-8.
8. Alper F, Kantarci M, Dane S, Gumustekin K, Onbas O, Durur I. Importance of anatomical asymmetries of transverse sinuses: An MR venographic study. Cerebrovasc Dis 2004;18:236-9.
9. Tantawy HF, Morsy MM, Basha MA, Nageeb RS. Different normal anatomical variations of the transverse dural sinus in magnetic resonance venography (MRV): Do age and sex matter? Eur J Anat 2020;24:49-56.
10. Shırodkar K, Reddy S, Dasappa N, Nandikoor S, Kumar GGS, Mallarajapatna G, editors. Assessment of Anatomical Variations in Cerebral Venous System Using Non Contrast Magnetic Resonance Venography 2017:European Society Of Radiology. European Congress Of Radiology: 2017. Poster no:C-2612 Available from https://epos.myesr.org/poster/esr/ecr2017/C-2612 DOI 10.1594/ecr/2017/C-2612. [Last accessed on 2020 Oct 14].
11. Ayanzen RH, Bird CR, Keller PJ, McCully FJ, Theobald MR, Heiserman JE. Cerebral MR venography: Normal anatomy and potential diagnostic pitfalls. AJNR Am J Neuroradiol 2000;21:74-8.
12. Sharma UK, Sharma K. Intracranial MR venography using low-field magnet: Normal anatomy and variations in Nepalese population. J Nepal Med Assoc 2012;52:61-5.
13. Lin L, Lin JH, Guan J, Zhang XL, Chu JP, Yang ZY. Falcine sinus: Incidence and ımaging characteristics of three-dimensional contrast-enhanced thin-section magnetic resonance ımaging. Korean J Radiol 2018;19:463-9.

Original Article

An Evaluation on the Morphology of the Nasal Bone, Piriform Aperture, and Choana on Dry Skulls

Anil Didem Aydin Kabakci, Duygu Akin Saygin, Şerife Alpa[1], Mustafa Buyukmumcu, Mehmet Tugrul Yılmaz

Department of Anatomy, Meram Faculty of Medicine, University of Necmettin Erbakan, [1]Department of Anatomy, Faculty of Medicine, University of Karatay, Konya, Turkey

Abstract

Introduction: *Piriform aperture (PA) and nasal bone (NBs) are important structures that contribute to the formation of the nose. Both anatomic structures show differences* based on ethnicity, gender, and age. *Hence, it is widely used to determine sex in science branches such as anthropology and forensic medicine. Furthermore,* morphometry of the PA and choana is an important criterion for physiological nasal respiration of individuals. *Recognition of structural differences of PA, NB, and choana along with all this information becomes important during maxillofacial procedures to be performed especially in plastic and reconstructive surgery.* The aim of the present study is to determine the individual differences in NBs, PA, and choana. **Material and Methods:** This *study was conducted on 83 Turkish dried skulls and PA, NBs, and choana was examined as morphometrically. PA was classified into* seven *types and NB was classified into* eight *subtypes.* **Results:** The most common type of PA was found type 5 (20%–24.1%) and the least most common type of PA was type 7 (4%–4.8%). *Type 1 was determined as the most common observed shape of the NB. The mean width of the choana on the right and left sides was found 13.21 ± 1.4 and 13.98 ± 1.81 mm, respectively. Moreover, the mean height of the choana on the right and left sides was found 25.56 ± 3.06 and 26.1 ± 2.5 mm, respectively.* **Discussion and Conclusion:** We believe that obtained data from our study will constitute a morphometric data set and will be useful in a wide range of fields from forensic science to reconstructive surgery.

Keywords: *Choana, morphometry, nasal bone, piriform aperture, variation*

Introduction

The piriform aperture (PA) and nasal bones (NBs) are important structures that contribute to the formation of facial structures. Morphological features of the PA and NBs are widely used in different areas, such as nasal reconstruction, rhinoplasty, and for surgical or aesthetic purposes. Further, they can be used in forensic facial reconstruction, which is a method used to identify the dead and determine sex for anthropological purposes.[1] Furthermore, the structure of the NB and the PA for physiological respiration is as important as the morphological structure of the choana and the length of the airway.[2]

The NB is an important structure in the center of the face. It is surrounded by the frontal bone on the superior. The superior margin of the NB is narrow, thick, and wavy, and articulated with the nasal notch of the frontal bone. The inferior margin of the NB is thin. This inferior margin clings to the lateral cartilages of the nose. The lateral margin of the NB is redented for articulation with the frontal process of the maxilla. The medial margin articulates with NB on the other side and superior this margin is thicker. The vertical part of the medial margin extending posteriorly is articulated with the spine of the frontal, the perpendicular plate of the ethmoid bone, and the septal cartilage of the nose.[2-4] The nose has three vaults, including the bony, upper cartilaginous, and lower cartilaginous vaults. The shape of the bony vault (comprising of paired NBs and the frontal process of the maxilla) is usually pyramidal and forms one-third of the external nose.[3-6]

The PA is located at the most anterior side of the bony nasal airway[7] and it is generally pear-shaped and surrounded by the NBs on the top, the frontal process of the maxilla on the left and right sides, and the palatine process of the maxilla below.[1] The region of the PA is the narrowest portion of the

How to cite this article: Kabakci AD, Akin D, Alpa S, Buyukmumcu M, Yilmaz MT. An evaluation on the morphology of the nasal bone, piriform aperture, and choana on dry skulls. J Anat Soc India 2020;69:XX-XX.

Article Info

Received: 16 January 2020
Accepted: 28 September 2020
Available online: ***

Address for correspondence:
Dr. Anil Didem Aydin Kabakçi, Department of Anatomy, Meram Faculty of Medicine, University of Necmettin Erbakan, 42080 Meram, Konya, Turkey.
E-mail: anil_didem_aydin@hotmail.com

Access this article online

Website: www.jasi.org.in
DOI: 10.4103/JASI.JASI_6_20
Quick Response Code:

bony nasal airway, and this region constitutes 2/3 of the total nasal resistance in the bony cavum.[8]

All surgical procedures in this region should be performed on the basis of NBs and PA differences. Rhinoplasty is a surgical procedure that should have as little margin of error as possible. Anatomical structural differences should be taken into account in surgeries performed in this area. Similarly, osteotomies are widely used for narrowing or widening the nasal base, improving bone deformities, and repairing open-roof deformities. NB osteotomies (especially lateral osteotomy) may be performed safely at the transition zone that exists along the frontal process of the maxilla from the PA to the radix, along the lateral nasal wall. Because of the fragmentation risk, osteotomies may be more difficult in patients who have short NBs.[3-6] A detailed understanding of the structure and function of the nasal region is critical for providing proper treatment. Besides knowing where the anatomical differences are, it is important to know how they contribute to clinical procedures. Thus, we aimed to determine if there is any difference in the NB, PA, and choana that may affect structurally the nasal respiration.

Material and Methods

Our study was performed with 83 Turkish dried skulls obtained from the bone collection at Necmettin Erbakan University and Karatay University. Permissions were obtained from Karatay University's, Pharmaceuticals, and Non-Medical Devices Research Ethics Board (2016/012). A digital caliper was used for skull measurements including the height of the NBs at the midpoint (HNB), the lateral edge height of the right NB (HNB-R), the lateral edge height of the left NB (HNB-L), the width of the NB at the top (WNBT), the width of the NB at the bottom (WNBB), the width of the right NB (RNB) and left NB (LNB) at the midpoint (WRNB and WLNB, respectively), the apex width of the PA (AWPA), the width of the PA at the level of the lower ends of the NBs (WPAT), the width of the PA at the bottom (WPAB), the height of the PA (HPA), the distance between the nasion and anterior nasal spine (N-ANS), the width of the right and left choana (CW1, CW2) at the level of the midpoint of the posterior bony aperture of the choana and the height of the right and left choana (CH1, CH2). The shape of the NBs and PA were classified.

A new classification derived from the Lang and Baumeister[9] classification was used for NB typing. NBs were classified into eight subtypes.

- Type 1 and Type 3: There is an angulation which becomes narrower from the edges toward the midline at the bottom. If the transverse thickness of the bone on the midline is greater than 4 mm, it is called type 1. If the thickness is lower than 4 mm, it is called type 3
- Type 2 and Type 6: There is an angulation which becomes narrower from the edges toward the midline on the top of the NB. If the transverse thickness of the bone is greater than 4 mm, it is called type 2. If the thickness is lower than 4 mm, it is called type 6
- Type 4 and Type 8: There is no angulation. Nasomaxillary sutures are parallel to each other on the midline. If the transverse thickness of the bone is greater than 8 mm, it is called type 8. If the thickness is lower than 4 mm, it is called type 4
- Type 5: There was an angulation at the midpoint of the NB
- Type 7: There was no angulation. The NB is wider at the bottom and narrower on the top [Figures 1-3].

The PA was classified into seven types, including 1-Pear shape, 2-Reverse heart shape, 3-Rhomboid shape, 4-Drop shape, 5-Ellipsoid shape, 6-Trapezoid shape, and 7-Round shape [Figures 4 and 5].

Statistical analysis

All data were evaluated using SPSS 21.0 (Statistical Package for the Social Science; IBM, Chicago, IL, USA). The mean values, standard deviations, maximum and minimum values, and percentages were determined for descriptive analyses. Furthermore, the relationship between RNB and LNB shape and PA shape was analyzed with multiple corresponding analyses.

Results

This study was conducted on 83 dried skulls (unknown gender). The mean values and standard deviations of the parameters of the NBs, PA, and choana were identified and are shown in Table 1. NB forms were categorized into eight subtypes by revising the classification of Lang and Baumeister [Figures 1-3].[9] Type 1 (narrowing from the edges to the midline, angulation at the lower part of the bone, bone mid thickness greater than 4 mm) was the most commonly observed shape of NB [Table 2, and Figures 1, 2a]. Type 3 was the least common type of NB [Table 2, Figure 1 and 2b]. The most common type of PA was Type 5 (ellipsoid shape, 20%–24.1%) and the least common type of PA was Type 7 (round shape, 4%–4.8%) [Table 3, Figures 4 and 5].

The association between shapes of the NB and PA was evaluated through multiple corresponding analyses (SPSS 21.0). The statistical analysis revealed that the shape of the PA tended to be in the form of a reverse heart, ellipsoid, or drop if the left NB was Types 2 or 7. The shape of the PA tended to be in the form of a trapezoid if the left NB was Type 3 or 6. Similarly, it was found that the shape of the PA tended to be in the form of a pear, round, or rhomboid if the left NB was Type 1, 4, or 8. Besides, it was observed that NBs that had an angulation at the midpoint, namely Type 5, did not contribute to the formation of the PA shape [Figure 6].

When the relationship between the RNB and the PA was examined, it was seen that pear and round shaped PA

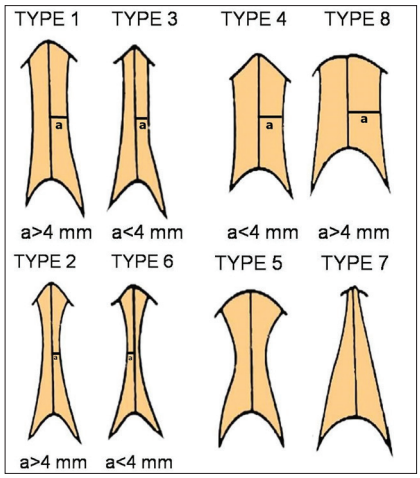

Figure 1: Schmeatic drawing of nasal bone types (Lang and Baumeister[9] classification was revised, a: midline transverse thickness)

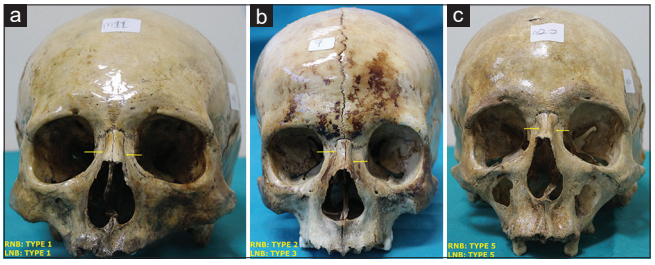

Figure 2: (a) Type 1 NB, (b) Type 2 and 3 NB, (c) Type 5 NB (NB: *Nasal bone*, RNB: Right nasal bone, LNB: Left nasal bone, yellow arrows show angulation level in nasal bones, angulation is in the lower part of the nasal bone in type 1 and type 3, in the upper part of type 2, and in the middle part in type 5)

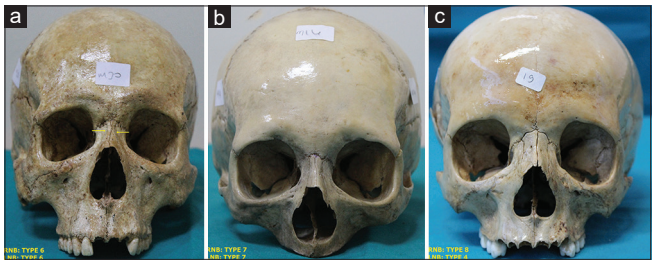

Figure 3: (a) Type 6 NB, (b) Type 7 NB, (c) Type 4 and 8 NB (NB: Nasal *bone*, RNB: Right nasal bone, LNB: Left nasal bone, yellow arrows show angulation level in nasal bones, *angulation is in the upper part of type 6)

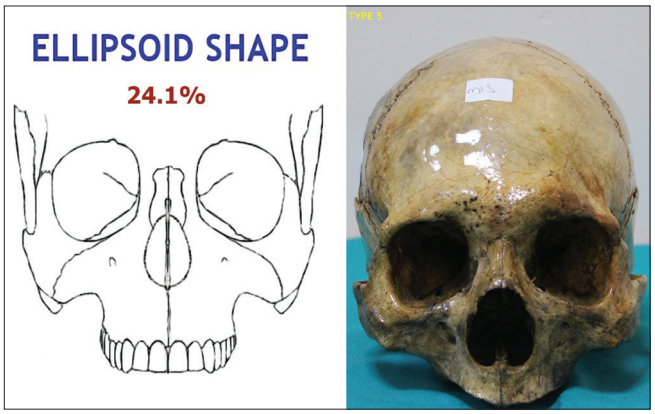

Figure 4: The most common type of piriform aperture (Type 5-Ellipsoid shape)

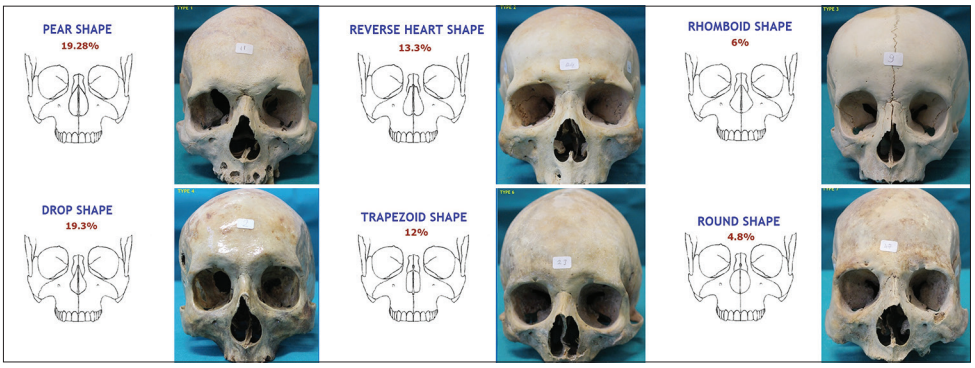

Figure 5: Other types of piriform aperture (pear shape, drop shape, reverse heart shape, trapezoid shape, rhomboid and round shape of piriform aperture)

were present with Type 4 and 7 RNBs. If the RNBs were Type 1 or 8 the PA tended to be in the form of a reverse heart, ellipsoid, or rhomboid. Similarly, if the RNB was in the form of Type 2, the PA tended to be in the form of a drop. In addition, Type 5 and 6 did not contribute to the formation of PA shapes [Figure 7].

Discussion

The NB, PA and choana were evaluated on 83 dried skulls of Turkish origin in this study. The size and morphology of the NB, PA, and choana are variables between different races, ethnic groups, genders, and ages.[6,7,10-14] The differences in these parameters revealed the importance of measurements of NB, PA, and choana in a wide range of fields from forensic medicine to maxillofacial surgery. There are studies that present the bone structure of the nasal through computed tomography (CT) and bone studies in the literature.[1,4,10,15,16-21] Although recent CT studies have gained momentum due to clear gender determination and high resolution, the shapes of the NB due to the angulation with the maxillary bone may be detected.[1]

The nose is located in the central part of the face and is physiologically and esthetically important. Esthetic and functional nasal surgeries are performed in plastic

Table 1: Maximum, minimum, mean values and standard deviations of the nasal bone, piriform aperture, and choana parameters (*n*: skull number, mm)

	n	Minimum	Maximum	Mean±SD
HNB	83	12.55	32.87	21.5±3.76
HNB-R	83	11.73	32.67	24.05±3.74
HNB-L	83	13.72	31.11	23.66±3.83
WNBT	83	6.52	18.08	12.65±2.68
WNBB	83	11.34	23.51	16.74±2.63
WRNB	83	3.69	12.18	7.73±1.69
WLNB	83	3.77	10.90	7.58±1.7
AWPA (width 1)	83	7.65	20.50	11.99±2.6
WPAT (width 2)	83	10.70	27.41	20.24±2.97
WPAB (width 3)	83	20.23	31.37	24.27±2.13
HPA	83	19.10	42.90	28.63±4.58
N-ANS	83	24.27	60.31	50.81±4.91
CW1	77	10.11	16.67	13.21±1.4
CW2	77	10.08	21.13	13.89±1.81
CH1	77	15.31	34.65	25.56±3.06
CH2	77	19.88	31.38	26.1±2.5

PA: Piriform aperture, HNB: The height of nasal bone at the midpoint, HNB-R: The lateral edge height of right nasal bone, HNB-L: The lateral edge height of left nasal bone, WNBT: The width of nasal bone at the top, WNBB: The width of nasal bone at the bottom, WRNB: The width of the right nasal bone at the midpoint, WLNB: The width of the left nasal bone at the midpoint, AWPA: The apex width of PA, WPAT: The width of the PA at the level of the lower ends of the nasal bones, WPAB: The width of PA at the bottom, HPA: The height of PA, N-ANS: The distance between nasion and anterior nasal spine, CW1, CW2: The width of the right and left choana, CH1, CH2: The height of right and left choana, SD: Standard deviation.

Table 2: Nasal bone types (%)

Type	Left, *n* (%)	Right, *n* (%)
Type 1	32 (38.6)	32 (38.6)
Type 2	22 (26.5)	19 (22.9)
Type 3	2 (2.4)	0 (0)
Type 4	6 (7.2)	6 (7.2)
Type 5	1 (1.2)	3 (3.6)
Type 6	2 (2.4)	2 (2.4)
Type 7	6 (7.2)	4 (4.8)
Type 8	12 (14.5)	17 (20.5)
Total	83 (100)	83 (100)

Table 3: Piriform aperture types (%)

PA	*n* (%)
Pear shape (Type 1)	17 (20.5)
Reverse heart shape (Type 2)	11 (13.3)
Rhomboid shape (Type 3)	5 (6)
Drop shape (Type 4)	16 (19.3)
Ellipsoid shape (Type 5)	20 (24.1)
Trapezoid shape (Type 6)	10 (12)
Round shape (Type 7)	4 (4.8)
Total	83 (100)

PA: Piriform aperture

surgery procedures worldwide.[4] Two-thirds of the nose isstructurallyimmobile and is comprised two separate anatomic parts, including the bony (upper) vault and the cartilaginous (middle) vault. The anatomical structure of the nasal region may be deformed after rhinoplasty procedures. Surgeons should be aware of the anatomical structure of the nasal region and the possible conditions of the nasal region to avoid potential risks (nasal valve obstructions-middle vault collapse). The incidence of collapse on the middle vault was higher in patients with shorter NBs, longer, weaker or upper lateral cartilages, and thinner skin compared to patients with longer NBs. The knowledge of the morphometric measures in the nasal region is of relevance for surgical procedures such as rhinoplasty, osteotomies, and aesthetic reconstructions.[22]

The most remarkable findings in NB measurements of this study that the mean NB width was 12.65 mm at the proximal location and the lateral side edges of the NBs stretched down, becoming concave at the midpoint (approximately 7.66 mm) [Table 1]. In comparison to other studies conducted on Turkish populations, it was observed that the NB height in our study was higher in the data obtained from the studies of Kaplanoglu *et al*.[15] and Yuzbasioglu *et al*.,[1] but lower than the data obtained from Karadag *et al*.[20] Our findings were consisted with the data of Uygur *et al*.[24] In this study, the NB height has been found lower than German, Austrian, Black American, Korean, and Iranian populations. Especially, this height was found to be higher than the Indian population [Table 4]. The NB width on the midpoint was lower than German, Korean, Indian population and also than in the Turkish population in the study of Yuzbasioglu *et al*.[1] [Table 4]. This finding confirms that the NB has a more concave structure toward the midline in our population.

The NB shape was categorized into eight types in the German population (79 dried skulls) by Lang and Baumeister.[9] Although the Lang and Baumeister[9]'s classification is quite wide, it is considered complex by some authors. Thus, other researchers have revised the classification into five types.[4,16-18] Type B and Type A were most common (52.3% and 43.2%, respectively-88 dried skulls from Korean adults) according to Hwang *et al*.[4] Similarly, Prado *et al*.[16] found that the most common type of NB was A (28.6% for female, 20.6% for male), while D (1% for female, 1% for male) was the least common type in both genders. They also emphasized that there was a significant difference between sexes. Asghar *et al*.[17] stated that the most common types of NB were Type A (45%) and Type C (20%), followed by Type B (15%), Type E (15%), and Type D (5%), without any significant sexual variation (P = 0.1443). It was emphasized that the Type A and Type B were the most common types of NBs in the most comprehensive studies about Turkish NB classifications which were performed by Yuzbasioglu *et al*.[1] and Kaplanoglu *et al*.[15] According to this classification, the most common NB types were Types

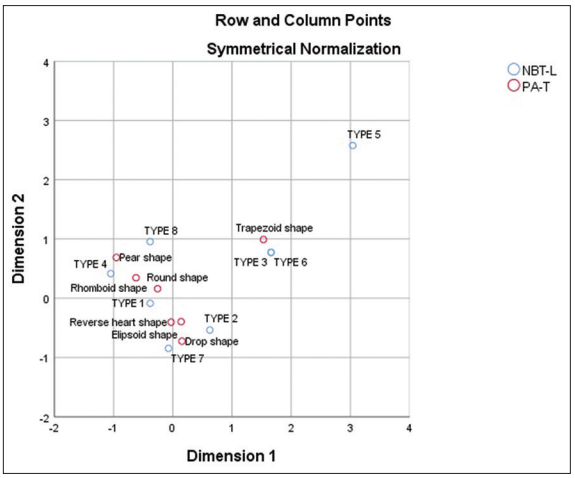

Figure 6: The multiple corresponding analysis graphic of the left nasal bone and piriform aperture

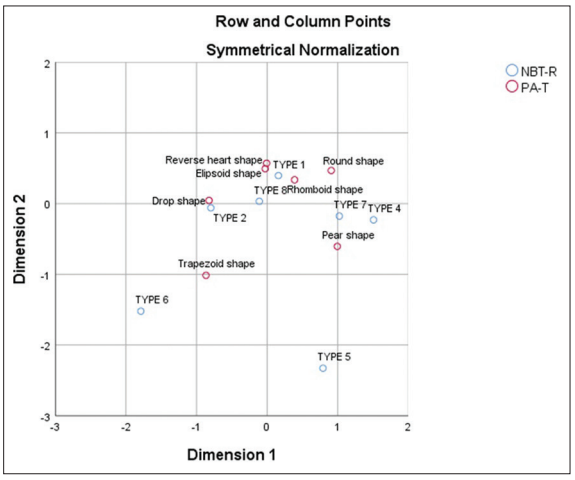

Figure 7: The multiple corresponding analysis graphic of the right nasal bone and piriform aperture

A (39.76%), B (27.11%), and E (24.7%), respectively. Unlike other researchers, type E has a significant value with a percentage of 24.7 [Table 5] [The types corresponding to type A, B, C, D, and E are given as an explanation at the bottom of Table 5]. When compared with other studies conducted on Turkish populations, type A was higher in this study than the data obtained by Kaplanoglu *et al*.[15] and Yuzbasioglu *et al*.,[1] but lower than the data obtained by Uygur *et al*.[24]

Anthropological studies have emphasized that nasal structures of individuals belonging to races living in different geographies are adapted for warming and moistening of inspired air. The length of the nasal airway is increased and the base is narrowed in colder and drier climates. Depending on the increase on the surface area, the period for warming and moistening of the inspired air is longer.[19] Hwang *et al*.[4] has been reported that the shape and size of the PA may be affected by environmental conditions.[4,15,16] Furthermore, morphological differences and dimensions of the PA have been reported as an important sex indicator. PA size and shape may be used as an anatomical landmark for determination of ethnic differentiation.[1,16] PA is a variant opening in terms of shape. These differences also affect the width and height of the opening. Therefore, the width measurement was performed on three different regions, including the apex, upper and lower part in this study.

Our study showed that the width of the PA ranged from 20–32 mm (the mean PA width was 24.27 mm) [Tables 1 and 4]. When compared with other studies conducted on the Turkish populations, it was observed that the PA width in our study was found consistent with the data of Aksu *et al*.,[2] Yuzbasioglu *et al*.[1] and Uygur *et al*.,[24] but also higher than the data obtained by Karadag *et al*.[20] In addition, the PA width data was similar to other races; however, it was found significantly larger than the study of Lopez *et al*.[25] [Table 4]. The mean PA height was found 28.63 mm in our study.

This data were lower than the findings of other researchers. This finding supports the ellipsoid shape, which was the most common PA shape observed in our study [Table 4].

Ofodile[19] emphasized that the PA was oval in the Ashanti population, triangular in White and Indian populations, and varied from oval to triangular in American individuals. Prescher *et al*.[30] evaluated 84 human skulls anthropologically. They declared that the PA area was larger in males and the shape of the PA was pear-shaped in both genders. Yuzbasioglu *et al*.[1] found the most common type of PA was Type 1 (pear-shape). Asghar *et al*.[17] and Durga *et al*.[18] classified the PA into four types (1-long and narrow, 2-triangular, 3-triangular to oval, and 4-tending to roundness), based on the shape and the PA index. Asghar *et al*.[17] and Durga *et al*.[18] found the most common PA type to be Type 3 (83.5% for Asghare *et al*.[17] and 45.09% for Durga *et al*.[18]). De Araújo *et al*.[21] stated that the most common PA shape was pear-shape (39.1%). Yuzbasioglu *et al*.[1] classification system was used in our study and the ellipsoid-shape (Type 5, 24.1%) was the most common PA aperture type [Table 3 and Figure 4].

Moreover, choana is the convex structure where the airflow passes from the posterior cavum to the nasopharynx. Therefore, choana width and length measurements are important parameters for NB and PA to warm and moisten the inspired air. The choana width at the level of the midpoint of the posterior bony aperture of the choana and choana height was found to be 13.21 ± 1.4 mm, 13.89 ± 1.81 mm, and 25.56 ± 3.06 mm, 26.1 ± 2.5 mm for the right and left side, respectively [Table 1]. Aksu *et al*.[2] determined this rate 13.09 ± 1.56 mm, 13.33 ± 1.36 mm and 24.45 ± 2.61 mm, 23.77 ± 2.42 mm, respectively.

Conclusion

This study provided information about the morphological structures of the NB, choana, and PA in the Turkish

Table 4: The comparison of the nasal bone and piriform aperture measurements according to the researchers (mm)

	Sample	The height of nasal bone at the midpoint	Nasal bone width	PA height	PA width 1	PA width 2	PA width 3
Lang and Baumeister[9]	German	24.9	13	29.1	-	16.3	23.6
Ofodile[19]	Austrian	30.2	-	-	-	-	21.6
Ofodile[19]	Black American	27.9	-	-	-	-	23.4
Hommerich and Riegel[23]	German	-	-	-	-	15.7	23.1
Hwang *et al*.[4]	Korean	25.2	9*	29.05	-	16.9	25.55
Uygur *et al*.[24]	Turkish	21.02	-	35.95	-	15.37	23.99
Lee *et al*.[10]	Korean	20.95	-	-	-		24.01
López *et al*.[25]	Brazilian	-	-	49.18	-	17.41	12.64
Karadag *et al*.[20]	Turkish	29.81	-	-	-	-	18.5
Prado *et al*.[16]	Brazilian	-	-	47.5	-	-	32.5
Aksu *et al*.[2]	Turkish	-	-	33.03	-	-	23.24
Moreddu *et al*.[26]	French	-	-	34.45	-	-	24.66
Nidugala *et al*.[27]	Indian	19.37	24.03**	-	-	-	-
Zamani Naser and Panahi Boroujeni[28]	Iranian	24.6	-	-	-	-	24.47
Yüzbaşioğlu *et al*.[1]	Turkish	18	11.9*	31.7	-	-	23.9
Roy *et al*.[7]	Caucasian	-	-	-	-	-	21.56
Abdelaleem *et al*.[29]	Egyptian	-	-	36.68	-	-	28.81
Asghar *et al*.[17]	Indian	17.58	12.2***	30.37	-	-	23.84
Kaplanoglu *et al*.[15]	Turkish	17.5	-	36.76	-	-	23.41
De Araújo *et al*.[21]	Brazilian	-	-	30.4	-	-	25.7
Durga *et al*.[18]	Indian	16.85	11.68***	29.2	-	16.1	24.22
Our study	Turkish	21.5	7.66***	28.63	11.99	20.24	24.27

*This measurement was taken from the top point of each side of nasal bones, **This width is a total breadth of each nasal bone at the midpoint, ***This width is a breadth that was taken from the midpoint of nasal bone. PA: Piriform aperture

Table 5: Nasal bone types according to some researchers (%)

Researchers	Sample	Type A (%)	Type B (%)	Type C (%)	Type D (%)	Type E (%)
Lang and Baumeister[4]	German population	68.3	10.1	1.3	10.1	10.1
Hwang *et al*.[3]	88 dried skulls (Korean population)	43.2	52.3	4.5	0	0
Uygur *et al*.[24]	38 cranium skeleton (Turkish population)	63.16	7.89	5.26	5.26	18.43
Lee *et al*.[10]	75 patients' CT images (Korean population)	53.41	14.77	17.05	0	0
Prado *et al*.[16]	97 individual's radiographs (Brazilian population)	49.48	27.84	13.40	2.06	7.22
Yüzbaşioğlu *et al*.[1]	120 MDCT images (Turkish population)	38.33	30	3.33	9.17	19.17
Asghar et al.[17]	40 dried skulls (Indian population)	45	15	20	5	15
Kaplanoglu *et al*.[15]	363 patients' CT images (Turkish population)	26.7	27.8	10.5	19.6	15.4
Durga *et al*.[18]	51 dried skulls (South Indian population)	35.2	19.6	17.6	15.6	11.7
Our study	83 dried skulls (Turkish population)	39.76	27.11	6.02	2.41	24.7

Type 1 and 3: Type A, Type 2 and 6: Type B, Type 7: Type C, Type 5: Type D, Type 4 and 8: Type E, CT: Computed tomography, MDCT: Multidetector CT

population. The anatomic data presented in this study on the width of the PA correlated with other studies. Compared to other investigators, we observed significant changes in the form of NBs. The data obtained from this study show a data series belonging to the Turkish population. Anatomical structures of races should be well-known to reduce postoperative complications and plan appropriate surgical techniques. We believe that results obtained from this study may provide information for selection of osteotomes in adequate sizes, procedures of corrective rhinoplasty, PA augmentation and resection.

Acknowledgment

This study conformed to the Helsinki Declaration. Permissions were obtained from Karatay University's, Pharmaceuticals and Non-Medical Devices Research Ethics Board (2016/012).

Financial support and sponsorship

Nil.

Conflicts of interest

There are no conflicts of interest.

References

1. Yüzbaşioğlu N, Yilmaz MT, Çicekcibasi AE, Şeker M, Sakarya ME. The evaluation of morphometry of nasal bone and pyriform aperture using multidetector computed tomography. J Craniofac Surg 2014;25:2214-9.
2. Aksu F, Mas NG, Kahveci O, Çırpan S, Karabekir S. Piriform Aperture and Choana Circles: An Anatomic Study. Dokuz Eylül Üniversitesi Tıp Fakültesi Dergisi 2013;27:1-6.
3. Rohrich RJ, Adams WP, Ahmad J, Gunter J. Dallas Rhinoplasty: Nasal Surgery by the Masters. CRC Press Taylor and Francis Group Publisher;2014.
4. Hwang TS, Song J, Yoon H, Cho BP, Kang HS. Morphometry of the nasal bones and piriform apertures in Koreans. Ann Anat 2005;187:411-4.
5. Ozturk C, Ozturk CN, Uygur S, Sullivan TB, Bozkurt M, Huettner F, *et al*. Craniometric analysis of the nasal skeleton and midface in Caucasian population. Eur J Plast Surg 2017;40:499-506.
6. Setabutr D, Sohrabi S, Kalaria S, Gordon K, Fedok FG. The relationship of external and internal sidewall dimensions in the adult Caucasian nose. Laryngoscope 2013;123:875-8.
7. Roy S, Iloreta AM, Bryant LM, Krein HD, Pribitkin EA, Heffelfinger RN. Piriform aperture enlargement for nasal obstruction. Laryngoscope 2015;125:2468-71.
8. Papesch E, Papesch M. The nasal pyriform aperture and its importance. Otolaryngol Head Neck Surg 2016;1:89-91.
9. Lang J, Baumeister R. Postnatal growth of the nasal cavity. Gegenbaurs Morphol Jahrb 1982;128:354-93.
10. Lee SH, Yang TY, Han GS, Kim YH, Jang TY. Analysis of the nasal bone and nasal pyramid by three-dimensional computed tomography. Eur Arch Otorhinolaryngol 2008;265:421-4.
11. Anderson KJ, Henneberg M, Norris RM. Anatomy of the nasal profile. J Anat 2008;213:210-6.
12. Palhazi P, Daniel RK, Kosins AM. The osseocartilaginous vault of the nose: Anatomy and surgical observations. Aesthet Surg J 2015;35:242-51.
13. Lazovic GD, Daniel RK, Janosevic LB, Kosanovic RM, Colic MM, Kosins AM. Rhinoplasty: The nasal bones-anatomy and analysis. Aesthet Surg J 2015;35:255-63.
14. Yaremchuk MJ, Vibhakar D. Pyriform aperture augmentation as an adjunct to rhinoplasty. Clin Plast Surg 2016;43:187-93.
15. Kaplanoglu H, Coskun H, Toprak U. Computed tomography evaluation of nasal bone and nasal pyramid in the turkish population. J Craniofac Surg 2017;28:1063-7.
16. Prado FB, Caldas RA, Rossi AC, Freire AR, Groppo FC, Caria PH, *et al*. Piriform aperture morphometry and nasal bones morphology in Brazilian population by postero-anterior Caldwell radiographys. Int J Morphol 2011;29:393-8.
17. Asghar A, Dixit A, Rani M. Morphometric study of nasal bone and piriform aperture in human dry skull of Indian origin. J Clin Diagn Res 2016;10:AC05-7.
18. Durga D, Archana R, Johnson W. Morphometric study of nasal bone and piriform aperture in human dry skull of South Indian origin. Int J Anat Res 2018;6:5970-73.
19. Ofodile FA. Nasal bones and pyriform apertures in blacks. Ann Plast Surg 1994;32:21-6.
20. Karadag D, Ozdol NC, Beriat K, Akinci T. CT evaluation of the bony nasal pyramid dimensions in Anatolian people. Dentomaxillofac Radiol 2011;40:160-4.
21. De Araújo TM, da Silva CJ, de Medeiros LK, Estrela YD, Silva ND, Gomes FB, *et al*. Morphometric analysis of piriform aperture in human skulls. Int J Morphol 2018;36:483-7.
22. Citardi MJ, Hardeman S, Hollenbeak C, Kokoska M. Computer-aided assessment of bony nasal pyramid dimensions. Arch Otolaryngol Head Neck Surg 2000;126:979-84.
23. Hommerich CP, Riegel A. Measuring of the piriform aperture in humans with 3D-SSD-CT-reconstructions. Ann Anat 2002;184:455-9.
24. Uygur M, Ertürk M, Akcan A, Kayalıoğlu G. Apertura piriformis ve os nasale'nin morfometrik özellikleri. Göztepe Tıp Dergisi 2006;4:174-7.
25. López MC, Galdames IC, Matamala DA, Smith RL. Sexual dimorphism determination by Piriform aperture morphometric analysis in Brazilian human skulls. Int J Morphol 2009;27:327-31.
26. Moreddu E, Puymerail L, Michel J, Achache M, Dessi P, Adalian P. Morphometric measurements and sexual dimorphism of the piriform aperture in adults. Surg Radiol Anat 2013;35:917-24.
27. Nidugala H, Bhargavi C, Avadhani R, Bhaskar B. Sexual dimorphism of the craniofacial region in a South Indian population. Singapore Med J 2013;54:458-62.
28. Zamani Naser A, Panahi Boroujeni M. CBCT evaluation of bony nasal pyramid dimensions in iranian population: A comparative study with ethnic groups. Int Sch Res Notices 2014; 2014:1-5.
29. Abdelaleem SA, Younis RH, Kader MA. Sex determination from the piriform aperture using multi slice computed tomography: Discriminant function analysis of Egyptian population in Minia Governorate. Egypt J Forensic Sci 2016;6:429-34.
30. Prescher A, Meyers A, Gerf von Keyserlingk D. Neural net applied to anthropological material: A methodical study on the human nasal skeleton. Ann Anat 2005;187:261-9.

Original Article

Morphological and Morphometric Study of the Acetabulum of Dry Human Hip Bone and Its Clinical Implication in Hip Arthroplasty

Archana Singh, Rakesh Gupta, Arun Singh[1]

Departments of Anatomy and [1]Community Medicine, Rohilkhand Medical College and Hospital, Bareilly, Uttar Pradesh, India

Abstract

Introduction: The objective was to study the morphology of the acetabular margin and articular surface and to measure the various dimensions of the acetabulum in dry human hip bones. **Material and Methods**: A cross-sectional morphological and morphometric study was performed on 92 undamaged acetabulum of adult dry human hip bone of unknown age and gender. The shape of anterior margin of the acetabulum and shape of the anterior and posterior ends of the articular surface of the acetabulum were observed. Morphometry was done using a Vernier caliper of accuracy of 0.01 mm. Vertical diameter (VD), transverse diameter (TD), anteroposterior diameter (APD), internotch distance (ND), and depth of the acetabulum were measured. Surface area (SA) and volume (V) of the acetabulum were calculated by mathematical calculation of dome. Statistical analysis was done using SPSS software version 22.0 (IBM, SPSS statistics, UNICOM GLOBAL, California, United States). The Pearson's correlation test was used. **Results:** In the present study, the anterior acetabular ridge was curved in 45.7% (42), angulated in 26.17% (24), straight in 13% (12), and irregular in 13% (12) bones. The anterior end of the lunate articular surface was angulated, and the posterior end was lunate in shape in 45.7% (42), whereas in 54.3% (50), bone both the ends were lunate in shape. Morphometric values and mean ± standard deviation were as follows: 48.21 mm ± 3.31 mm (VD), 47.81 mm ± 3.37 mm (TD), 48.79 mm ± 4.08 mm (APD), 23.58 mm ± 2.77 mm (ND), 27.45 mm ± 3.02 mm (D), 4162.56 mm^2 ± 755.58 (SA), and 36,563.65 mm^3 ± 9408.67 (V). **Discussion and Conclusion:** The knowledge of these acetabular parameters is necessary for the creation of acetabular prosthesis and surgical procedures such as acetabular reconstruction in hip joint surgeries.

Keywords: *Acetabular prosthesis, acetabulum, lunate articular surface*

Introduction

The acetabulum is a cup-shaped cavity present on the lateral side of the hip bone. In Latin, the meaning of the acetabulum is a shallow vinegar cup.[1] Acetabulum articulates with the head of the femur to form the hip joint which is a ball-and-socket variety of synovial joint. The acetabulum has a lunate articular surface and a nonarticular fossa on the center of the floor of the acetabulum. The lunate articular surface is covered by hyaline cartilage, and the acetabular fossa is filled with fibroelastic fat and covered with the synovial membrane. All the three bones such as ileum, ischium, and pubis contribute to form the acetabulum. The pubis forms the anterior one-fifth, the ileum forms posterosuperior two-fifth, and the ischium forms posteroinferior two-fifth of the acetabulum. The articular surface is deficient inferiorly, known as the acetabular notch, and is bridged by transverse acetabular ligament. The depth of acetabulum (DH) is increased by the attachment of fibrocartilaginous rim known as acetabulum labrum. It holds the femoral head and maintains the joint stability.[2]

Anterior acetabular ridge's morphology is helpful in the diagnosis of congenital acetabular dysplasia and during acetabular surgeries. Previous studies evaluate the anterior acetabular ridge morphology.[3-5]

The diameters and DH are valuable for surgical treatments like total hip arthroplasty. It will also helpful to the anthropologist in determining the gender, and it is also enlightening to the radiologist and prosthetist. According to Kulkarni,[6] the acetabulum is divided into three zones to find the degree of slacking of the acetabulum.

How to cite this article: Singh A, Gupta R, Singh A. Morphological and morphometric study of the acetabulum of dry human hip bone and its clinical implication in hip arthroplasty. J Anat Soc India 2020;69:XX-XX.

Article Info

Received: 06 November 2020
Accepted: 22 May 2020
Available online: ***

Address for correspondence:
Dr. Archana Singh, Department of Anatomy, Rohilkhand Medical College and Hospital, Bareilly, Uttar Pradesh, India.
E-mail: drarchana279@gmail.com

Access this article online

Website: www.jasi.org.in
DOI: 10.4103/JASI.JASI_214_19
Quick Response Code:

Because of variation in the shape of the acetabulum, the joint congruencies are much frequent even with minor anatomical variations.[7] Incongruencies of joint may be prone to the degenerative changes in comparison to the normal joint anatomy.[8]

Aims and objectives

Aim

The aim was to know the morphological features of the acetabulum and to measure various dimensions of the acetabulum in dry human hip bone.

Objectives

To observe the shape of anterior margin and lunate articular surface of the acetabulum, to measure the various parameters and to calculate the surface area (SA) and volume (V) of acetabulum. To find the correlation between depth and V and depth and SA of acetabulum.

Material and Methods

This cross-sectional study was conducted after getting the permission from the institutional ethics committee. A total of 92 dry adult human hip bones of unknown gender were taken from the Department of Anatomy of Medical College of Uttar Pradesh. The following morphological and morphometric parameters were recorded.

Morphological features were as follows:

1. Anterior acetabular ridge: [9] the shape of ridge was evaluated and classified as curved, straight, angular, and irregular
2. Ends of lunate surface: [9] the shape of anterior and posterior ends of the lunate surface was noted as curved or angular (pointed).

Morphometric parameters were as follows: measured by a digital Vernier caliper in millimeters [Figures 1 and 2].

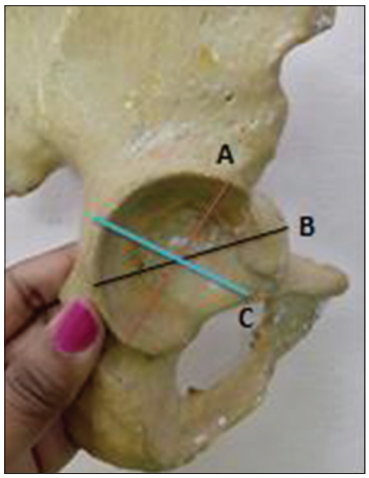

Figure 1: Morphometric measurements of the acetabulum; (A) vertical diameter, (B) transverse diameter, (C) anteroposterior diameter

1. Vertical diameters (VDs): farthest distance on the acetabular margin in vertical plane (at the line from the anterior superior iliac spine to the most prominent point on the ischial tuberosity)[10]
2. Transverse diameters (TD): farthest distance on acetabular rim in horizontal plane[10]
3. Anteroposterior diameter (APD): farthest distance on acetabular rim in anteroposterior axis[10]
4. DH: thin metallic scale was placed across the acetabulum. With the help of sliding Vernier caliper, the depth was measured[10]
5. Width of acetabular notch distance (ND): distance between the two ends of lunate articular surface.
6. SA and V: measurement of SA and V of acetabular cavity was challenging. SA and V were calculated by mathematical formulas for dome.

Mathematical calculations of a dome (the hemispherical concavity of the radial head) are as follows: [Figure 2].

Formulas:[11] $\boldsymbol{SA = \pi\,(h^2 + r^2)}$

$\boldsymbol{v = 1/6\pi h\,(3r^2 + h^2)}$

Results

Out of the total 92 hip bones, 42 were of the right side and 50 were of the left side. The acetabular anterior margin was found to be curved in 45.7% (57.1% in the right side and 36% in the left side), angulated in 26.1% (23.8% in the right side and 28% in the left side), straight in 15.2% bones (14.3% in the right side and 16% in the left side), and irregular in 13% acetabulum (4.8% in the right side and 20% in the left side) [Figure 3]. The anterior end of the articular margin was angulated in 45.7% of acetabulum and lunate in 54.3% of bones. The posterior end of the articular margin of the acetabulum was lunate in shape in all the acetabulum [Table 1 and Figure 4].

On morphometry of the acetabulum, the mean VD was 48.21 mm ± 3.31, TD was 47.81 mm ± 3.37 mm, APD

Table 1: Different shapes of the anterior margin of the acetabulum and shape of ends of lunate articular surface of the acetabulum in the present study

	Right (*n*=42), % (*n*)	Left (*n*=50), %(*n*)	Total (*n*=92), % (*n*)
Anterior margin of acetabulum			
Curved	57.1 (24)	36 (18)	45.7 (42)
Angulated	23.8 (10)	28 (14)	26.1 (24)
Straight	14.3 (6)	16 (8)	15.2 (14)
Irregular	4.8 (2)	20 (10)	13 (12)
Anterior end			
Angulated	38.1 (16)	52 (26)	45.7 (42)
Lunate	61.9 (26)	48 (24)	54.3 (50)
Posterior end			
Angulated			
Lunate	100 (42)	100 (50)	100 (992)

Table 2: Morphometric values of the acetabulum of the right side, left side, and total

	Right (*n*=42)		Left (*n*=50)		Total (*n*=92)	
	Mean±SD	Minimum-maximum	Mean±SD	Minimum-maximum	Mean±SD	Minimum-maximum
VD (mm)	48.00±3.56	40.36-53.87	48.38±3.12	43.92-53.99	48.21±3.31	40.36-53.99
TD (mm)	47.43±3.43	41.97-53.54	48.13±3.33	42.12-54.69	47.81±3.37	41.97-54.69
APD (mm)	48.70±4.54	40.79-57.19	48.86±3.68	42.73-57.86	48.79±4.08	40.79-57.86
ND (mm)	23.11±2.70	17.35-29.5	23.98±2.79	19.55-29.86	23.58±2.77	17.35-29.86
DH (mm)	26.73±3.06	22.69-33.21	28.04±2.88	21.68-34.65	27.45±3.02	21.68-34.65
SA (mm^2)	4044.68±801.07	3084.5-5811.42	4261.58±708.08	2926.1-6191.08	4162.56±755.58	2926.1-6191.08
V (mm^3)	55,098.26±9950.5	22,760.72-58142.48	37,794.58±8841.16	21,048.1-63,695.5	36,563.65±9408.67	21,048.1-63,695.5

VD: Vertical diameter, TD: Transverse diameter, APD: Anteroposterior diameter, ND: Notch distance, DH: Depth of acetabulum, SA: Surface area, V: Volume of acetabulum, SD: Standard deviation

Table 3: Comparison of morphometric values of the right and left sides of the acetabulum

	Right	Left	*t*	*P*
Mean diameter (mm±SD)	48.04±3.67	48.23±2.93	0.244	0.809
ND (mm±SD)	23.11±2.7	23.67±2.81	0.876	0.386
Depth (mm±SD)	26.73±3.06	27.96±2.5	1.83	0.073
SA (mm^2±SD)	4044.67±801.07	4208.47±638.18	0.95	0.346
V (mm^3±SD)	35,098.25±9950	37,313.76±7833.98	1.01	0.316

SA: Surface area, V: Volume of acetabulum, SD: Standard deviation

Table 4: Correlation between depth, surface area, and volume of the acetabulum of the hip bone

	Pearson's value	*P*	Significance
Depth versus surface area	0.913	<0.001	Yes
Depth versus volume	0.955	<0.001	Yes
Surface area versus volume	0.945	<0.001	Yes

was 48.79 mm ± 4.08 mm, ND was 23.58 mm ± 2.77 mm, depth was 27.45 mm ± 3.02 mm, SA was 4162.56 mm^2 ± 755.58, and V was 36,563.65 mm^3 ± 9408.67 [Table 2].

On paired *t*-test, there was no significant difference found between the right and left side values [Table 3]. Statistical analysis using Pearson's correlation test proved an existing correlation between depth versus SA, depth versus V, and SA versus V [Table 4].

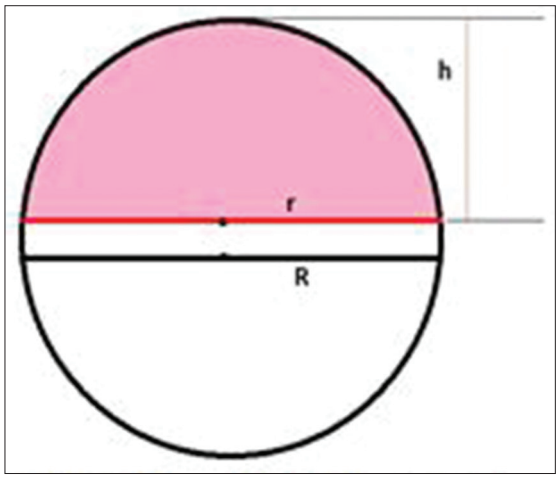

Figure 2: Measurements related to the surface area and volume of the acetabulum; *h* = depth of articular surface = radius of articular surface, *R* = radius of hemisphere

Discussion

Knowledge of morphology of the anterior acetabular ridge is very important for total hip arthroplasty. Posterior acetabular ridge almost always forms a simple semicircle. However, the anterior acetabular ridge shows variations, and because of these variations, the amount of anteversion is affected by the point of measurement along the anterior ridge.[3] In the present study, the most common shape of the anterior margin of the acetabulum was curved, followed by angular, straight, and irregular; similar finding was reported by Thoudam and Chandra,[8] whereas Maruyama *et al*.[3] and Govsa *et al*.[5] reported most common shape as curved, followed by angular, irregular than straight [Table 5].

Anterior and posterior ends of the articular surface were angulated and lunate. In the present study, all posterior

Table 5: Different shapes of the anterior acetabular margin reported by different studies

Shape of anterior margin	Maruyama *et al.* (2001)[3]	Govsa *et al.* (2005)[5]	Aksu *et al.* 2006[12]	Gaurang *et al.* 2014[13]	Thoudam and Chandra 2014[8]	Gangavarapu and Muralidhar 2017[9]	Present study 2019
Curved, % (*n*)	60.50 (121)	43.36 (98)	46.1 (71)	61 (61)	61 (60)	43.75 (35)	45.7 (42)
Angulated, % (*n*)	25.50 (51)	28.33 (64)	16.88 (26)	0	27 (27)	22.56 (18)	26.17 (24)
Straight, % (*n*)	4.50 (09)	11.94 (27)	23.37 (36)	20 (20)	4 (4)	27.5 (220	15.2 (14)
Irregular, % (*n*)	9.50 (19)	16.37 (37)	13.63 (21)	19 (19)	9 (9)	6.2 (5)	13 (12)
Total	200	226	154	100	100	80	92

Table 6: Comparison of shape of the anterior and posterior ends of the lunate surface of the acetabulum

Anterior and posterior ends of articular surface	Yugesh and Kumar 2016[14]	Gangavarapu and Muralidhar 2017[9]	Present study 2019
Anterior end (%)			
Angulated	95.00	85	45.70
Lunate	5	15	54.30
Posterior end (%)			
Angulated	1.70	5	0
Lunate	98.30	95	100

Table 7: Mean diameter and depth of the acetabulum reported by various studies

	Mean diameter (mm±SD)	Mean depth (mm±SD)
Aksu *et al*.[12] (*n*=71)	54.29±3.8	29.49±4.2
Gaurang *et al*.[13]	42.54±3.6	19.07±2.47
Thoudam and Chandra[8]	50.99±1.99	28.32±1.32
Yugesh and Kumar[14]	Right: 47.4±0.23 Left: 48.0±0.37	Right: 29.9±0.21 Left: 29.7±0.23
Gangavarapu and Muralidhar[9]	Right: 49.40±3.5 Left: 48.06±5.65	Right: 24.09±2.69 Left: 25.16±2.84
Khobragade and Vatsalaswamy[18] (*n*=110)	-	26.1±2.83
Salamon *et al*.[16] (*n*=30)	-	30±3.2
Saikia *et al*.[17] (*n*=92)	-	25±8
Present study (*n*=92)	48.27±3.34	27.45±3.02

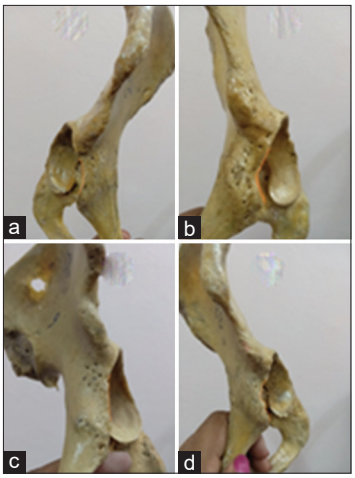

Figure 3: Shape of the anterior acetabular margin; (a) curved, (b) angular, (c) straight, (d) irregular

end was lunate in shape which differed from other findings [Table 6].

The mean diameter of the acetabulum of the present study was 48.27 mm ± 3.34 mm, which was similar with the findings reported by Yugesh and Kumar[14] and Gangavarapu and Muralidhar,[9] whereas Aksu *et al*.[12] and Thoudam and Chandra[8] reported higher values and Gaurang *et al*.[13] reported less value of the mean diameter of the acetabulum [Table 7].

The mean VD, TD, and AP diameter of the acetabulum were measured as 48.21 mm ± 3.31 mm, 47.81 mm ± 3.37 mm, and 48.79 mm ± 4.08 mm, respectively, in the present study, which was almost similar with the findings of the Jadhav *et al*.[15] [Table 8].

DH measured by Yugesh and Kumar[14]and Salamon *et al*.[16] was higher than that of the present study. In the present study, DH was 27.45 mm ± 3.02 mm, which was higher than the findings of Gaurang *et al*.[13] and Saikia *et al*.,[17] whereas findings of Thoudam and Chandra[8] and Khobragade and Vatsalaswamy[18] have similar values of DH as the present study [Table 7].

SA in the present study was calculated by mathematical formulas whereas other studies used different methods to calculate the SAs. Jadhav *et al*.[15] recorded the SA in female as 1900 mm², in male as 2300 mm², and Salamon *et al*.[16] reported 2294 mm² ±329.5. In the present study, SA was 4162.56 mm² ±755.58, which was higher; it may be because of different methods used for measuring the SAs [Table 8].

In the present study, V of the acetabulum was calculated by mathematical formulas, and it was 36,563.65 mm³ (36.56 ml). Other studies used different other methods to measure the V of the acetabulum. Tan

Table 8: Various diameters and surface area of the acetabulum measured by different studies

	Vertical diameter	Transverse diameter	Anteroposterior diameter	Surface area (mm²)
Jadhav *et al*., 2017[15] (*n*=72)	Female: 48±3.9	Female: 46.8±3.2	Female: 48±3.4	Female: 1900
	Male: 52±3	Male: 51.6±3.2	Male: 52±3.6	Male: 2300
Salamon *et al*.[16] (*n*=30)				2294±329.5
Present study (*n*=92)	48.21±3.31	47.81±3.37	48.79±4.08	4162.56±755.58

Table 9: Volume of acetabular cavity measured by different authors

	Volume of acetabulum
Tan *et al*. (*n*=55), 2001[19]	31.5 cm³
Kordelle *et al*. (*n*=32), 2001[20]	26.3 mm³
Chung *et al*. (*n*=17), 2008[21]	14.2 ml
Khobragade and Vatsalaswamy (*n*=100), 2014[18]	20.74 ml
Vivekbabu *et al*. (*n*=40), 2018[22]	Male: 23.13 ml
	Female: 17.88 ml
Present study (*n*=92), 2019	36,563.65 mm³

Table 10: Internotch distance of the acetabulum measured by various authors

	Width of acetabular notch	
	Right side (mm)	Left side (mm)
Yugesh *et al*.[14]	30.8±0.42	31.1±0.72
Gangavarapu *et al*.[9]	22.25±2.97	22.52±2.46
Present study	23.11±2.7	23.67±2.81

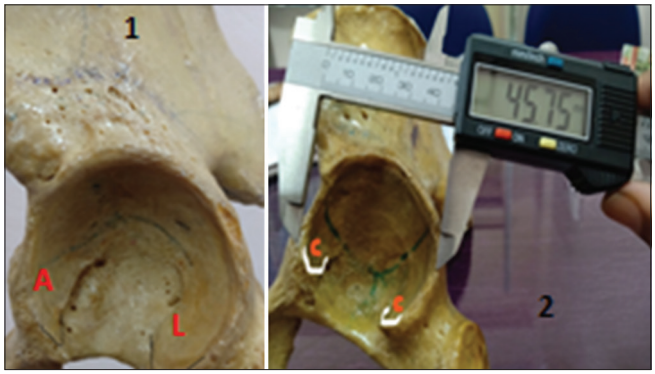

Figure 4: Shape of ends of lunate articular surface. 1 – Anterior end angulated; posterior end lunate 2 – Both ends lunate

et al.[19] measured V which was almost same as the present study (31.5 cm³), whereas other authors such as Kordelle,[20] Chung *et al*.,[21] Khobragade and Vatsalaswamy,[18] and Vivekbabu *et al*.[22] reported less value than the present study [Table 9].

The width of acetabular notch (inter ND) in the present study was measured as 23.58 mm ± 2.77 mm. The finding was similar to the findings of Gangavarapu and Muralidhar.[9] Yugesh and Kumar[14] reported higher values than that of the present study [Table 10].

Conclusion

Clinically, the knowledge of morphology of the anterior acetabular ridge and various dimensions of the acetabulum is very important to orthopedician for hip surgeries and to construct suitable prostheses. The data of the present study may also help the forensic science faculty, orthopedicians, and prosthetists.

Financial support and sponsorship

Nil.

Conflicts of interest

There are no conflicts of interest.

References

1. Last RJ. Lower limb. In: McMinn RM, editor. Last's Anatomy Regional and Applied. 9th ed. New York: Churchill Livingstone; 1996. p. 215-6.
2. Standring S. Pelvic girdle, gluteal region and hip joint. In: Williams A, editor. Grays Anatomy: The Anatomical Basis of Clinical Practice. 39 ed. New York: Elsevier Churchill Livingstone; 2005. p. 1421, 1440.
3. Maruyama M, Feinberg JR, Capello WN, D'Antonio JA. The Frank Stinchfield Award: Morphologic features of the acetabulum and femur: Anteversion angle and implant positioning. Clin Orthop Relat Res 2001;1:52-65.
4. Varodompun N, Thinley T, Visutipol B, Ketmalasiri B, Pattarabunjerd N. Correlation between the acetabular diameter and thickness in Thais. J Orthop Surg (Hong Kong) 2002;10:41-4.
5. Govsa F, Ozer MA, Ozgur Z. Morphologic features of the acetabulum. Arch Orthop Trauma Surg 2005;125:453-61.
6. Kulkarni GS. Surgical anatomy of hip joint. Total Hip Arthroplasty. Textbook of Orthopedics and Trauma. 1st ed. New Delhi: Jaypee Brothers Medical Publishers Pvt. Ltd.; 1999. p. 2910, 3685.
7. Sadler TW. Langman's Medical Embryology. 7th ed. Maryland: Lippincott Williams and Wilkins; 1995. p. 154-60.
8. Thoudam BD, Chandra PX. Actabulaum-morphological and morphometrical study. Res J Pharma Biol Chem Sci 2014;5:793-9.
9. Gangavarapu S, Muralidhar RS. The study of morphology and morphometry of acetabulum on dry bones. Int J Anat Res 2017;5:4558-62.
10. Davivongs V. The pelvic girdle of the Australian aborigine; sex differences and sex determination. Am J Phys Anthropol 1963;21:443-55.
11. Andrei D, Alexander V. Handbook of Mathematics for Engineers and Scientists. 1st ed. Florida: CRC Press; 2006. p. 1544.
12. Aksu FT, Ceri NG, Arman C, Tetik S. Morphology and

morphometry of the acetab-ulum. DEÜ Tip Fakültesi Derg 2006;20:143-8.
13. Gaurang P, Reliab SR, Patel SV, Patel SM, Jethvaa N. Morphology and morphometry of acetabulum. Indian J Biol Med Res 2013;4:2924-6.
14. Yugesh K, Kumar SS. Morphometric analysis of acetabulum and its clinical correlation in South Indian population. IJAR 2016;2:1011-4.
15. Jadhav S, Rokade S, Nomulwar S, Ahire P, Bahetee B. Morphometric study of acetabulum. Appl Physiol Anat Dig 2017;2:26-34.
16. Salamon A, Salamon T, Sef D, Jo-Osvatic A. Morphological characteristics of the acetabulum. Coll Antropol 2004;28 Suppl 2:221-6.
17. Saikia KC, Bhuyan SK, Rongphar R. Anthropometric study of the hip joint in Northeastern region population with computed tomography scan. Indian J Orthop 2008;42:260-6.
18. Khobragade L, Vatsalaswamy P. Morphometric study of depth of acetabulum. Int J Res Med Sci 2017;5:3837-42.
19. Tan V, Seldes RM, Katz MA, Freedhand AM, Klimkiewicz JJ, Fitzgerald RH Jr., *et al*. Contribution of acetabularlabrum to articulating surface area and femoral head coverage in adult hip joints: An anatomic study in cadavera. Am J Orthop (Belle Mead NJ) 2001;30:809-12.
20. Kordelle J, Richolt JA, Millis M, Jolesz FA, Kikinis R. Development of the acetabulum in patients with slipped capital femoral epiphysis: A three-dimensional analysis based on computed tomography. J Pediatr Orthop 2001;21:174-8.
21. Chung CY, Choi IH, Cho TJ, Yoo WJ, Lee SH, Park MS, *et al*. Morphometric changes in the acetabulum after dega osteotomy in patients with cerebral palsy. J Bone Joint Surg Br 2008;90:88-91.
22. Vivekbabu B, Yuvarajbabu K, Ganeshmohanraj K. Morphological and morphometrical analysis of acetabulum with special reference to volume in dry human pelvic bone. Drug Invention Today 2018;10:1921-3.

Original Article

Polymorphic Study of Ataxin 3 Gene in Eastern Uttar Pradesh Population

Barkha Singh, Prasenjit Bose, S. N. Shamal, Deepika Joshi[1], Royana Singh

Departments of Anatomy and [1]Neurology, Institute of Medical Sciences, Banaras Hindu University, Varanasi, Uttar Pradesh, India

Abstract

Introduction: Spinocerebellar ataxia type 3 (SCA3), or Machado-Joseph disease (MJD), is a prevalent autosomal dominant-inherited disease that causes progressive problems with movement. Abnormal repetitive expansion of CAG trinucleotide in the ATXN3 gene results in SCA3. This study was done to review the corporation of CAG repeats and polymorphisms in definitive genes with the occurrence of SCA3 in the Indian community, especially in the eastern UP population. **Material and Methods:** The 40 Ataxia's patient and their parents were listed after obtaining written consent from the participant's attendant/guardians. Out of these, we have identified polymorphism in three patients. **Results:** In one patient, we have found a single base change, *g.31483A>T* in *Exon 10*, which changes the nucleotide from Adenine to Thymine (*A31483T*), while in the second patient, we have identified an intronic change at *g.35690A>G* in *Exon 10*, which changes the nucleotide from Adenine to Guanine (*A35690G*) and in the third patient DNA sequence analysis identified an intronic change at *g.35587A>G* Exon 10, which changes the nucleotide from Adenine to Guanine (*A35587G*). **Discussion and Conclusion:** Although the partial loss of ATXN3 function may also contribute, the disease mechanism in MJD is believed to be a toxic gain-of-function. Several pathogenic cascades have been reported to be triggered by mutant ATXN3, but the critical molecular events driving MJD pathogenesis stay unresolved. While significant developments in studies have enhanced our knowledge of MJD, there is presently a lack of preventive treatment. Results presented here also expand our knowledge about MJD found in the eastern UP population.

Keywords: *ATXN3 gene, Machado-Joseph disease, polymerase chain reaction, polymorphism, Spinocerebellar ataxia type 3*

Introduction

Spinocerebellar ataxia type 3 (Machado-Joseph disease [MJD]/SCA3), also known as MJD is the prevalent autosomal dominant-inherited cerebellar ataxia.[1,2] MJD is diagnosed with molecular genetic testing to detect an abnormal repetitive expansion of CAG trinucleotide in the ATXN3 gene. The gene ATXN3 is found on chromosome 14q32.1 and is suggested in people with progressive cerebellar ataxia and pyramidal signs as well as dystonia, ophthalmoplegia, action-induced facial and lingual fasciculation-like movements, and bulging eyes.[3,4] Current therapy is symptomatic without inhibiting neuronal cell death or delaying the age of onset. Identifying molecular pathways of disease is, therefore, essential for unraveling future therapeutic goals. SCA3 is a polyglutamine (polyQ) neurodegenerative disorder. Normal alleles range from 11 to 44 repeats of CAG, while pathogenic expansions range from 61 to 87 CAGs.[5]

A range of clinical characteristics can be found in subjects with ≥52 CAG units.[6-8] The identification of founders with Portuguese-Azorean ancestry was noted in the first linkage studies.[9]

The trials find the interactions of ataxin-3 with two proteins, HHR23A and HHR23B, both homologs of the DNA repair protein Rad23.[10] Additional research disclosed ataxin-3 as a bona fide deubiquitinating (DUB) enzyme,[11,12] giving vital insight into ataxin-3's normal function. More lately, ataxin-3 has been shown to communicate with the transcription factor FOXO4 in the oxidative stress reaction as a transcriptional coactivator.[13] Thus, while some very fundamental ataxin-3 features have been identified, these developments have produced nonintersecting inquiry lines and have not given an underlying mechanism for the pathogenesis of SCA3 disease. To determine the prevalence and

How to cite this article: Singh B, Bose P, Shamal SN, Joshi D, Singh R. Polymorphic study of ataxin 3 gene in eastern Uttar Pradesh population. J Anat Soc India 2020;XX:XX-XX.

Article Info

Received: 08 August 2019
Accepted: 24 October 2020
Available online: ***

Address for correspondence:
Prof. Royana Singh,
Department of Anatomy,
Institute of Medical Sciences,
Banaras Hindu University,
Varanasi - 221 005,
Uttar Pradesh, India.
E-mail: royanasingh@bhu.ac.in

Access this article online

Website: www.jasi.org.in
DOI: 10.4103/JASI.JASI_107_19
Quick Response Code:

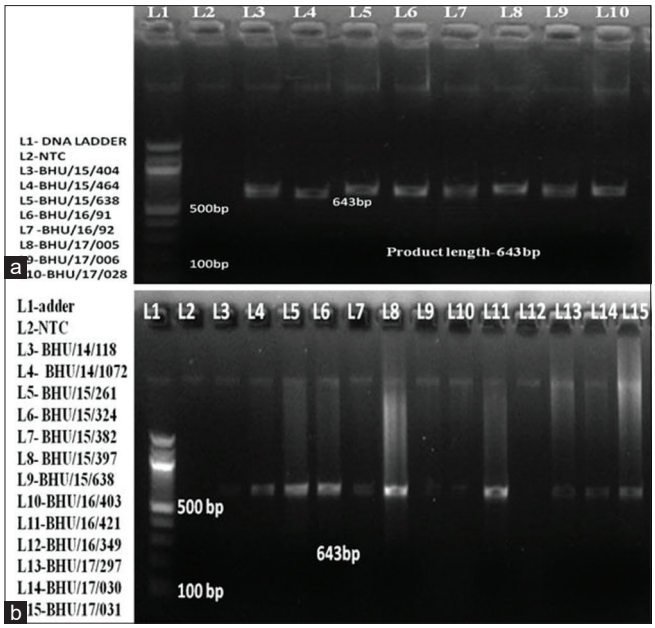

Figure 1: (a and b) Showing gel pictures of amplified genomic DNA (Exon 10 of ATXN 3 Gene) of SCA3 samples

Figure 2: (a) Showing picture of SCA3 Patient, ID- BHU/15/638, (b) Pedigree of Patient BHU/15/638, (c) Sequence analysis of Patient BHU/15/638, (d) Sequence analysis demonstrates single nucleotide change at g.31483A>T position in Exon10 where Adenine was replaced by Thymine (A31483T), (e) MUTATION TASTER result showing polymorphic site

distribution of MJD/SCA3 in the Cuba, a clinical and molecular genetic study of a cohort of SCA3 families was created. Also assessed were the ordinary variation of repeats of CAG and their volatile conduct.

Due to the low prevalence of intermediate alleles at this locus, SCA3 was not validated in the replication cohorts. The major symptoms are as gait ataxia as the disease's initial symptom. Other cerebellar characteristics were dysdiadochokinesia, dysmetria, cerebellar dysarthria, and kinetic tremor. Pathological nystagmus was the most significant oculomotor sign.

Material and Methods

This study was done to review the corporation of CAG repeats and polymorphisms in definitive genes with the occurrence of SCA 3 in the Indian community, especially in the eastern UP population. The study will also help us in concluding the genetic explanation of these CAG/polyQ repeat expansion in the SCA3 gene. We looked for Atxn3 polymorphism in a subset of genomic DNA (DNA isolation from blood samples). The 40 Ataxia's patient and their parents were listed after obtaining written consent from the participant's attendant/guardians. A particular admission precedent was based on clinically recognizing cerebellar ataxia. It was determined by the study of medical records. Blood samples from the proband, mother and their various controls were collected from the OPD of the Department of Neurology (Sir Sunderlal Hospital, Institute of Medical Sciences, Banaras Hindu University [BHU], Varanasi) and evicted to Cytogenetic lab (Institute of Medical Sciences, BHU, Varanasi) for genetic studies in ethylenediaminetetraacetic acid vials and stored at 4°C under sterile condition till further scrutiny. Genomic DNA was isolated from blood using materials like heparinized blood.

After isolation of genomic DNA, quantification of DNA was measured for the further experiment using the *Nanodrop-Spectrophotometer*. After quantification, primers were designed for the coding region of ATXN3 gene including exon/intron boundaries. The ATXN3 gene contains 10 Exons. The primers were designed using Primer3 software version 0.4.0 (http://frodo.wi.mit.edu/primer3/).

Polymerase chain reaction

In molecular biology, the polymerase chain reaction (PCR) was used as a technique to amplify the single or a few copies of a piece of DNA across multiple order of magnitude, generating thousands to millions of copies of particular DNA sequence. The PCR was carried out on an *AppliedBiosystem, 96 well Veriti Thermal Cycler* (Applied Biosystem, USA).

During the study, molecular analysis was done for *Exon 1-10*. Primers were designed to amplify across each of the exons including *Exon 10*. Sequencing analysis was done to

Table 1: showing polymorphism detected in 3 cases out of 40 families (3 familial and 37 sporadic cases)

BHU ID	Age	Gender	Age of onset	Repeat size (test sample) normal	Repeat size (test sample)
BHU/15/404	35 years	Male	6 years	CAG-28	CAG-22
BHU/15/261	16 years	Male	8 years	CAG-28	CAG-32
BHU/15/297	65 years	Male	5 months	CAG-28	CAG-20
BHU/15/382	36 years	Female	7 years	CAG-28	CAG-20
BHU/15/508	42 years	Male	22 years	CAG-28	CAG-22
BHU/15/533	40 years	Male	5 years	CAG-28	CAG-20
BHU/15/565	19 years	Male	5 years	CAG-28	CAG-21
BHU/15/638	58 Years	Male	6 months	CAG-28	CAG-27 Intronic Changes
BHU/16/91	54 years	Male	5 years	CAG-28	CAG-22
BHU/16/92	40 years	Male	12 years	CAG-28	CAG-24
BHU/16/188	54 years	Male	6 months	CAG-28	CAG-20
BHU/16/334	50 years	Male	5 years	CAG-28	CAG-20
BHU/16/335	39 years	Male	2 years	CAG-28	CAG-22
BHU/16/349	58 years	Male	6 months	CAG-28	CAG-18
BHU/17/05	40 years	Male	1 year	CAG-28	CAG-07
BHU/17/06	45 years	Male	26 years	CAG-28	CAG-27
BHU/17/25	48 years	Female	10 years	CAG-28	CAG-22
BHU/17/28	40 years	Male	2 year	CAG-28	CAG-18 Polymorphism
BHU/17/31	17 year	Male	3 year	CAG-28	CAG-15
BHU/17/34	65 years	Female	15 years	CAG-28	CAG-24
BHU/17/41	40 years	Male	5 years	CAG-28	CAG-10
BHU/17/42	35 years	Male	3 years	CAG-28	CAG-22
BHU/17/43	45 years	Male	2 years	CAG-28	CAG-18
BHU/17/54	75 years	Male	4 years	CAG-28	CAG-15
BHU/17/79	17 years	Male	6 years	CAG-28	CAG-10
BHU/17/145	30 years	Male	2 years	CAG-28	CAG-22
BHU/17/146	32 years	Female	4 years	CAG-28	CAG-11
BHU/17/149	52 years	Female	12 years	CAG-28	CAG-15
BHU/17/152	24 years	Female	5 years	CAG-28	CAG-22
BHU/17/170	18 years	Male	2 years	CAG-28	CAG-22
BHU/18/28	55 years	Male	7 years	CAG-28	CAG-24
BHU/18/29	28 years	Female	2 years	CAG-28	CAG-22
BHU/18/32	40 years	Female	1 year	CAG-28	CAG-22
BHU/18/35	61 years	Male	5 years	CAG-28	CAG-22
BHU/18/36	32 years	Female	2 years	CAG-28	CAG-22
BHU/15/463	24 years	Female	2 years	CAG-28	CAG-21
BHU/15/464	35 years	Male	6 years	CAG-28	CAG-21 Polymorphism
BHU/15/429	40 years	Male	1 year	CAG-28	CAG-18
BHU/15/30	40 years	Male	2 year	CAG-28	CAG-10
BHU/17/28	40 years	Male	5 years	CAG-28	CAG-20

The table shows repeat size found in Ataxin 3 gene of three Cerebellar ataxia patients out of 40 families.

determine polymorphism in all the patients and control for *Exon 1-10*; however, polymorphism and intronic changes were observed only in *Exon 10*.

Gel electrophoresis

After running PCR, the PCR products were subjected to gel electrophoresis. We have done gel electrophoresis at temperature of 100°C and after that, with the help of the Gel doc system or gel imaging, we have measured and recorded the labeled nucleic acid or DNA. Gel results of amplified genomic DNA of Exon10 can be seen in Figure 1. We run PCR for all collected samples and after that, we had carried out the gel electrophoresis to see the amplification. In [Figure 1a and b], we can see that the Exon10 of the ATXN3 gene would get amplified at 643bp. After that all the samples were sent for sequencing. In sequencing, mutation was observed in *Exon10*. After that, the analysis was performed in dry lab using Mutation Taster is free web-based application to evaluate DNA sequence variants for their disease causing potential.

The study was performed to determine the impact of the polymorphic site. None of the unaffected members of the family and none of the control individuals had this abnormal conformer. One polymorphism and one intronic changes have been found in the gene ATXN3.

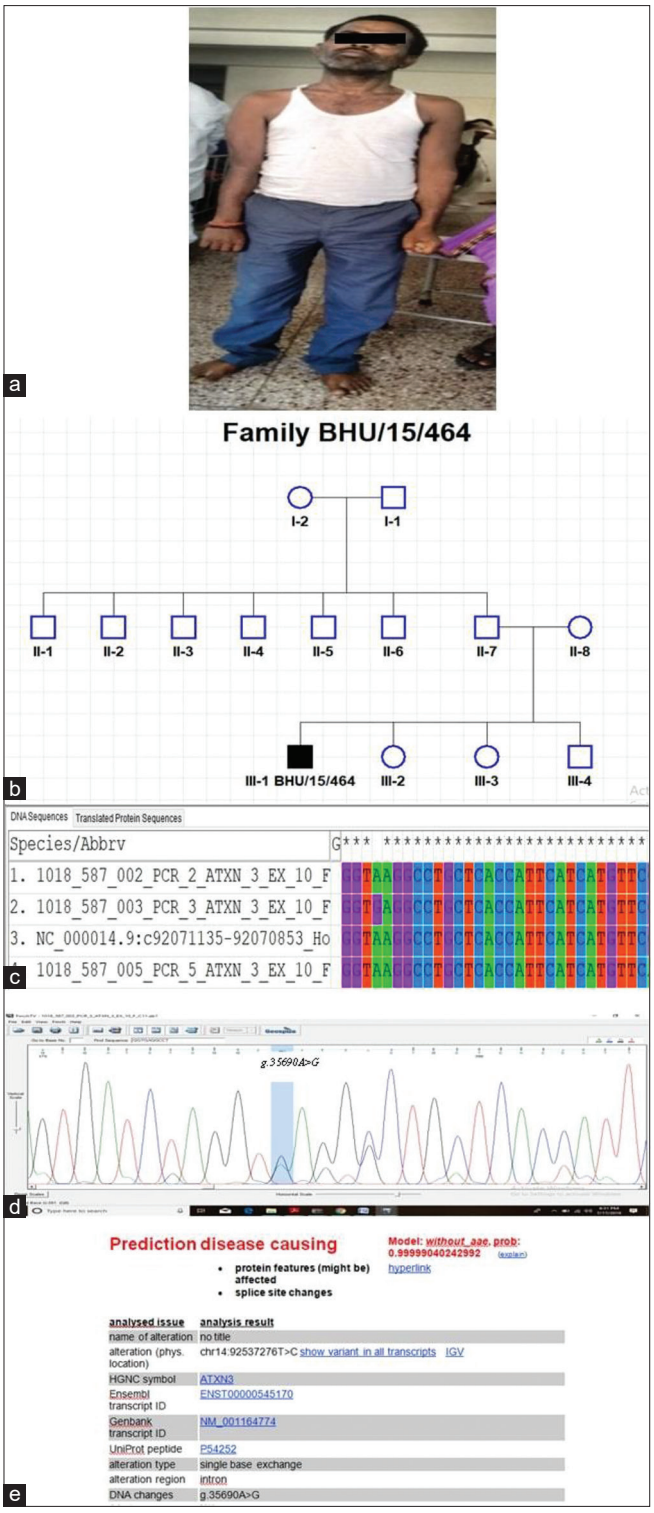

Figure 3: (a) Showing picture of SCA3 Patient, ID- BHU/15/464, (b) Pedigree of Patient BHU/15/464, (c) Sequence analysis of Patient BHU/15/464, (d) Sequence analysis demonstrates single nucleotide change at g.35690A>G in Exon 10, which changes the nucleotide from Adenine to Guanine (A35690G), (e) mutation taster result showing polymorphic site

Results

Gel results of amplified genomic DNA of Exon 1 to Exon 10 as shown in Figure 1. We run PCR for all collected samples (40 patients and 20 Controls) as shown in table 1 and had carried out the gel electrophoresis to see the amplification. We can see that the Exon 10 of the *Atxn 3* gene would get amplified at 638 bp.

Phenotypic analysis

Three familial and sporadic patients ranging in age from 16 years to 65 years with clinically apparent ataxia presenting with nystagmus, decreased saccade velocity; amyotrophy fasciculations, sensory loss, and evaluated by history taking and physical examination, magnetic resonance imaging and computed tomography scan for SCA 3 were identified.

Molecular analysis

During the study, molecular analysis was done for Exon 1-10**.** Primers were designed to amplify across each of the Exons, including Exon 10. Sequencing analysis was done to determine polymorphism in all the patients and control for Exon 1-10; however, polymorphism was observed only in Exon 10. During the study, *in silico* analysis was done to determine the impact of the polymorphic site.

In the first case, a male aged 58 years whose ID is BHU/15/638 was detected with no family history (sporadic case) as shown in Figure 2. Chromatogram demonstrates a single base change, *g.31483A>T* in *Exon 10*, where adenine was replaced by Thymine (*A31483T*) (Ensembl transcript ID ENST00000545170), these alteration takes place in intron. With the help of *MUTATION TASTER* software, the polymorphic site was detected, wild type gDNA sequence compare to altered gDNA sequence, in these sequences A altered to T, Multiple sequence alignment was done to determine the single base exchange of A>T.

In the second case, also a male aged 35 years whose ID is BHU/15/464 was detected with no familial history (as shown in Figure 3). Multiple sequence alignment was done to determine a single base exchange of A>G. Chromatogram demonstrates single nucleotide change at *g.35690A>G* in *Exon 10*, which changes the nucleotide from Adenine to Guanine (*A35690G*) (Ensembl transcript ID ENST00000398590), these alteration takes place in the intron. *MUTATION TASTER* result showing the polymorphic site as disease causing. Wild-type gDNA sequence compares to altered gDNA sequence, in this sequence A altered to G.

In the third case, a male aged 40 years whose ID is BHU/17/28 was detected with no family history (sporadic case) as shown in Figure 4. Multiple sequence alignment was done to determine a single base exchange of *A>G.* (D) Chromatogram demonstrates single nucleotide change at *g.35587A>G* in *Exon 10*, which changes the nucleotide from Adenine to Guanine (*A35587G*), (Ensembl transcript ID ENST00000545170), *MUTATION TASTER* result showing the polymorphic site as disease causing. Wild type gDNA sequence compared to altered gDNA sequence, in this sequence A altered to G.

Table 2: Single base exchange variation identified in Atxn 3 in spinocerebellar ataxia patients with their position of nucleotide according to ensemble and position of amino acid

Gender	Cerebellar ataxia	Ensembl ID and position of nucleotide	Polymorphism	Synonymous/nonsynonymou (mutation taster prediction)
Male BHU/18/30	Ataxin 3 (Type I)	(ENST00000545170) 31483A	Adenine to Thymine *(A31483T)*	Synonymous Changes
Male BHU/15/464	Ataxin 3 (Type I)	(ENST00000398590) 35690A	Adenine to Guanine *(A35690G)*	Synonymous Changes
Male BHU/17/28	Ataxin 3 (Type I)	(ENST00000545170) 35587A	Adenine to Guanine *(A35587G)*	Nonsynonymous Changes

Variations are analyzed by using Mutation Taster (In silico study)

Figure 4: Pedigree of Patient BHU/17/28. (a) Picture of SCA3 patient, ID- BHU/17/28, (b) Pedigree of patient BHU/17/28, (c) Multiple sequence alignment was done to determine single base exchange of A > G. (d) Chromatogram demonstrates single nucleotide change at g. 35587A > G in Exon 10, which changes the nucleotide from adenine to guanine (A35587G), (e) MUTATIONTASTER result showing polymorphic site as disease causing. (f) Wild type gDNA sequence compared to altered gDNA sequence, in this sequence A altered to G

Discussion

MJD, the most common dominantly inherited ataxia in the world, is triggered by an expansion of polyQ in the DUB enzyme ataxin-3. The polyQ repeat expansion is thought to give the various polyQ-encoding proteins a toxic gain-of-function, potentially supporting their misfolding and aggregation, but the accurate mechanism of disease pathogenesis remains unknown. The ATXN3 gene offers directions for the production of an enzyme called ataxin3, which is found in cells throughout the body. Ataxin3 is engaged in a mechanism called the ubiquitinproteasome system, which destroys surplus and damaged proteins and gets rid of them. The molecule ubiquitin attaches (binds) to unneeded proteins and marks them within cells to be broken down (degraded). Ataxin3 removes (cleaves) the ubiquitin from these unwanted proteins just before it is degraded to allow the ubiquitin to be reused. Ataxin3 is known as a DUB enzyme because of its function in slicing ubiquitin from proteins.

We observed polymorphism in three patients of SCA3 and those were polymorphism and intronic changes as

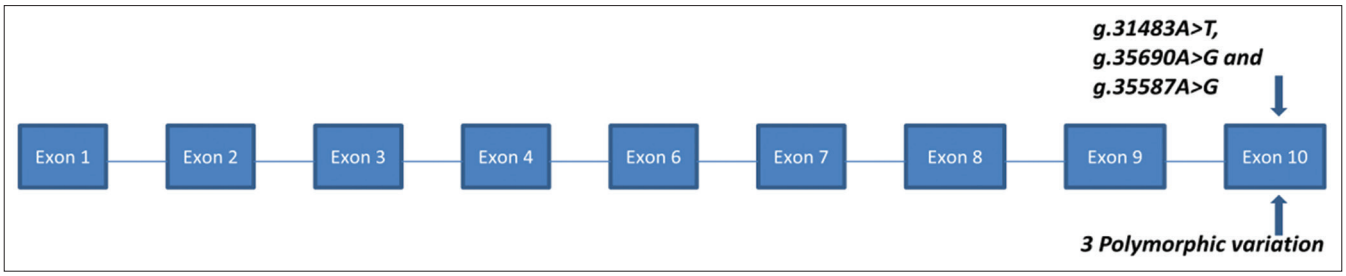

Figure 5: Polymorphism detected in Exon 10 in all the three cases

depicted in Table 2 and Figure 5. SCA3 is a polyglutamine neurodegenerative disorder. Normal alleles range from 11 to 44 repeats of CAG, while pathogenic expansions range from 61 to 87 CAGs. A range of clinical features can be found in subjects carrying ≥52 CAG units. This has led us to speculate on the existence of common features in Ataxia type 1 disorder. While well characterized at the molecular level, the encoded protein function is not currently known.

Normally, *ATXN3* helps to control the stability and activity of multiple proteins in various cellular pathways. Mutant (expanded) *ATXN3* is susceptible to form insoluble aggregates and to undergo proteolysis that produces fragments containing polyQ that further encourage aggregation. Although the partial loss of the *ATXN3* function may also contribute, the disease mechanism in MJD is believed to be a toxic gain-of-function. Several pathogenic cascades have been reported to be triggered by mutant *ATXN3,* but the critical molecular events driving MJD pathogenesis stay unresolved. In the pursuit of MJD treatment, several pathways have been targeted, but none have yet progressed to human clinical trials.

The single-nucleotide change in the first patient was at *g.31483A>T* position in Exon10, where Adenine was replaced by Thymine (*A31483T*) as shown. The change of nucleotide was in the intronic region. While, in the second patient, a single base change was observed at *g.35690A>G* in *Exon 10*, which changes the nucleotide from Adenine to Guanine (*A35690G*). It can be predicted as disease causing by altering the nucleotide variants as shown.

In the third patient, the nucleotide change occurred at site *g.35587A>T* position in Exon10, where Adenine was replaced by Guanine (A>G), as shown. This nucleotide change represents single base change. A study was done to screen polymorphism through mutation taster.

Conclusion

Mutations in the ATXN3 gene mostly affect nerve cells and other types of brain cells. SCA3 is associated with cell death in the portion of the brain attached to the spinal cord (the brainstem), the part of the brain engaged in coordinating motions (the cerebellum), and other brain regions. This condition is also associated with the death of nerve cells in the spinal cord. Over time, the brain and spinal cord cell loss cause distinctive signs and symptoms of SCA3. While significant developments in studies have enhanced our knowledge of MJD, there is presently a lack of preventive treatment. Results presented here also expand our knowledge about MJD found in the eastern UP population. These findings deserve confirmation in a second population and more in-depth research in cellular and animal models.

Financial support and sponsorship

Nil.

Conflicts of interest

There are no conflicts of interest.

References

1. Schöls L, Bauer P, Schmidt T, Schulte T, Riess O. Autosomal dominant cerebellar ataxias: Clinical features, genetics, and pathogenesis. Lancet Neurol 2004;3:291-304.
2. Ranum LP, Lundgren JK, Schut LJ, Ahrens MJ, Perlman S, Aita J, *et al*. Spinocerebellar ataxia type 1 and Machado-Joseph disease: Incidence of CAG expansions among adult-onset ataxia patients from 311 families with dominant, recessive, or sporadic ataxia. Am J Hum Genet 1995;57:603-8.
3. Lima L, Coutinho P. Clinical criteria for diagnosis of Machado-Joseph disease: Report of a non-Azorena Portuguese family. Neurology 1980;30:319-22.
4. D'Abreu A, Franca MC, Jr., Paulson HL, Lopes-Cendes I. Caring for Machado-Joseph disease: Current understanding and how to help patients. Parkinsonism Relat Disord 2010;16:2-7.
5. Whaley NR, Fujioka S, Wszolek ZK. Autosomal dominant cerebellar ataxia type I: A review of the phenotypic and genotypic characteristics. Orphanet J Rare Dis 2011;6:33.
6. Maciel P, Costa MC, Ferro A, Rousseau M, Santos CS, Gaspar C, *et al*. Improvement in the molecular diagnosis of Machado-Joseph disease. Arch Neurol 2001;58:1821-7.
7. Paulson HL. Dominantly inherited ataxias: Lessons learned from Machado-Joseph disease/spinocerebellar ataxia type 3. Semin Neurol 2007;27:133-42.
8. van Alfen N, Sinke RJ, Zwarts MJ, Gabreëls-Festen A, Praamstra P, Kremer BP, *et al*. Intermediate CAG repeat lengths (53,54) for MJD/SCA3 are associated with an abnormal phenotype. Ann Neurol 2001;49:805-7.
9. Martins S, Calafell F, Gaspar C, Wong VC, Silveira I, Nicholson GA, *et al*. Asian origin for the worldwide-spread mutational event in Machado-Joseph disease. Arch Neurol 2007;64:1502-8.
10. Wang G, Sawai N, Kotliarova S, Kanazawa I, Nukina N. Ataxin-3, the MJD1 gene product, interacts with the two human homologs of yeast DNA repair protein RAD23, HHR23A and

HHR23B. Hum Mol Genet 2000;9:1795-803.

11. Winborn BJ, Travis SM, Todi SV, Scaglione KM, Xu P, Williams AJ, *et al*. The deubiquitinating enzyme ataxin-3, a polyglutamine disease protein, edits Lys63 linkages in mixed linkage ubiquitin chains. J Biol Chem 2008;283:26436-43.
12. Burnett B, Li F, Pittman RN. The polyglutamine neurodegenerative protein ataxin-3 binds polyubiquitylated proteins and has ubiquitin protease activity. Hum Mol Genet 2003;12:3195-205.
13. Araujo J, Breuer P, Dieringer S, Krauss S, Dorn S, Zimmermann K, *et al*. FOXO4-dependent upregulation of superoxide dismutase-2 in response to oxidative stress is impaired in spinocerebellar ataxia type 3. Hum Mol Genet 2011;20:2928-41.

Original Article

An Anatomical Description of the Vermian Fossa: The Reappraisal of an Overlooked Entity

Jeshika S. Luckrajh, J. Naidoo, L. Lazarus

Department of Clinical Anatomy, School of Laboratory Medicine and Medical Sciences, College of Health Sciences, University of Kwazulu-Natal, Westville Campus, Durban, South Africa

Abstract

Introduction: The vermian fossa (VF) is a shallow depression at the inferior end of the internal occipital crest, which lodges the inferior part of the cerebellar vermis. Published literature describes the VF as having a highly variable incidence and morphology. The present study is aimed to investigate the incidence, morphology, and morphometry of the VF within a select South African population and to conduct a review of the literature regarding this structure. **Material and Methods:** A total of 100 dry, adult skulls of South African origin were analyzed to determine the morphological and morphometric parameters of the VF. **Results:** The VF was found to be present in 62% of cases. The shape of the VF was classified as triangular (27%), quadrangular (8%), and atypical (27%). The average length of the VF was 13.78 mm, and the average width was 11.62 mm. The morphometric findings of this study correlate with that of previous studies; however, the incidence of atypical shaped VF (27%) is higher in comparison to previous studies (9.7%). **Discussion and Conclusion:** The detailed anatomical description of the VF may aid in the study of diseases which cause alterations in the size and morphology of the vermis of the cerebellum as well as in transvermian approaches to tumors within the fourth ventricle. Furthermore, due to the paucity of anatomical descriptions of the VF, a reappraisal of this structure is warranted as it is of prime importance to clinicians operating in or interpreting radiological images of the posterior cranial fossa.

Keywords: *Cerebellar vermis, posterior cranial fossa, vermian fossa*

Introduction

The vermian fossa (VF) is a shallow endocranial depression located between the inferior end of the internal occipital crest and the posterior border of the foramen magnum.[1] The function of the VF and the reason for its development in the posterior cranial fossa has been a mystery to anatomists and anthropologists for centuries.[2,3] Lombroso, known as the father of criminology, who proposed the atavistic tendencies of criminals, had identified the VF as one of the anatomical features of a criminal.[2] This author, who referred to the VF as the median occipital fossa, had made this conclusion after identifying an enlarged vermis and VF during the postmortem of one who had committed "atrocious crimes."[2] In 1926, East had attributed an enlarged VF to intracranial pressure as the result of hydrocephaly in a 4-month-old infant.[3] These seemingly strange attributions of the VF are not acknowledged in current times and literature regarding the VF is quite brief in standard anatomical texts. According to Grays Anatomy (41st edition), the VF "may exist" which alludes to the variability of this structure, and this may account for the absence of VF literature in other anatomical textbooks.[1] However, there is a necessity for anatomists and medical educators to have a thorough knowledge of all structures, which may lead to a higher quality of medical education. Furthermore, in the present era of radiological imaging, structures of the skull may serve as an important role in diagnostic medicine. Berge and Bergman stated that knowledge of the size and incidence of structures and variations of the skull may aid in the diagnostic evaluation of radiologic images and acknowledged that the absence of essential anatomic data on normal variations is a severe deficiency of modern anatomy textbooks.[4] The VF has been identified as one such structure which has been sparsely described from an anatomical perspective.

In addition, the anatomy of the VF and its variations may be of relevance to the surgeon employing a transventricular

How to cite this article: Luckrajh JS, Naidoo J, Lazarus L. An anatomical description of the vermian fossa: The reappraisal of an overlooked entity. J Anat Soc India 2020;69:XX-XX.

Article Info

Received: 17 September 2019
Accepted: 14 September 2020
Available online: ***

Address for correspondence:
Dr. L. Lazarus,
Department of Clinical Anatomy, School of Laboratory Medicine and Medical Sciences, College of Health Sciences, University of Kwazulu-Natal, Westville Campus, Private Bag X54001, Durban 4000, South Africa.
E-mail: ramsaroopl@ukzn.ac.za

Access this article online

Website: www.jasi.org.in
DOI: 10.4103/JASI.JASI_131_19
Quick Response Code:

and supracerebellar infratentorial approach to remove midline tumors of the posterior cranial fossa or a transvermian approach to remove tumors within the fourth ventricle.[5,6] A detailed description of the VF may also aid in the study of diseases that cause alterations in the size and morphology of the vermis of the cerebellum, as it has been reported that certain cases of cerebellar cortical dysplasia are associated with VF variations.[5]

Therefore, the present study is aimed to investigate the anatomical parameters of the VF by determining its incidence, morphology, and morphometry.

Material and Methods

A total of one hundred adults, dry skulls were obtained from the Department of Clinical Anatomy, University of KwaZulu-Natal, South Africa. Ethical approval was obtained from the Institutional Ethics Committee (BREC Ref No: 256/19). The specimens were of South African origin; however, the gender of each specimen was unknown.

The incidence, shape, length, and width of the VF were recorded. A digital Vernier caliper (Linear Tools, 2012, 0–150 mm, LIN 86500963) was employed to measure the morphometric parameters. The shape of the VF was classified as Type 1 (Triangular), Type 2 (Quadrangular), and Type 3 (Atypical), according to the classification system used by Kale and Öztürk.[7] In cases of quadrangular and atypically shaped VF, the length and width were taken at the longest and widest part of the VF, respectively.

Descriptive statistics (incidences) were used to describe the results of this study.

All specimens with macroscopic damage or lesions of the posterior cranial fossa were excluded from this study, and only specimens without macroscopic damage or lesions of the posterior cranial fossa were included.

Results

The VF was found to be present in 62% of cases [Table 1]. The shape of the VF was classified as Triangular in 27% of cases, Quadrangular in 8% of cases, and Atypical in 27% of cases [Figure 1 and Table 1]. The average length of the VF was 13.78 mm, and the average width was 11.62 mm [Table 2].

Discussion

The term "Vermian" is related to the cerebellar vermis, which is commonly known to be the primary structure found within the VF. The Latin term *vermis* is translated worm and this may refer to the shape of the cerebellar vermis, which includes the tuber, pyramid, uvula, and nodule.[1] However, Kunc *et al*. highlighted that there is no true contact of the occipital bone with the vermis of the cerebellum and therefore suggested that the term "Vermian Fossa" should be replaced with "triangular eminence" (eminentia triangularis) and defined as flat triangular prominence at the inferior end of the internal occipital crest, formed by the attached margins of the falx cerebelli.[13] The descriptions of the VF in anatomical textbooks are either brief or absent altogether. There are several studies in the literature which describe the VF; however, these studies represent data largely from Asian populations. Murlimanju *et al*. suggested that VF morphology may be influenced by racial differences; it is therefore of value to analyze this structure within different population groups.[5] The results of this study represent data

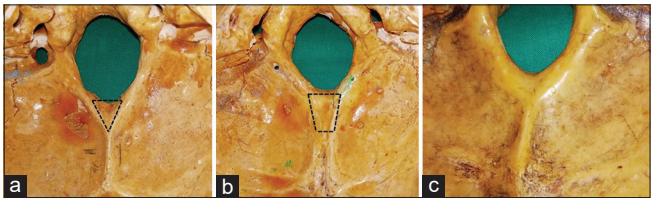

Figure 1: Morphological presentation of the Vermian fossa. (a) Type 1 - triangular; (b) Type 2 - quadrangular; (c) Type 3 – atypical

Table 1: Incidence and morphological presentation of the Vermian fossa

Author (year)	Sample size (*n*)	Population	Incidence (%)	Morphology (%)		
				Triangular	Quadrangular	Atypical
Cireli *et al*. (1990)	210	-	11.4%	-	-	-
Berge and Bergman (2001)[4]	100	USA	4	-	-	-
Kale and Öztürk (2008)[7]	158	Turkey	8.2	4.4	2.5	1.3
Murlimanju *et al*. (2013)[5]	35	India	71.4	76	8	16
Yadav *et al*. (2014)[8]	55	India	72.7	72.5	10	17.5
Ranjan *et al*. (2015)[9]	110	India	80	70.5	8	21.6
Archana *et al*. (2017)[10]	50	India	72	80.6	11.1	8.3
Singh and Gupta (2017)[11]	60	India	66.7	80	20	0
Pandey *et al*. (2018)[12]	40	India	80	90.6	6.3	3.1
Kunc *et al*. (2020)[13]	1042	Czech Republic	29.7	-	-	-
Weighted mean			32.9	54.2	8.1	9.2
Present study (2019)	100	South Africa	62	27	8	27

Table 2: Morphometry of the Vermian fossa

Author (year)	Sample size (*n*)	Length (mm)	Width (mm)
Kale and Öztürk (2008)[7]	158	27.8	18.4
Murlimanju *et al*. (2013)[5]	35	13.6	11.9
Yadav *et al*. (2014)[8]	55	14.2	12.1
Ranjan *et al*. (2015)[9]	110	13.4	12.1
Archana *et al*. (2017)[10]	50	14.6	12.6
Singh and Gupta (2017)[11]	60	17	13.5
Pandey *et al*. (2018)[12]	40	16.7	18
Weighted mean		18.8	14.7
Present study (2019)	100	13.8	11.6

from a select South African population to add to the global body of knowledge.

The literature revealed a weighted mean incidence of the VF in 32.9% of cases; however, the present study recorded the VF in 62% of cases [Table 1]. This finding is lower than that of recent literature, which records the incidence of the VF ranging from 66.7% to 80% [Table 1]. However, earlier studies by Cireli *et al*., Berge and Berman and Kale and Öztürk recorded significantly lower incidences of 11.4%, 4%, and 8.2%, respectively [Table 1].[4,7,14] It is notable that the latter studies were done in the USA and Turkey, respectively, whereas the studies reflecting higher incidences were conducted in India. The significant difference in incidence between the studies as well as the consistency in results from the Indian studies, supports the hypothesis that racial and geographic distribution may contribute to the variation of the VF.[5,7,8,12] The incidence of the VF within a select South African population, as is recorded in this study, has not been previously reported and is of clinical relevance to surgeons during the preoperative planning of surgeries within the posterior cranial fossa.

The morphological characteristics of the VF are variable and have been described as Type 1–3, according to the classification system proposed by Kale and Öztürk.[7] Type 1 represents a triangular fossa, Type 2 represents a quadrangular fossa, and Type 3 represents an atypically shaped fossa [Figure 1].[7] Type 1 was found in 27% of cases in the present study. This is the most commonly found shape in the literature, and the weighted mean incidence of Type 1 in the literature was 54.2% (range: 4.4%–90.6%) [Table 1].

Type 2, quadrangular VF, was found in 8% of cases in this study. This correlates closely with the findings of Ranjan *et al*. and Pandey *et al*., who recorded Type 2 VF in 8% and 6.3%, respectively [Table 1].[9,12] The weighted mean incidence of Type 2, as depicted in the literature, was 8.1% (range 2.5%–20%), which correlates closely with the findings of the present study. Kale and Öztürk stated that a few authors termed the quadrangular VF as fossa occipitalis mediana since it was deeper than other cases.[7] However, in developing the classification of VF morphology, Kale and Öztürk classified fossa occipitalis mediana as Type 2 VF since the locations of the two are the same, the only difference being the depth of the fossa.[7] Furthermore, Kale and Öztürk hypothesized that the distinction in the depth of the VF may be attributed to the size and shape of the inferior cerebellar vermis and therefore concluded that this classification may be indicative of the size and shape of the inferior cerebellar vermis.[7]

Type 3 VF described atypical cases which presented with a morphology which was neither triangular nor quadrangular but did display a fossa. In the present study, Type 3 was recorded in 27% of cases; this finding is higher than the weighted mean incidence of 9.2% (range: 1.3%–21.6%) in the literature [Table 1].

The average length of the VF in the present study was 13.8 mm. This finding was lower than the weighted mean length of the VF in the literature, which was 18.8 mm. The average width of the VF was 11.6 mm, in the present study. This finding is less than the weighted mean width recorded in the literature (14.7 mm) [Table 2].

Sanudo *et al*. stated that both diagnosis and therapeutic performance may be augmented by studies of morphological variations.[15] Despite its high incidence, the VF is currently considered an anatomical variation and is an overlooked entity in many standard anatomical texts. Further to highlighting the VF as a distinguished structure of skull anatomy, the present study reported morphological and morphometric parameters of the VF. These results may aid the surgeon operating in the posterior cranial fossa during procedures such as the transventricular and supracerebellar infratentorial removal of midline tumors or the transvermian approach to tumors within the fourth ventricle.[9]

The closest anatomical structures to the VF are the posterior cerebromedullary cistern from the superior aspect and the division of the occipital sinuses continuing into the marginal sinuses from the lateral aspect. Surgeons operating in this area may benefit from knowing the incidence of variations of the VF, which may influence surrounding structures such as a duplicated falx cerebelli.[13,16] Furthermore, the detailed knowledge of the anatomical parameters of the VF may aid in the study of diseases which cause alterations in the size and morphology of the cerebellar vermis as cerebellar cortical dysplasia are associated with VF variations.[5]

Conclusion

Considering the paucity of literature regarding the VF in anatomical texts as well as the clinical relevance of this structure, this study highlights the need for a reappraisal of the VF. It is recommended that future studies include larger sample sizes, with biographical data for more comprehensive statistical analysis. Accurate knowledge of the anatomy and variations of the VF is of importance to anatomists, radiologists, and surgeons and may aid in mitigating iatrogenic injuries.

Financial support and sponsorship

Nil.

Conflicts of interest

There are no conflicts of interest.

References

1. Standring S, Anand N, Birch R, Collins P, Crossman AR, Gleeson M, *et al*. Gray's Anatomy E-Book: The Anatomical Basis of Clinical Practice. Edinburgh: Elsevier Health Sciences; 2016.
2. Lombroso C. Criminal Man. USA: Duke University Press; 2006.
3. East CF. A rare abnormality of the occipital bone. J Anat 1926;60:416-7.
4. Berge JK, Bergman RA. Variations in size and in symmetry of foramina of the human skull. Clin Anat 2001;14:406-13.
5. Murlimanju BV, Prabhu LV, Sharmada KL, Saralaya VV, Pai MM, Kumar CG, *et al*. Morphological and morphometric study of the "Vermian Fossa" in Indian human adult skulls. J Morphol Sci 2013;30:148-51.
6. Ebrahim KS, Toubar AF. Telovelar approach versus transvermian approach in management of fourth ventricular tumors. Egypt J Neurosurg 2019;34:10.
7. Kale A, Öztürk A. Vermian fossa An anatomical study. Journal of Istanbul Faculty of Medicine 2008;71:4.
8. Yadav A, Chauhan K, Nigam GL, Sharma A, Yadav A. Morphological and morphometrical analysis of the vermian fossa in dry adult skulls of western Uttar Pradesh population: An osteological study. Int J Anat Res 2014;2:478-80.
9. Ranjan RK, Kataria DS, Yadav U. Vermian fossa: An anatomical study of Indian human dry skull. Int J Health Sci Res 2015;8:238-42.
10. Archana R, Jinu MK, Sathyapriya B, Johnson WM. Morphology of vermian fossa in south Indian human adult skull bones. Int J Anat Radiol Surg 2017;6:AO01-4.
11. Singh A, Gupta R. Morphological and morphometric study of vermian fossa. Int J Adv Integr Med Sci 2017;2:198-200.
12. Pandey AK, Suma Latha S, Kotian SR. A cadaveric study of the internal occipital crest and vermian fossa with its clinical significance. Int J Anat Res 2018;6:5520-4.
13. Kunc V, Fabik J, Kubickova B, Kachlik D. Vermian fossa or median occipital fossa revisited: Prevalence and clinical anatomy. Ann Anat 2020;229:151458.
14. Cireli E, Ozturk L, Yurtseven M, Ba Alolu K. An examination of the skull in the occipitalis interna area and fossa vermiana. Ege Tp Dergisi 1990;29:793-6.
15. Sanudo JR, Vázquez R, Puerta J. Meaning and clinical interest of the anatomical variations in the 21st century. Eur J Anat 2003;7:1-3.
16. Shoja MM, Tubbs RS, Khaki AA, Shokouhi G. A rare variation of the posterior cranial fossa: Duplicated falx cerebelli, occipital venous sinus, and internal occipital crest. Folia Morphol (Warsz) 2006;65:171-4.

Original Article

Considering the Surface Area and Sagittal Angle in a Pair of Lumbosacral Facets: Determining the Structural Relevance of Asymmetric Facets at the Lumbosacral Junction

Uchenna Kenneth Ezemagu[1,2], F. Chinedu Akpuaka[1,3], Emmanuel C. Iyidobi[4], Chike P. Anibeze[1,5]

[1]Department of Anatomy, Faculty of Basic Medical Sciences, College of Medicine, Abia State University, Uturu, [2]Department of Anatomy, Alex Ekwueme Federal University Ndufu Alike Ikwo, Ebonyi State, [3]Department of Surgery, College of Medicine, Chukwuemeka Odumegwu Ojukwu University, Uli Campus, Anambra State, [4]Department of Orthopaedic, National Orthopaedic Hospital, [5]Department of Anatomy, Enugu State University of Science and Technology, Enugu, Nigeria

Abstract

Introduction: The mechanism of spine dysfunction that was linked to asymmetry in facet joint planes remains poorly understood. We determined the surface area and sagittal angle in a pair of L4, L5, and S1 vertebral facets. We aimed to explain the structural relevance of asymmetric facets at the lumbosacral junction. **Material and Methods:** Vertebral columns of 45 adult male human cadavers were cut at the L3–L4 intervertebral disc. Each section was macerated and tied together in a sequence to obtain the value of sagittal angle of the superior facets of L4, L5, and S1 vertebrae and area of the inferior facets of L4 and L5 vertebrae, using a modified protractor and graph paper method, respectively. Asymmetry was determined using the formula propound by Plochocki (2002). **Results:** The mean value of surface area of the left and right inferior facets of L4 and the left and right inferior facets of L5 was 161 ± 24 and 168 ± 23 mm^2 and 200 ± 28 and 218 ± 33 mm^2, respectively. The mean value of sagittal angle of the left and right superior facets of L4, L5, and S1 was 37.71° ± 4.38°, 36.18° ± 4.8°, 46.96° ± 6.49°, 48.51° ± 6.25°, 52.49° ± 5.1°, and 54.67° ± 5.25°, respectively. The degree of asymmetry in the area of the inferior facets of L4 and L5 ranges from 0% to 30% and 0%–32.26%, respectively, and that for sagittal angle of the superior facets of L4, L5, and S1 was 0%–37.93%, 0%–30.95%, and 0%–26.32%, respectively. **Discussion and Conclusion:** This study would suggest that despite the statistically significant mean differences in the paired variables, the vertebrae were free of any pathological change but with consequent adaptive features. However, the stress effects would suggest that the left lumbosacral facet joints are predisposed to dysfunction of mechanical origin.

Keywords: *Adaptation, back pain, biomechanics, bipedal posture, body weight*

Introduction

The extent of asymmetry in a pair of vertebral facets that becomes clinically relevant remains challenging to orthopedic surgeons and chiropractors. We cannot overemphasize the significance of facet asymmetry in medical practice. It may precipitate disc degeneration and hernia,[1] contributes to the development of different types of idiopathic scoliosis,[2] and predicts the occurrence of facet cyst and low back pain.[3,4] Although the incidence of asymmetry in a pair of the superior facets at the thoracolumbar region of the spine was rare,[5] some authors[6] queried its relevance in facet joint disease at the lumbosacral junction.

Second, in anthropology, lumbosacral weakness[7] and certain spine derangements around the lumbosacral junction of a modern man were considered to be consequences of skeletal modifications to enhance stability, yet the reason remains vague.[7,8] Although little research has focused on asymmetry in the lower body,[9] this study could suggest a clear reason for the above proposal and explain in part some factors in the puzzle of lumbosacral adaptation to bipedal posture.

Third, the lumbosacral junction transmits the weight of the upper body to the pelvis, and it is the most frequent site of back pain and facet cyst.[3,4] Mechanical forces, static and dynamic stress,[10,11] higher body mass index,[12,13] and a smaller relative cross-sectional area of the paraspinal muscle[14] were linked to disc degeneration and back pain. Similarly, authors[8,15,16] explained the pattern of weight transmission at the lumbosacral

How to cite this article: Ezemagu UK, Akpuaka FC, Iyidobi EC, Anibeze CP. Considering the surface area and sagittal angle in a pair of lumbosacral facets: Determining the structural relevance of asymmetric facets at the lumbosacral junction. J Anat Soc India 2019;XX:XX-XX.

Article Info

Received: 13 May 2019
Accepted: 13 January 2020
Available online: ***

Address for correspondence:
Dr. Uchenna Kenneth Ezemagu, Department of Anatomy, Alex Ekwueme Federal University Ndufu Alike Ikwo, Ebonyi State, P.M.B. 1010, Nigeria. E-mail: uchennaezemagu@gmail.com

Access this article online

Website: www.jasi.org.in
DOI: 10.4103/JASI.JASI_53_19
Quick Response Code:

junction and noted that lumbosacral facets were subjected to mechanical stress.

Given these findings, necessitated studies designed to determine the extent of asymmetry in surface area and sagittal angle in a pair of vertebral facets at the lumbosacral junction and explain how each facet responds to the stress of upper body weight. It would be of benefit in the management of spine derangement of mechanical origin.

Material and Methods

After institutional review board approval for this study in line with the conditions of the Medical Research Ethics Committee, a total of 45 adult male human cadavers (age range: 25–35 years, mean: 28 years) were involved since there were no female cadavers available during the study. The cadavers were being dissected by medical students during gross anatomy dissection curriculum.

The vertebral columns were cut at the L3–L4 intervertebral disc, using a hand saw [Figure 1]. Vertebrae that belong to each section were obtained through the process of maceration. All the vertebrae were reported by a pathologist to be fully ossified and free of any pathological change or inborn abnormality. The value of the left and right inferior facet areas of the fourth and fifth lumbar vertebrae was obtained in a sequence using graph paper method.[8,15] The number of squares covered on the graph paper was independently counted and determined by the three researchers to minimize interobserver error. The value of the sagittal angle of L4, L5, and S1 vertebrae was obtained in a sequence using a modified protractor.[5,17]

The extent of asymmetry in facet area and sagittal angle was calculated as follows: ([left side − right side] ÷ right side) × 100 as adopted by Plochocki.[9] The descriptive statistics of the data showed that the continuous random variables were normally distributed as shown in Figure 2a-c. Therefore, we adopted a paired sample *t*-test to compare the two means of paired inferior facet area and sagittal angle to establish the level of significance of the mean differences. Furthermore, regression analyses were conducted on paired variables.

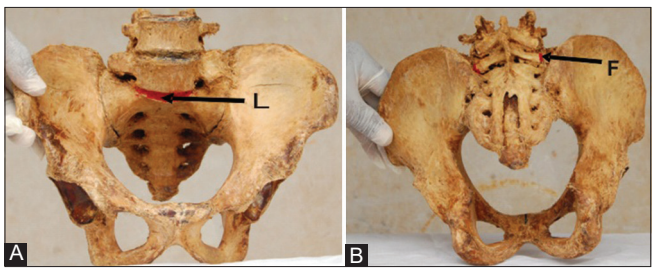

Figure 1: Anterior (A) and posterior (B) views of lower portion of the spine (L4 – coccyx) and pelvic girdle of a dissected cadaver, showing the Lumbosacral junction(L) and right L5/S1 facet joint(F)

Results

The statistics in Table 1 showed that the mean values of surface area of the left facet of the fourth lumbar vertebra (L4LF), the right facet of the fourth lumbar vertebra (L4RF), the left facet of the fifth lumbar vertebra (L5LF), and the right facet of the fifth lumbar vertebra (L5RF) were 161 ± 24, 168 ± 23, 200 ± 28, and 218 ± 33 mm^2, respectively. The mean values of the sagittal angle of the left (L4LSA) and right (L4RSA) superior facets of L4, the left (L5LSA) and right (L5RSA) superior facets of L5, and the left (S1LSA) and right (S1RSA) superior facets of S1 were $37.71° \pm 4.38°$, $36.18° \pm 4.8°$, $46.96° \pm 6.49°$, $48.51° \pm 6.25°$, $52.49° \pm 5.1°$, and $54.67° \pm 5.25°$, respectively. The result was characterized by increase in sagittal angle in a sequence from the fourth lumbar to the first sacral vertebra.

The range of asymmetry in the area of corresponding inferior facets of L4 and L5 was –23.16%–30.00% and −32.26%–20.99%, respectively, and that for sagittal angle of L4, L5, and S1 was −14.29%, 37.93%; -30.95%, 25.58% and -26.32%, 20.00%, respectively. [Figure 2a-c]. Having adopted the formula propound by Plochocki[9] to determine the proportion of asymmetry in a pair of corresponding structures, the negative value implied that the right parameter was greater than the left counterpart in some cases.

The correlation matrices and mean differences between the paired variables in Table 2 showed that the mean value of surface area of L4RF and L5RF was significantly ($P < 0.05$) higher than that of L4LF and L5LF, respectively. Likewise, the mean value of L4LSA, L5RSA, and S1RSA was significantly ($P < 0.05$) higher than that of L4RSA, L5LSA, and S1LSA, respectively.

The regression analyses in Table 3 showed that the regression coefficients of the predictors were highly significant ($P < 0.01$), indicating that predictions made on the resultant regression equations are reliable. Likewise, the multiple regression analyses revealed a linear relationship of the sagittal angle in a sequence from L4 to S1, which could be predicted with the following equations:

$$L5LSA\ (°) = -9.689 + 0.946\ L4LSA + 0.399\ S1LSA$$

$$L5RSA\ (°) = 4.873 + 0.706\ L4RSA + 0.331\ S1RSA.$$

Discussion

The analysis of the work was a setback for lack of a statistical package determining asymmetry in a pair of structures among individuals in a given population. Although manual measurement of vertebral column angulations was valid in assessment of spine derangement,[18] a simple diagnostic tool and methodology determining the sequential relationship of the vertebral facets of an individual is essential. The regression equations in Table 3 could serve as functional matrices to adopt during identification of an individual sacrum and lower

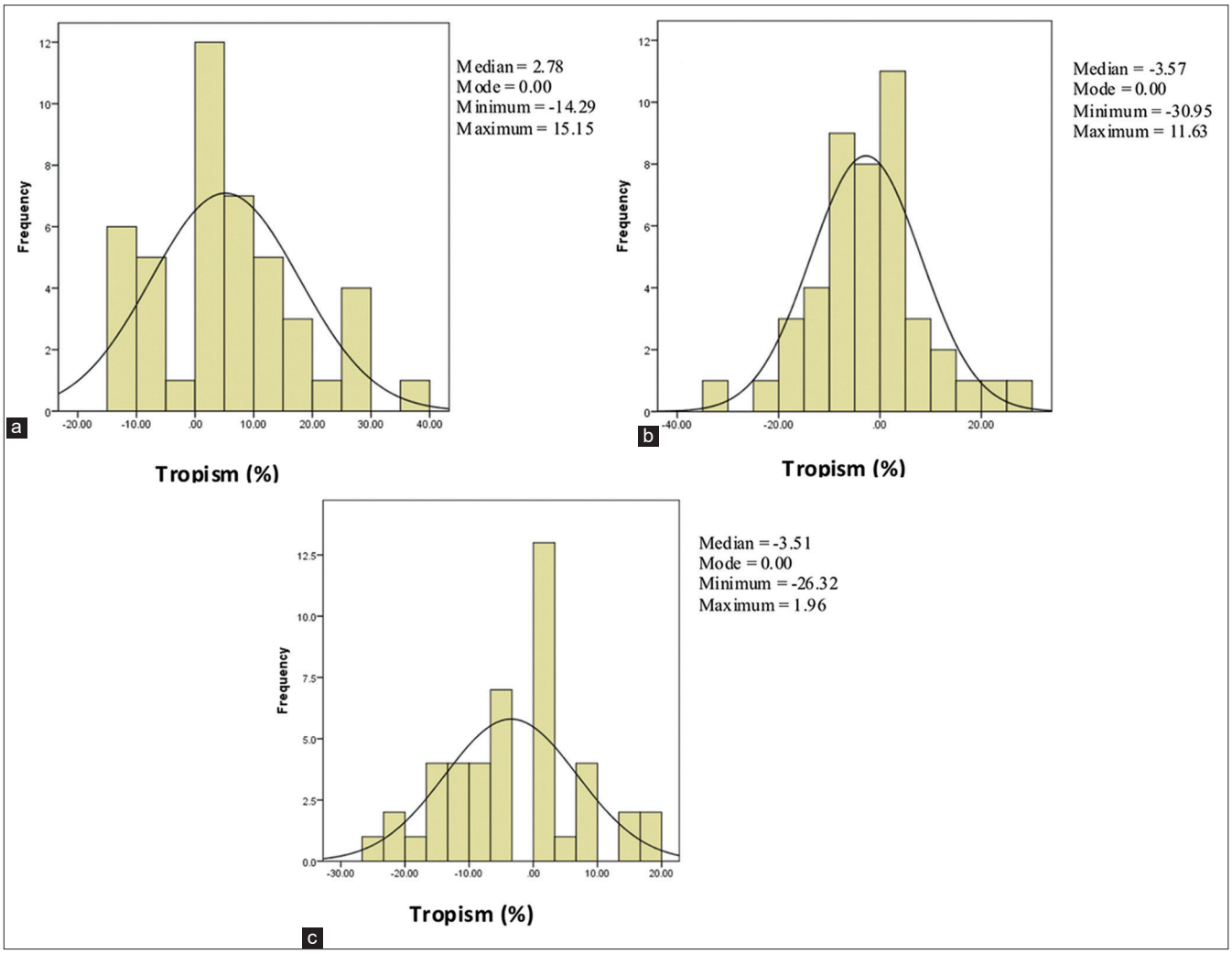

Figure 2: (a-c) Frequency distribution of degree of facet joint tropism of L4 (a), L5 (b), and S1 (c), showing a normal distribution curve

Table 1: Descriptive statistics of L4, L5, and S1 variables

	L4FL	L4FR	L4LSA	L4RSA	L5FL	L5FR	L5LSA	L5RSA	S1LSA	S1RSA
Mean	161.11	168.13	37.71	36.18	200.18	217.96	46.96	48.51	52.49	54.67
SEM	3.63	3.42	0.65	0.71	4.16	4.94	0.97	0.93	0.76	0.78
Median	156.00	172.00	38.00	36.00	202.00	218.00	48.00	48.00	53.00	56.00
Mode	156.00	172.00	40.00	37.00	208.00[a]	216.00	50.00	43.00[a]	54.00	57.00
SD	24.37	22.94	4.38	4.77	27.90	33.16	6.49	6.25	5.12	5.25
Range	120.00	92.00	17.00	21.00	116.00	124.00	32.00	26.00	21.00	23.00
Minimum	112.00	132.00	30.00	27.00	148.00	156.00	29.00	34.00	40.00	42.00
Maximum	232.00	224.00	47.00	48.00	264.00	280.00	61.00	60.00	61.00	65.00

a: Two modes exist and the least value was chosen. Number of valid cases=45. L4FL: Surface area of the left inferior facet of the fourth lumbar vertebra (mm^2), L4FR: Surface area of the right inferior facet of the fourth lumbar vertebra (mm^2), L4LSA: Sagittal angle of the left superior facet of the fourth lumbar vertebra (°), L4RSA: Sagittal angle of the right superior facet of the fourth lumbar vertebra (°), L5FL: Surface area of the left inferior facet of the fifth lumbar vertebra (mm^2), L5FR: Surface area of the right inferior facet of the fifth lumbar vertebra (mm^2), L5LSA: Sagittal angle of the left superior facet of the fifth lumbar vertebra (°), L5RSA: Sagittal angle of the right superior facet of the fifth lumbar vertebra (°), S1LSA: Sagittal angle of the left superior facet of the first sacral vertebra (°), S1RSA: Sagittal angle of the right superior facet of the first sacral vertebra (°)

lumbar vertebrae in a forensic anthropology laboratory. Second, the equations might be useful to orthopedic surgeons during reconstructive spine intervention procedures that aim to retain the original alignment of the facets. Such techniques include vertebroplasty and kyphoplasty,[19] in conjunction with pedicle screw-based instrumentation used for treating certain spinal geometric distortion.[20-22]

Table 2: The test of mean differences between L4, L5, and S1 corresponding variables

	Paired differences						
	Mean difference	SD	SEM	95% confidence interval of the differences		*t*-statistics	Significant (two-tailed)
				Lower	Upper		
L4FL−L4FR	−7.022	21.052	3.138	−13.347	−0.697	−2.238	0.030
L4LSA - L4RSA	1.533	4.288	0.639	0.245	2.822	2.399	0.021
L5FL−L5FR	−17.778	26.178	3.903	−25.643	−9.913	−4.556	0.000
L5LSA - L5RSA	−1.556	4.998	0.745	−3.057	−2.054	−2.088	0.043
S1LSA - S1RSA	−2.178	5.614	0.837	−3.864	−0.491	−2.602	0.013

Based on the *P* value column, all the tests are significant ($P<0.05$). L4FL: Surface area of the left inferior facet of the fourth lumbar vertebra (mm^2), L4FR: Surface area of the right inferior facet of the fourth lumbar vertebra (mm^2), L4LSA: Sagittal angle of the left superior facet of the fourth lumbar vertebra (°), L4RSA: Sagittal angle of the right superior facet of the fourth lumbar vertebra (°), L5FL: Surface area of the left inferior facet of the fifth lumbar vertebra (mm^2), L5FR: Surface area of the right inferior facet of the fifth lumbar vertebra (mm^2), L5LSA: Sagittal angle of the left superior facet of the fifth lumbar vertebra (°), L5RSA: Sagittal angle of the right superior facet of the fifth lumbar vertebra (°), S1LSA: Sagittal angle of the left superior facet of the first sacral vertebra (°), S1RSA: Sagittal angle of the right superior facet of the first sacral vertebra (°). SD: Standard deviation, SEM: Standard error of mean

Table 3: Regression analysis summary for L4, L5, and S1 corresponding variables

Variables		Coefficients					
		Constant			Independent variable		
Dependent	Independent	*B*	*t*-statistics	*P*	*B*	*t*-statistics	*P*
L4FR	L4FL	76.313	4.101	0.000	0.570	4.989	0.000
L4LSA	L4RSA	18.972	4.498	0.000	0.518	4.480	0.000
L5FR	L5FL	64.611	2.308	0.026	0.766	5.529	0.000
L5LSA	L5RSA	12.092	2.168	0.036	0.719	6.301	0.000
S1LSA	S1RSA	30.364	4.085	0.000	0.405	2.990	0.005

L4FL: Surface area of the left inferior facet of the fourth lumbar vertebra (mm^2), L4FR: Surface area of the right inferior facet of the fourth lumbar vertebra (mm^2), L4LSA: Sagittal angle of the left superior facet of the fourth lumbar vertebra (°), L4RSA: Sagittal angle of the right superior facet of the fourth lumbar vertebra (°), L5FL: Surface area of the left inferior facet of the fifth lumbar vertebra (mm^2), L5FR: Surface area of the right inferior facet of the fifth lumbar vertebra (mm^2), L5LSA: Sagittal angle of the left superior facet of the fifth lumbar vertebra (°), Sagittal angle of the right superior facet of the fifth lumbar vertebra (°), S1LSA: Sagittal angle of the left superior facet of the first sacral vertebra (°), S1RSA: Sagittal angle of the right superior facet of the first sacral vertebra (°).Regression equations: L4FR=76.313 + 0.570 L4FL, L4LSA=18.972 + 0.518 L4RSA, L5FR=64.611 + 0.766 L5FL, L5LSA=12.092 + 0.719 L5RSA, S1LSA=30.364 + 0.405 S1RSA

In support of the results in Table 1, some authors[15] observed that average inferior facet area of L4 and L5 was 1.49 ± 0.25 and 1.69 ± 0.31 cm^2, respectively. Likewise, the mean value of the left sagittal angle of the superior facets of L4, L5, and S1 was 35° ± 11°, 44° ± 13°, and 55° ± 15°, respectively, and that of the right counterpart was 40° ± 14°, 41° ± 13°, and 36° ± 17°, respectively.[17] The values from this study were within the range of mean value of the figures above except for the value of the right sagittal angle of S1 vertebra. The difference was attributed to race[17] or biomechanical environment.[23,24] Moreover, inherent error due to approximation and difficulty in locating anatomic landmarks might have contributed to the difference. However, independent assessments by the three researchers were adopted in this study to minimize these sources of error.

Although some authors[7,25] observed tropism on the lumbosacral joint planes, others[2,26] had no evidence of asymmetry in the superior or inferior facets of the lumbar vertebrae in children. Most likely, asymmetry in the facet area or facet joint planes at the lumbosacral junction in adults could be an outcome of uneven distribution of upper body weight and stress on the pair of facets during vertebral bone growth and remodel. Similarly, Rubbery[27] reported that the increase in sagittal angle of the lumbar vertebral facets in a sequence inclines the facet joint at the lumbosacral junction toward the coronal plane. Thus, the superior facet of S1 acts as an anterior wedge to the matching inferior facet of L5. The alignment was likely to enable a load on the body of vertebrae to gradually shift to their facets and also resist shear of the spine due to vertically directed axial load on the lumbosacral angle [Figure 1].

Notably, the vertebral column works as a driving shaft, and facet joints guide the extent and direction of its movements. If an axial torque rotation is applied at one end of it, every segment should be subjected to a twisting moment, in a direction perpendicular to the radius of the segment. Therefore, facet asymmetry presents an absence of common center of curvature for the left and right facets during hyperextension, flexion, and rotation of the spine. Precisely, it creates a rotational stress to the facet joint structures, leading to a plastic deformation,[28] especially on the counterpart with smaller radius and surface area. Stress is a measure of the force, an object experience per unit

cross-sectional area, indicating an inverse relationship with surface area.

Therefore, mechanical strength of a vertebral facet, subject to the pressure from the pull of gravity on body weight and load, depends on its cross-sectional area. This would suggest that the left facet joint structures of the lower lumbar vertebrae were predisposed to stress effects and facet dysfunction of mechanical origin because of their smaller surface area when compared with the right corresponding facets.

However, the fifth lumbar vertebra gives origin to iliolumbar ligaments and relatively thickest mammillary processes and muscles that reinforce its superior facets.[10] The ligament and muscles attach to the pelvis. Ardently, we observed that the mammillary tubercle of the superior facet of S1 that aligned with the relatively larger inferior facet of L5 was likely to protrude more than its counterpart. The above-observed adaptive features might have reinforced the facets enabling them to accommodate the asymmetrical stress and also transmit it to the pelvis through the ligaments and muscles.

This study would suggest that despite the statistically significant mean differences in the paired variables in Table 2, the vertebrae were free of any pathological change. It could be an indication that stresses encountered by the pair of facets were within the range of their allowable and working stresses. However, it might have explained in part why earlier researchers in anthropology attributed weakness and low back pain to the lumbosacral junction. Moreover, it revealed a structural variation in the skeletal framework of a modern man, and how it could affect his biomechanical environment, as well as offered insight to this paleontological puzzle.

Conclusion

The increase in sagittal angle of the lumbar vertebral facets in a sequence led to a wedge alignment of the inferior facets of L5 and superior facets of S1. This arrangement could resist shear due to vertically directed axial load on the lumbosacral angle. Second, the mammillary tubercle of the superior facet of S1 that aligns with the relatively larger inferior facet of L5 was likely to protrude more than that of its corresponding facet. Furthermore, the mean value of the right facet area and sagittal angle greater than the left counterpart predisposed the left facets to stress effects and facet dysfunction of mechanical origin.

Acknowledgment

The authors would like to thank Dr. C. O. Ani (MD, FWACS) for proofreading the manuscript. We thank Dr. G. Ndukwe and Dr. S. Danborno for granting us access to the facilities at the Gross Anatomy laboratories of Abia State University and Ahmadu Bello University, Zaria, respectively, and Dr. Felix Aguboshim for the statistical analysis of this work.

Financial support and sponsorship

Nil.

Conflicts of interest

There are no conflicts of interest.

References

1. Noren R, Trafimow J, Andersson GB, Huckman MS. The role of facet joint tropism and facet angle in disc degeneration. Spine (Phila Pa 1976) 1991;16:530-2.
2. Masharawi YM, Peleg S, Albert HB, Dar G, Steingberg N, Medlej B, *et al.* Facet asymmetry in normal vertebral growth: Characterization and etiologic theory of scoliosis. Spine (Phila Pa 1976) 2008;33:898-902.
3. Rahimizadeh A. Bleeding in a lumbar juxtafacet cyst with Cauda Equina syndrome: Report of a case and review of the literature. World Spinal Column J 2011;2:46-51.
4. Cassidy JD, Loback D, Yong-Hing K, Tchang S. Lumbar facet joint asymmetry. Intervertebral disc herniation. Spine (Phila Pa 1976) 1992;17:570-4.
5. Patel MM, Singel TC. Modification of protractor to measure the sagittal angle of superior articular facets of vertebrae. J Anat Soc India 2003;52:15.
6. Murtagh FR, Paulsen RD, Rechtine GR. The role and incidence of facet tropism in lumbar spine degenerative disc disease. J Spinal Disord 1991;4:86-9.
7. Giles LG, Singer KP. Clinical Anatomy and Management of Low Back Pain Series. Oxford: Butterworth Heinemann; 1997.
8. Ezemagu UK, Anibeze CP, Akpuaka CF. Considering the inferior surface area of lower lumbar vertebrae: Determining weight transmission pattern at the lumbosacral junction. Anat Sci Int 2018;93:277-83.
9. Plochocki JH. Directional bilateral asymmetry in human sacral morphology. Int J Osteoarchaeol 2002;12:349-55.
10. Sowa GA, Coelho JP, Bell KM, Zorn AS, Vo NV, Smolinski P, *et al.* Alterations in gene expression in response to compression of nucleus pulposus cells. Spine J 2011;11:36-43.
11. Louie PK, Presciutti SM, Iantorno SE, Bohl DD, Shah K, Shifflett GD, *et al.* There is no increased risk of adjacent segment disease at the cervicothoracic junction following an anterior cervical discectomy and fusion to C7. Spine J 2017;17:1264-71.
12. Ezemagu UK, Anibeze CI, Ani CO, Ossi GC. Correlation of body mass index with low back pain amongst patients without injury in a Nigeria population. Int J Curr Microbiol Appl Sci 2016;5:371-8.
13. Bono OJ, Poorman GW, Foster N, Jalai CM, Horn SR, Oren J, *et al.* Body mass index predicts risk of complications in lumbar spine surgery based on surgical invasiveness. Spine J 2018;18:1204-10.
14. Kim JY, Ryu DS, Paik HK, Ahn SS, Kang MS, Kim KH, *et al.* Paraspinal muscle, facet joint, and disc problems: Risk factors for adjacent segment degeneration after lumbar fusion. Spine J 2016;16:867-75.
15. Aruna N, Rajeshwari T, Rajangam S. Transmission of weight through the neural arch of lumbar vertebrae in man. J Anat Soc India 2003;52:128-31.
16. Pal GP, Routal RV. Transmission of weight through the lower thoracic and lumbar regions of the vertebral column in man. J Anat 1987;152:93-105.
17. Patel MM, Gohil DV, Singel TC. Orientation of superior articular facets from C3 to S1 vertebrae. J Anat Soc India 2004;53:35-9.
18. Langensiepen S, Semler O, Sobottke R, Fricke O, Franklin J,

Schönau E, *et al.* Measuring procedures to determine the cobb angle in idiopathic scoliosis: A systematic review. Eur Spine J 2013;22:2360-71.
19. Limthongkul W, Karaikovic EE, Savage JW, Markovic A. Volumetric analysis of thoracic and lumbar vertebral bodies. Spine J 2010;10:153-8.
20. Mai HT, Mitchell SM, Hashmi SZ, Jenkins TJ, Patel AA, Hsu WK, *et al.* Differences in bone mineral density of fixation points between lumbar cortical and traditional pedicle screws. Spine J 2016;16:835-41.
21. Ponnusamy KE, Iyer S, Gupta G, Khanna AJ. Instrumentation of the osteoporotic spine: Biomechanical and clinical considerations. Spine J 2011;11:54-63.
22. Janssen I, Ryang YM, Gempt J, Bette S, Gerhardt J, Kirschke JS, *et al.* Risk of cement leakage and pulmonary embolism by bone cement-augmented pedicle screw fixation of the thoracolumbar spine. Spine J 2017;17:837-44.
23. Williams PL. Gray's Anatomy. 38th ed.. Edinburgh: Churchill Livingstone; 2000.
24. Trummer M, Flaschka G, Tillich M, Homann CN, Unger F, Eustacchio S, *et al.* Diagnosis and surgical management of intraspinal synovial cysts: Report of 19 cases. J Neurol Neurosurg Psychiatry 2001;70:74-7.
25. Putz R. The functional morphology of the superior articular processes of the lumbar vertebrae. J Anat 1985;143:181-7.
26. Ledet EH, Sanders GP, DiRisio DJ, Glennon JC. Load-sharing through elastic micro-motion accelerates bone formation and interbody fusion. Spine J 2018;18:1222-30.
27. Rubbery TP. Degenerative Spondylolisthesis. Orthopedics 2001;12:83.
28. Labrom RD. Growth and maturation of the spine from birth to adolescence. J Bone Joint Surg Am 2007;89 Suppl 1:3-7.

Original Article

In vivo Cross-Sectional Topographic Anatomy at Sternal Angle on Magnetic Resonance Imaging

Rohit Aggarwal, Sreedhar Muthukrishnan Calicut[1], Raheem Abdul Sheik, Vijaya Sagar Theegala[2], Indrani Mukhopadhyay[3]

Departments of Radiology, 7 Air Force Hospital, Kanpur, Uttar Pradesh, [1]Commandant, Military Hospital, Kirkee, [3]Department of Obstetrics and Gynaecology, Armed Forces Medical College, Pune, Maharashtr, [2]Department of Anatomy, Sri Ramachandra Medical College and Research Institute, Chennai, Tamil Nadu, India

Abstract

Introduction: The manubriosternal angle, first described by Louis in 1825, is an important landmark in the anatomy of the thorax and has been conventionally described as corresponding to the T4–5 IV disc level based on cadaveric dissections. The objective of this study was to document the level of the angle of Louis and various anatomic structures that also correspond to the same level in living individuals based on multiplanar magnetic resonance (MR) images. **Material and Methods:** We reviewed MR scans of the cervicodorsal spine of 262 individuals comprising 174 males and 88 females in the age range 14–76 years. For each individual, the vertebral level of the following structures was noted on T1-weighted (T1W)/T2-weighted (T2W) turbo spin echo (TSE) coronal and sagittal images, namely tracheal bifurcation (TB), aortic arch (AA), and sternal angle (SA). **Results:** The SA was most commonly seen corresponding to the T5 vertebral body level (45.20%) and at T4–5 IV disc level in only 20.45% of the individuals. The convexity of the arch of the aorta was seen in the majority of the individuals corresponding to the T3 vertebral body level (47.96%). TB was seen at T4 level in 34.35% and only in 22.69% at the T4–5 IV disc level. **Discussion and Conclusion:** The anatomical level of the SA, AA, and TB in living individuals as assessed on MR images is significantly different from the traditionally held belief based on cadaveric dissections.

Keywords: *Aortic arch, magnetic resonance imaging, sternal angle, tracheal bifurcation*

Introduction

Sternal angle (SA), the forward prominence formed by the manubriosternal joint, is an important landmark in the anatomy of the thorax. Based on cadaveric studies, conventional anatomical textbooks mention the SA plane and surface marking of SA to correspond to many anatomical structures including tracheal bifurcation (TB) and aortic arch (AA).[1-3] However, this belief has been challenged by many authors using computed tomography (CT)-based *in vivo* studies. All these studies conducted on different ethnic populations have shown results contrary to this traditional belief, and there has been a very wide variation in the vertebral levels of these structures in living human beings. Furthermore, there is a variable correlation among AA, TB, and SA plane. There is also variable evidence regarding age and gender differences in the levels of these structures.[4-8] Surface anatomy and markings are essential components of curriculum for medical students, and it is prudent to update this knowledge with availability of modern cross-sectional imaging modalities. This information is vital for planning and execution of many lifesaving interventions. There are few *in vivo* studies in medical literature that have assessed the anatomy of SA in human beings using magnetic resonance imaging (MRI) as an anatomical tool. MRI by virtue of its direct multiplanar imaging capability and superior contrast resolution is an excellent modality for depicting anatomy. The *in vivo* anatomical details of various anatomical landmarks that are traditionally believed to lie at the SA plane can be accurately depicted using MRI. In addition, results obtained from free-breathing MRI scans are likely to be closest to the normal physiology in human subjects. This study is an attempt to review the traditional anatomical descriptions of the SA plane and other thoracic structures (AA and TB) with respect to their corresponding vertebral levels and also in relation to each other using free-breathing MRI scans of the upper thorax in living individuals.

How to cite this article: Aggarwal R, Calicut SM, Sheik RA, Theegala VS, Mukhopadhyay I. *In vivo* cross-sectional topographic anatomy at sternal angle on magnetic resonance imaging. J Anat Soc India 2020;69:XX-XX.

Article Info

Received: 09 May 2020
Accepted: 28 August 2020
Available online: ***

Address for correspondence:
Dr. Rohit Aggarwal,
Department of Radiology,
7 Air Force Hospital,
Kanpur - 208 004,
Uttar Pradesh, India.
E-mail: rohitaggy@gmail.com

Access this article online

Website: www.jasi.org.in
DOI: 10.4103/JASI.JASI_85_20
Quick Response Code:

Material and Methods

We reviewed 262 MRI scans of the cervicodorsal spine of patients done between September 2018 and December 2019 at our institution using a Philips Achieva 1.5 Tesla scanner (Philips Medical Systems, Veenpluis 4-6, The Netherlands). Institutional ethical committee clearance was obtained. The following categories of patients were excluded from the study:

- Patients with scoliosis of the cervical and/or dorsal spine
- Patients with basilar invagination
- Patients with collapse vertebrae
- Patients with any congenital vertebral anomaly
- Patients with evidence of sternotomy
- Suboptimal visualization of structure under study.

All the MRI scans were performed in supine position with both arms lying parallel to and by the side of the torso. The routine protocol for MRI of the cervicodorsal spine at our institution consisted of T1-weighted (T1W) and T2-weighted (T2W) TSE sagittal and coronal and T2W gradient recalled echo (GRE) axial images, respectively, of which only the T1W and T2W coronal and sagittal images were reviewed for the purpose of this study.

The imaging parameters for the MR scan were as follows:

- T1W TSE sagittal: Repetition time (TR) – 407 ms and time to echo (TE) – 14 ms
- T2W TSE sagittal: TR – 4000 ms and TE – 115 ms
- T1W TSE coronal: TR – 400 ms and TE – 15 ms.

All the scans were done at a field of view of 280 mm, slice thickness 3 mm, and with a matrix size 512 × 512.

For each individual, the vertebral levels corresponding to each of the following structures were noted: TB, AA, and SA. The vertebral levels were counted from above downward with the C2 vertebra as the reference due to its unique appearance on sagittal and coronal images. The sagittal images were used to evaluate the vertebral levels corresponding to the SA and AA, respectively, whereas the coronal images were used to evaluate the vertebral levels of the TB. A reference line was generated across the entire set of images in a series using an inbuilt software tool, which ensured that the line corresponded to the same coordinates on all the images of a series. A horizontal line drawn from the anterior aspect of the manubriosternal joint and another horizontal line drawn along the inferior surface (summit of concavity) of the AA were extended posteriorly across the vertebral column on sagittal images to assess the level of the SA [Figure 1] and the AA [Figure 2], respectively. The carinal angle was identified on coronal images, and a horizontal line corresponding to the inferior surface of the carina was generated across all the coronal images in the series to identify the corresponding vertebral level [Figure 3]. The vertebral body level or the IV disc level at which these lines passed through the vertebral column was noted. For ease of statistical analysis, these vertebral levels were further grouped into three broad groups [Figure 4]:

- Level 1: Superior to T4 vertebral body level
- Level 2: At the T4 vertebral body and T4–5 IV disc level
- Level 3: Inferior to T4–5 IV disc level.

Age groups were classified into three subgroups as <30 years, 30–50 years, and >50 years.

Figure 1: T2-weighted mid-sagittal image of the cervicodorsal spine with horizontal reference line to evaluate the vertebral level of sternal angle (white arrow)

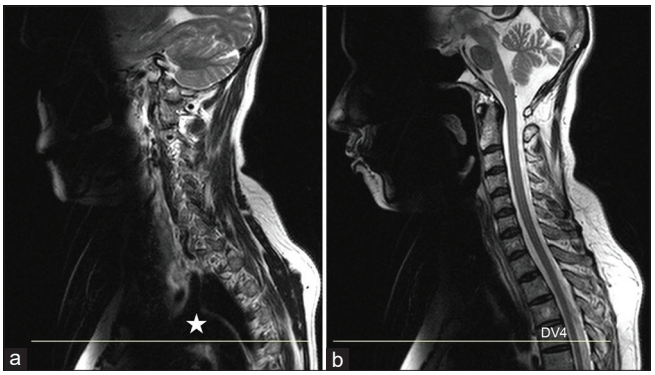

Figure 2: T2-weighted sagittal images. (a) Reference line across the summit of inferior concavity of aortic arch (star). (b) Reference line extending up to the fourth dorsal vertebra

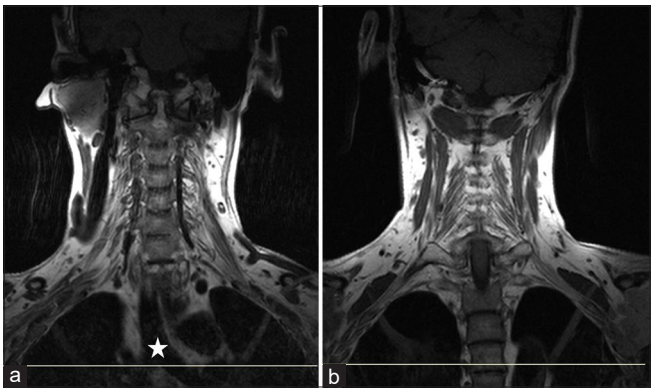

Figure 3: T1-weighted coronal images. (a) Reference line across carina (star). (b) Reference line extending up to the dorsal vertebra

Chi-square test and mean test were used to assess the statistical significance in various data subsets. The relationship between the superior surface of AA and the manubrium sterni was also evaluated by drawing an additional horizontal line posteriorly from the sternal notch toward the vertebral column.

Results

We analyzed the MRI scans of 262 individuals comprising 174 males and 88 females of the age range 14–76 years. Out of the total study group of 262 individuals, only the number of scans, as shown in Table 1, was included in the data subset for studying the respective structures.

The SA corresponded to Level 3 in the majority of the individuals (58.91%) [Table 2]. A statistically significant difference was noted in the levels of the SA between males and females. Among females, the SA corresponded to Level 3 in 74%, whereas in males, it corresponded to Level 2 (46.71%) and 3 (49.63%), respectively ($P < 0.001$) [Figure 5]. The age distribution was as per Figure 6.

The undersurface of the AA corresponded to Level 2 in the majority of the individuals (72.73%) [Table 3]. In the majority of both males (76.11%) and females (67.44%), the concavity of the AA corresponded to Level 2 [Figure 5]. In the majority of the individuals of all the age groups, the undersurface of the AA corresponded to Level 2 [Figure 6].

The bifurcation of the trachea corresponded to Level 2 in the majority of the individuals (54.07%) [Table 4]. In the majority of both females (55.35%) and males (57.90%), the TB corresponded to Level 2 [Figure 5]. A statistically significant difference was noted in the level of the TB in individuals below 50 years (<30 years – 71.40% and 30–50 years – 57.73% at Level 2) and those above 50 years (57.14% at Level 3) ($P < 0.05$) [Figure 6].

No significant difference was noted in levels of TB and AA in males and females. Furthermore, no significant difference was noted in levels of SA and AA in different age groups ($P > 0.05$). On comparing levels of various structures in the same individual, AA and SA corresponded to the same level in 36.87% of the individuals (Level 2 in 29.03% and Level 3 in 7.83%). The AA was higher to the SA in 56.68% of the individuals ($n = 217$).

The TB and SA were at the same level in 41.13% of the individuals (Level 2 in 24.05% and Level 3 in 17.08%). In 42.4% of the individuals, the TB corresponded to a level higher to the SA ($n = 158$). The AA and TB were at the same level in 57.24% of the individuals (Level 1 in 46.20% and Level 3 in 11.03%). In 35.17%, the TB was below the SA ($n = 145$). Out of 133 individuals in whom we could evaluate the vertebral level of all the three structures, it was noted that they were at the same level in only 20.30% of the individuals (15.78% at Level 2 and 4.51% at Level

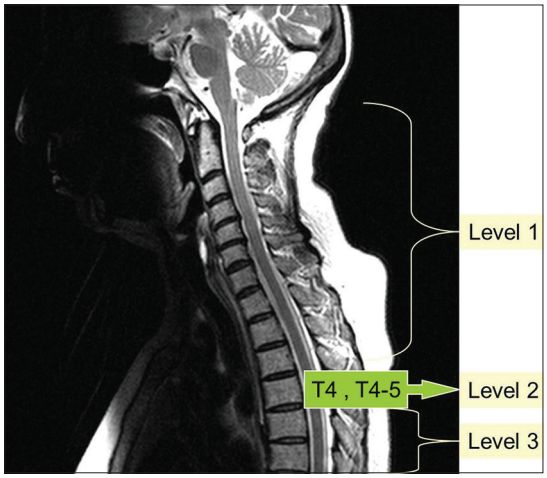

Figure 4: T2-weighted sagittal image showing grouping of vertebral levels

Table 1: Number of cases included in the data subset

Parameter	Excluded	Studied
Sternal angle	43	219
Arch of aorta	42	220
Tracheal bifurcation	90	172

Table 2: Vertebral levels of the sternal angle

Level	Number of individuals	Level-wise distribution (%)
T3	3	Level 1: 2.28
T3-4	2	
T4	40	Level 2: 38.81
T4-5	45	
T5	99	Level 3: 58.91
T5-6	16	
T6	12	
T6-7	2	

Table 3: Vertebral levels of the arch of the aorta

Level	Number of individuals	Level-wise distribution (%)
T3-4	9	Level 1: 4.09
T4	94	Level 2: 72.73
T4-5	66	
T5	48	Level 3: 23.18
T5-6	3	

Table 4: Vertebral levels of tracheal bifurcation

Level	Number of individuals	Level-wise distribution (%)
T2	1	Level 1: 2.90
T2-3	1	
T3	2	
T3-4	1	
T4	56	Level 2: 54.07
T4-5	37	
T5	53	Level 3: 43.03
T5-6	19	
T6	2	

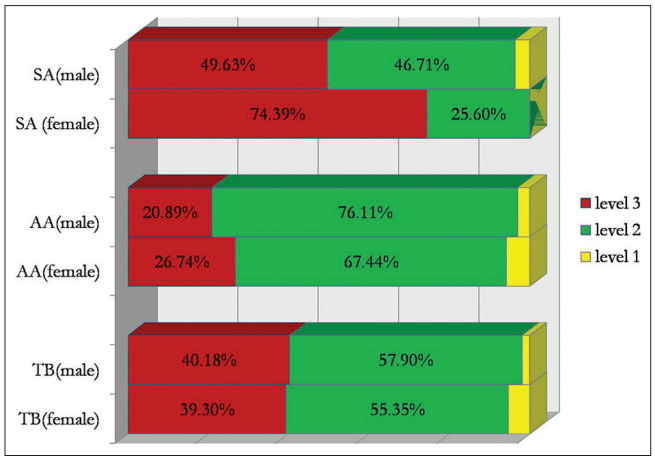

Figure 5: Clustered stacked chart depicting sex distribution of sternal angle, aortic arch, and tracheal bifurcation

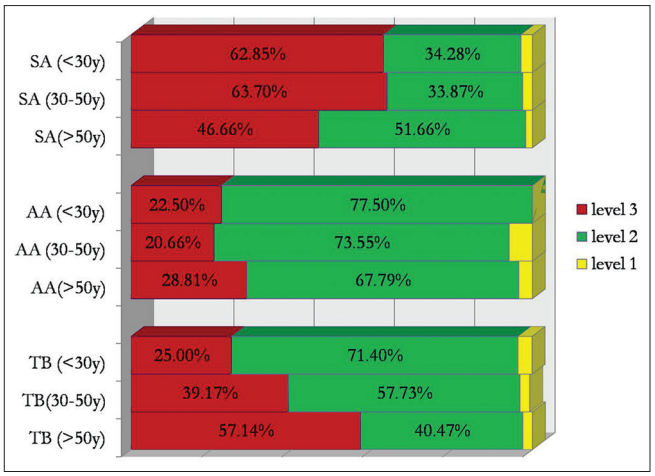

Figure 6: Clustered stacked chart depicting age distribution among various age groups of sternal angle, aortic arch, and tracheal bifurcation

3). In these individuals, the median level of the SA was at Level 3, whereas the median level of the AA and TB, respectively, corresponded to Level 1. This difference was statistically significant using median test ($P < 0.001$).

The relationship of the upper surface of the AA to the manubrium sterni was separately evaluated in 90 individuals as part of the study. It was noted that in all these individuals, the upper surface of the AA was consistently above the level of the SA. In 61.11% of the individuals, it corresponded to the superior half of the manubrium sterni, whereas in 31.11%, it corresponded to the level of the sternal notch or higher.

Discussion

Pierre Charles Alexander Louis (1787–1872) was an expert French morbid anatomist who has to his credit the description of the manubriosternal joint which is eponymously called the angle of Louis. It is a subject of debate among medical historians whether he actually ever described the angle at the junction of the manubrium and the body of the sternum (SA) due to insufficient medical literature on the same. Essom-Sherrier and Neelon[9] state that, in the year 1910, Edward Goodman reviewed Louis's work and found a comprehensive description of the SA. Louis had described the SA as a bulging in the chest of patients with emphysema in the *Journal of the Society of Medical Observations* in 1837. Morton and Norman state that Louis described the SA in "Recherches antomico – pathologique sur la phthisie" in the year 1825,[10] but in an English translation of the same by Walshe[11] and in another article by Chukwuemeka *et al*.,[4] no specific description of the SA was found.

The mediastinum is strictly the partition between the lungs and includes the mediastinal pleura, although it is commonly applied to the region between the two pleural sacs. It is bounded anteriorly by the sternum and posteriorly by the thoracic vertebral column extending vertically from the thoracic inlet to the diaphragm. Conventionally, most of the anatomical texts divide the mediastinum into the superior and inferior mediastinum by a plane which passes from the manubriosternal joint to the vertebral column. The vertebral level corresponding to this plane is another debatable issue. Grant *et al*. mention that "at this level the trachea bifurcates, the arch of the aorta traverses the thorax from right to left in a posterolateral direction."[1] Last RJ states that this is a horizontal plane passing horizontally through the SA backward to the lower border of the fourth thoracic vertebra.[2] The same author also mentions about the various other structures corresponding to this plane, stating that "the plane passes through the bifurcation of the trachea, the concavity of the arch of the aorta and just above the bifurcation of the pulmonary trunk. On the plane, the azygos vein enters the superior vena cava and the thoracic duct reaches the left side of the esophagus in its passage upward from the abdomen. Also lying in the plane are the ligamentum arteriosum and the superficial and deep parts of the cardiac plexus." Williams *et al*. state that "the plane of division into upper and lower mediastinum traverses the manubriosternal joint and the junction of fourth and fifth thoracic vertebra."[3] In a subsequent edition, Williams *et al*. state that "the plane of division into upper and lower mediastinum traverses the manubriosternal joint and the lower surface of the fourth thoracic vertebra."[12]

Various imaging modalities have been used to study the level of SA in relation to the other mediastinal structures and vertebral levels. Arora and Singh in an editorial have comprehensively reviewed the role of imaging in assessing the SA. They suggested that CT and MR are preferred modalities for accurate depiction of mediastinal anatomy. They also noted that there is significant individual variation in the level of mediastinal structures in various studies.[13] Various authors have studied the cross-sectional anatomy of various mediastinal structures on CT.[4-8] Similarly, Shabshin *et al*.[14] studied sagittal MRI sections of thorax

and localizer images of the cervicothoracic region to assess the reliability of various anatomical landmarks for accurate identification of dorsal vertebrae. In this study, the vertebral levels of the sternal apex, aortic bifurcation, and pulmonary bifurcation were assessed in 67 patients. In another study, Sharan *et al*.[15] studied the vertebral level of the sternal notch on T1 scout mid-sagittal MRI images in 106 consecutive patients to determine the appropriate surgical approach for thoracic spinal reconstruction without using thoracotomy or sternotomy. Connor *et al*.[16] have studied the utility of various anatomical landmarks in accurate identification of thoracic vertebrae on thoracic MRI. In this study, a total number of ten bony and soft-tissue anatomical landmarks such as sternal notch, inferior angle of the carina, and superior surface of AA were retrospectively studied in 100 thoracic MRI scans, and the authors found poor interobserver agreement, suggesting that the only reliable way of identifying the thoracic vertebrae is by identifying the C2 vertebra and counting down from thereon.

In the literature review, no other study could be found that has assessed vertebral levels of SA on MRI. However, many authors have assessed the same using CT scan.[4-8] Chukwuemeka *et al*. have shown that in the majority of the individuals, SA passed through the upper half of the T5 vertebral body (52.9%) with the level ranging from T4 to T6.[4] Similarly, Garg *et al*. have reported that the vertebral level of SA varied widely from T3/4 to T6/7, with the most common level being at T4/5 (35%).[5] Badshah *et al*. report the most common level to be at T5.[6] Uzun *et al*.[7] and Shen *et al*.[8] have reported the most common level of SA to lie at or above T4–5 IV disc. In our study, the SA passed through Level 3 in maximum cases (58.9%), followed by Level 2 (38.8%) with a range of T3 to T6/7 [Table 2]. Thus, the findings in our study broadly match the findings of other CT-based studies with respect to wide variation in level. Our findings are also similar to Chukwuemeka *et al*., Garg *et al*., and Badshah *et al*. with respect to the level of SA.[4-6] However, these findings are in variance with description of the SA in standard anatomy textbooks.[2,3,12] One of the possible explanations could be the movement of the thorax during inspiration, while CT images are acquired as opposed to previously described studies in cadavers. We found a statistically significant difference in vertebral levels of SA between males and females, wherein the SA was at a lower level in females. These findings are in variance with the findings of other authors where they found no statistical difference in the level of SA in relation to gender.[4,5,7,8] No plausible explanation could be found or suggested by authors for this difference. With respect to age distribution, our study also does not show any significant difference similar to other studies.[4-8]

Garg *et al*.[5] have reported the undersurface of AA to be at or higher than T3–4 IV disc level in 75% of the cases, whereas Uzun *et al*.[7] reported the same in 62%. Our study revealed that in a majority of individuals (72%), the undersurface of AA corresponded to Level 2 which correlates with the traditionally held belief described in most textbooks of anatomy. Similar results have also been shown by Badshah *et al*.[6] and Shen *et al*.[8] The concavity of the arch of the aorta has been variably reported to be corresponding to plane of the SA in 7%–59%.[4,5,7,8] In our study, however, the concavity of the arch of the aorta was at the level of SA in 36.8% and at a higher level in 56.68% of the cases. Interestingly, the level of the arch of the aorta did not show any such sex- or age-related variability in any of the studies. Although wide variation in the vertebral levels of TB has been reported with 63%–91% at or below T5.[5-8] Our findings are at variance to this as only in 43.03% of the cases TB were at or below T5. With respect to correlation with SA plane, TB and SA are at the same plane in 4%–31% of the individuals and lower in up to 91% of the individuals.[4,5,7,8] Our findings are at variance with these studies as we found TB and SA to be at the same plane in 41.13% of the cases. Furthermore, in another 42.4% of the cases in our study, TB was at a higher level than SA. The TB is seen to lie at a lower level with progression of age in our study. A significant difference was seen in the levels of TB in individuals below 50 years and above 50 years of age. The possible explanation for this difference could be age-related loss of elasticity of tracheobronchial cartilage, however, this needs to be studied further. Uzun *et al*. have reported a significant difference in levels of TB with respect to gender; however, no such difference was seen in our study.[7]

Shabshin *et al*.[14] correlated the superior margin of the aorta with the vertebral level and found it to vary from T2–T4 level, with only 8% of the cases above the level of T3 vertebra. Similarly, Connor *et al*.[16] have found that the mean vertebral level of the superior surface of AA is T3 with a range of T2–T5. In our study, the superior margin of AA was correlated with sternal notch instead of vertebral levels, and we found that in 31% of the cases, the superior margin of AA was above the level of sternal notch. AA was seen to correspond to the upper half of the manubrium or higher in more than 92% of the individuals. From an imaging perspective, the suprasternal approach for ultrasonography of the AA should be effective in the majority of the individuals due to this reason.

Conclusion

The conventional teaching in anatomy textbooks has been that SA, TB, and AA lie at the same cross-sectional plane which corresponds to T4–5 vertebral level. This description is based on historical cadaveric dissections and is probably governed by the dictates of convenience rather than on statistical data in living individuals in contrary to this traditionally held belief. Our study involving a sizeable number of living individuals using MRI as an anatomical tool has shown that these three anatomical landmarks lie at the same plane in only a minority of individuals. Even

among these individuals, a further smaller number show that the corresponding cross-sectional plane is at T4–5 level.

Financial support and sponsorship

Nil.

Conflicts of interest

There are no conflicts of interest.

References

1. Grant JC, John VB, Charles ES. Grant's Method of Anatomy: A Clinical Problem-Solving Approach. 11th ed. Baltimore: Williams & Wilkins; 1989. p. 69.
2. Last RJ, McMinn RM. Last's Anatomy: Regional and Applied. 9th ed. Edinburgh: Churchill Livingstone; 1994. p. 254.
3. Williams PL, Warwick R, Dyson M, Bannister LH. Splanchnology. In: Gray's Anatomy. 37th ed. Edinburgh: Churchill Livingstone; 1989. p. 1245-475.
4. Chukwuemeka A, Currie L, Ellis H. CT anatomy of the mediastinal structures at the level of the manubriosternal angle. Clin Anat 1997;10:405-8.
5. Garg S, Gulati A, Aggarwal A, Gupta T, Mirjalili SA, Sahni D. Retrospective analysis of adult thoracic surface anatomy in Indian population using computed tomography scans. J Anat Soc India 2019;68:39-45.
6. Badshah M, Soames R, Khan MJ, Marwat MI, Khan A. Revisiting thoracic surface anatomy in an adult population: A CT evaluation of vertebral level. Clin Anat 2017;30:227-36.
7. Uzun C, Atman ED, Ustuner E, Mirjalili SA, Oztuna D, Esmer TS. Surface anatomy and anatomical planes in the adult Turkish population. Clin Anat. 2016;29:183-190.
8. Shen XH, Su BY, Liu JJ, Zhang GM, Xue HD, Jin ZY, *et al*. A reappraisal of adult thoracic and abdominal surface anatomy via CT scan in Chinese population. Clin Anat 2016;29:165-1.
9. Essom-Sherrier C, Neelon FA. The names and faces of medicine. Angle of Louis. N C Med J 1989;50:21.
10. Morton LM, Norman JM. Morton's Medical Bibliography. 5th ed. Aldershot England: Scholar Press; 1991. p. 264.
11. Louis PC. Researches on Pthisis Anatomical, Pathological and the Rapeutical. In: Walshe WH, editor. Vol. 8. Translator. London: Sydenham Society; 1844.
12. Williams PL, Bannister LH, Berry MM, Collins P, Dyson M, Dussek JE, *et al*. Gray's Anatomv: The Anatomical Basis of Medicine and Surgery. 38th ed. Edinburgh: Churchill Livingstone; 1995. p. 1677.
13. Arora VK, Singh V. Sternal angle revisited – From anatomy to radiology. J Anat Soc India 2013;62:95-97.
14. Shabshin N, Schweitzer ME, Carrino NA. Anatomical landmarks and skin markers are not reliable for accurate labelling of thoracic vertebra on MRI. Acta Radiol 2010;51:1038-42.
15. Sharan AD, Przybylski GJ, Tartaglino L. Approaching the upper thoracic vertebrae without sternotomy or thoracotomy. Spine 2000;25:910-6.
16. Connor SE, Shah A, Latifoltojar H, Lung P. MRI-based anatomical landmarks for the identification of thoracic vertebral levels. Clin Radiol 2013;68:1260-7.

Case Report

Ectopic Pelvic Kidney and its Renal Artery from the Common Iliac Artery

Sevda Lafci Fahrioglu, Musa Muhtaroglu, Selda Onderoglu, Sezgin Ilgi

Department of Anatomy, Faculty of Medicine, Near East University, Nicosia, Cyprus

Abstract

The pelvic kidney is the most common type of renal ectopia. It is clinically asymptomatic in general but are more prone to the urinary infections. It has also been associated with an increased risk of nephrolithiasis. The 37-year-old man was admitted to the emergency room with complaints of left flank pain, nausea and vomiting. In addition to this flank pain, the patient had an intermittent pain in the lower abdomen and pelvic region for 6 years with no history of fever. The renal ultrasound demonstrating several shadowing echogenic areas consistent with nephrolithiasis in both kidneys. In addition, while the right kidney was in the normal size and location, the left kidney was located on the ectopic site, just above the bladder. Doppler examination revealed double renal arteries originating from the aorta on the right side. Our case indicates the importance of the ectopic pelvic kidney location when planning surgical procedures in patients with renal and pelvic pathology, kidney transplantation and nephrectomy.

Keywords: *Ectopic kidney, double renal artery, renal anatomy*

Introduction

During the normal fetal developmental stages, the kidney does not yet reach its adult anatomical location.[1] If it continues to remain in the pelvic region after the fetal stages, it will be called pelvic kidney.[2] The pelvic kidneys which reside in the pelvis minor are clinically asymptomatic in general but are more prone to urinary infections and stone formation.[2,3]

The congenital anomalies of the kidney and the urinary system are common congenital organ malformations, with an incidence of 0.03%–0.16%.[3] The pelvic kidney is the most common type of renal ectopia. The ectopic kidney can rarely be found at the thorax.[2,3] The pelvic kidney can cause deep vein thrombosis due to its pressure on the iliac vein.[4] Ectopic kidney has also been associated with an increased risk of nephrolithiasis.[5] Furthermore, transitional cell carcinoma of a pelvic kidney is also observed, but it has a more rare occurrence.[6-8]

Embryology

Initially, the kidneys are located near the tail of the embryo in the early stages of embryogenesis.[1] The metanephric diverticulum and metanephric blastema, which are the main parts of the permanent kidney, develop from methanephrosis in the pelvis. The kidneys migrate to the lumbar region with the effect of the abdominal wall growth during the intra-uterine period. The kidneys also rotate medially during migration to renal fossa.[2,4] The vascular buds from the kidneys grow toward and invade the common iliac arteries. The genetic and teratogenic risk factors may affect the physiological development of the kidneys and lead to congenital disabilities. The congenital abnormalities of the kidney and urinary system are one of the common congenital organ malformations. It has two subgroups, which are the congenital malformations of the kidney and the anomalies of the lower urinary system.[2,3,9] The most common type of renal ectopia is a pelvic kidney. During the fetal period in the normal developmental stages, the kidney does not reach the anatomic location, and if it remains in the pelvic region is called the pelvic kidney.[5]

Case Report

In September 2018, the 37-year-old male was admitted to the emergency room with complaints of left flank pain, nausea, and vomiting. In addition to this flank pain, the patient had intermittent pain in the lower abdomen and pelvic region for 6 years with

How to cite this article: Fahrioglu SL, Muhtaroglu M, Onderoglu S, Ilgi S. Ectopic pelvic kidney and its renal artery from the common iliac artery. J Anat Soc India 2020;69:XX-XX.

Article Info

Received: 03 December 2019
Accepted: 22 May 2020
Available online: ***

Address for correspondence:
Assoc. Prof. Sevda Lafci Fahrioglu,
Department of Anatomy, Faculty of Medicine, Near East University, TRNC, Nicosia, Cyprus.
E-mail: sevdalafci@gmail.com

Access this article online

Website: www.jasi.org.in
DOI: 10.4103/JASI.JASI_210_19
Quick Response Code:

no history of fever. On careful investigation of the patient's medical history, it was discovered that he was admitted to the emergency department with the same flank pain complaint after seeing several physicians in different hospitals over many years. The patient was thin and tall. A kidney stone was suspected, and the renal ultrasound demonstrated several echogenic areas consistent with nephrolithiasis in both kidneys. In addition, while the right kidney was in the normal size and location, the left kidney was located on the ectopic site, just above the bladder. The left ectopic kidney was slightly malrotated with its pelvis oriented posteriorly. The size of the left kidney was 94 mm × 61 mm × 52 mm, and the renal pelvis was in the right and posterior position [Figure 1]. The size of the right kidney was 129 mm × 51 mm × 45 mm [Figure 2]. The thickness of the parenchyma of the right and the left kidneys were 11–12 mm and 12–13 mm, respectively. The cortical and medullary echogenicity of both kidneys were normal, and a parenchymal band was present in the middle, but there was no double collecting system. In addition, 8–10 stones were found in the calyces of both kidneys, ranging in size from 3 to 11 mm.

The computed tomography (CT) scan performed after ultrasound demonstrated multiple renal stones, but no double collecting systems in both kidneys [Figures 3 and 4].

Doppler examination revealed double renal arteries originating from the aorta on the right side. The diameter of the right renal arteries was 4 mm and 3.5 mm. The diameter of the left renal artery was 5 mm, and it originated from the left common iliac artery immediately after the aortic bifurcation. The vascularization of both kidneys was symmetrical and normal. Segmental and interlobar arteries were normal, and resistivity indices up to arcuate arteries were normal. There was no renal artery stenosis in both kidneys.

Discussion

The kidneys that develop in the pelvis move to a more proximal site and merge with the adrenal gland. The growth of the lumbar and sacral regions of the embryo in length causes the kidneys to "ascend" to their final position in the upper lumbar region at the 9th week of gestation.[4] During this migration, as the kidneys rise, they continue to have new blood vessels at their new level and leave behind their old blood vessels to regress. As the kidneys migrate upward, the renal hilum turns 90° medially, and thereby, the renal hilum is finally located at the medial side of the kidney.[1] Absence of the kidney in the renal

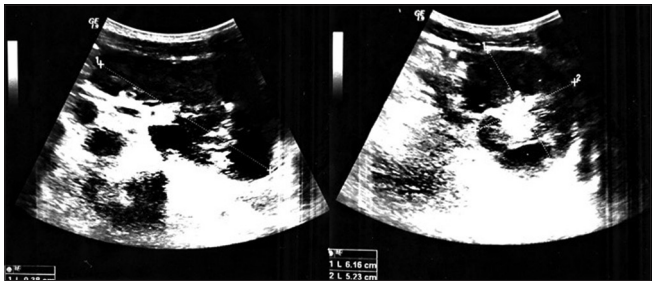

Figure 1: Renal ultrasonography demonstrating of the left kidney

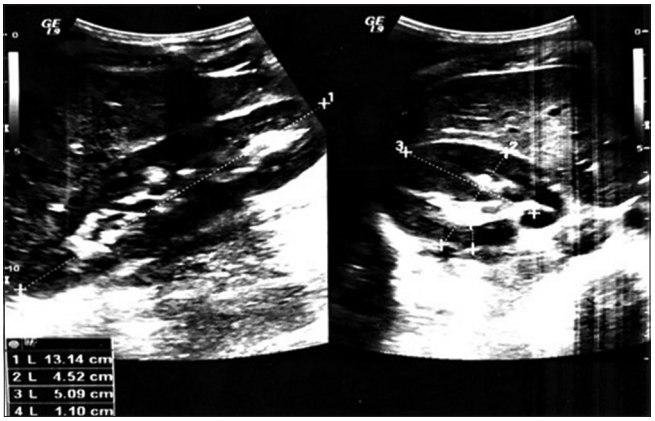

Figure 2: Renal ultrasonography demonstrating of the right kidney

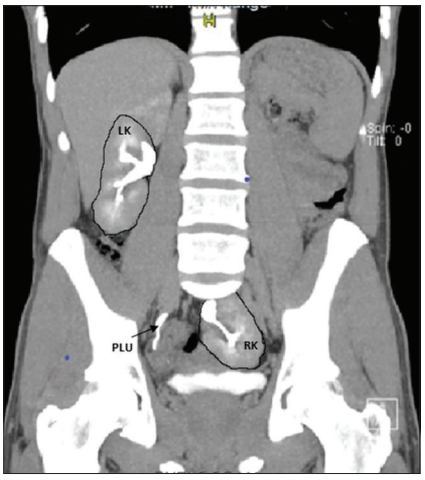

Figure 3: Computed tomography urogram demonstrating the right kidney, the left kidney, and the pelvic part of the right ureter

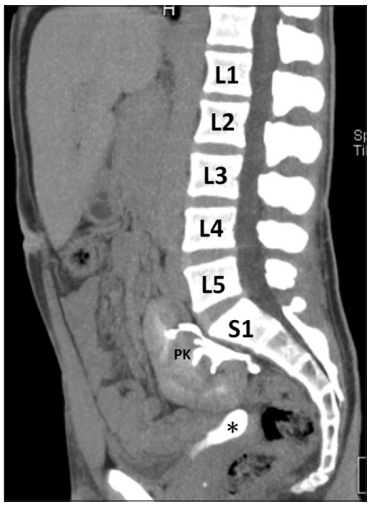

Figure 4: The sagittal section of the computed tomography urogram demonstrating the left kidney, which is located at the top of the bladder. *: Urinary bladder

fossa (also called "Empty renal fossa") indicates renal agenesis; ectopic kidney is kidney located in an abnormal ectopic position which arises due to the failure of ascent or arrest of the ascent of the kidney.[3] The pelvic ectopia is a type of renal ectopia, which is caused by faulty migration from the pelvis during the embryological process. Although the ectopic kidney can be found in the lower lumbar, abdominal, and thoracic locations, the left pelvic region is the most common site for the ectopic kidney. In addition, contralateral and crossed ectopic kidneys can also occur.[5]

Urinary system anomalies can be detected in about 10% of the population. The presence of pelvic kidneys may not be noticed early in life unless it is detected by kidney ultrasound or abdominal tomography for different reasons. The pelvic kidney, which is the most common type of renal ectopia, can be seen in adults at the rate of 1/1000.[6] The incidence of a normal and a pelvic kidney ranges from 1:800 to 1:3000.[9] The pelvic kidneys are mostly asymptomatic. In the presence of an ectopic kidney, genital system abnormalities such as undescended testicles, urethral duplication, and hypospadias may also be defined. The malrotated ectopic kidney is one of the risks of stones formation, which may present as renal colic and hematuria, like in our case.

Since the renal vessels are shaped according to the normal anatomical position of the kidney, the position of the ectopic kidney also affects the origin of the kidney vessels. As we found in our patient, the artery of a distally located ectopic kidney may originate from a common iliac artery close to the aortic bifurcation, as well as from the inferior mesenteric artery, distal aorta, or external iliac artery.[9]

Although the ectopic kidney is asymptomatic, the patients should be monitored with ultrasound at regular intervals since these patients have a higher risk of developing nephrolithiasis. They should be alerted against complications such as secondary infection and hydronephrosis.[10-12] The treatment of hydronephrotic pelvic kidney involves various difficulties, as the kidney can be found in front of the sacrum, behind the lower gastrointestinal system and internal genital organs. Although the prevalence of renal cancer in the pelvic kidneys is exceedingly rare, it should also be kept in mind.[6-8,11]

Surgical removal of the pelvic kidney may be complicated because of its neighboring anatomical structures or the presence of a tortuous ureter in the presence of abnormal neurovascular structures.[10,12] For this reason, it is important to have information about the anatomical locations of the pelvic kidney. Our case indicates the importance of the ectopic kidney location when planning surgical procedures in patients with renal and pelvic pathology, kidney transplantation, and nephrectomy.

Declaration of patient consent

The authors certify that they have obtained all appropriate patient consent forms. In the form the patient(s) has/have given his/her/their consent for his/her/their images and other clinical information to be reported in the journal. The patients understand that their names and initials will not be published and due efforts will be made to conceal their identity, but anonymity cannot be guaranteed.

Financial support and sponsorship

Nil.

Conflicts of interest

There are no conflicts of interest.

References

1. Standring S. Kidney and urether. In: Gray's Anatomy: The Anatomical Basis of Clinical Practice. 40th ed. Edinburgh (UK): Churchill Livingstone Elsevier; 2008. p. 2248-57.
2. Arslan H, Aydogan C, Orcen C, GonIllu E. A rare case: Congenital thoracic ectopic kidney with diaphragmatic eventration. J Pak Med Assoc 2016;66:339-41.
3. Al-Saqladi AW, Akares SA. Intrathoracic kidney in a child with literature review. Saudi J Kidney Dis Transpl 2015;26:349-54.
4. Eng JM, Walor DM, Michaels LA, Weiss AR. An unusual presentation of May-Thurner syndrome in a pediatric patient with a pelvic kidney. J Pediatr Urol 2013;9:e72-5.
5. Koh Y, Imanaka T, Tsujimura G, Kinjo T, Nomura H, Yoshioka I, *et al*. A case report: Lithiasis of the left ectopic pelvic kidney. Nihon Hinyokika Gakkai Zasshi 2018;109:54-7.
6. Rezaee ME, Shetty Z, Pridmore D, Dave CN, Shetty SD. Robot-assisted laparoscopic nephroureterectomy for transitional cell carcinoma of a right pelvic kidney. J Endourol Case Rep 2016;2:131-4.
7. Gharbi M, Chakroun M, Chaker K, Zaghbib S, Saadi A, Bouzouita A, *et al*. Renal cell carcinoma in an ectopic pelvic kidney: About a case report. Urol Case Rep 2018;23:46-7.
8. Halalsheh O, Ghawanmeh HM, Alshammari A, Sahawneh F, Al-Okour R, Al Karasneh A, *et al*. Upper tract urothelial carcinoma in ectopic pelvic kidney. Urol Case Rep 2017;11:42-3.
9. Eid S, Iwanaga J, Loukas M, Oskouian RJ, Tubbs RS. Pelvic kidney: A review of the literature. Cureus 2018;10:e2775.
10. Antonelli A, Peroni A, Furlan M, Palumbo C, Zamboni S, Veccia A, *et al*. Robot-assisted partial nephrectomy and bilateral pyelolithotomy in ectopic pelvic kidneys. Urology 2019;129:235.
11. Alokour RK, Ghawanmeh HM, Al-Ghazo M, Lafi TY. Renal cell carcinoma in ectopic-pelvic kidney: A rare case with review of literature. Turk J Urol 2018;44:433-6.
12. Giorlando F, Recaldini C, Leonardi A, Macchi E, Fugazzola C. Duplex collecting system in a pelvic kidney – An unusual combination. J Radiol Case Rep 2017;11:8-15.

Case Report

Turner Syndrome Associated with Cerebellar Abnormalities

Tanya T. Kitova, Ekaterina H. Uchikova[1], Kristina P. Kilova[2], Veselin T. Belovejdov[3]

Departments of Anatomy, Histology and Embryology, [2]Medical Informatics, Biostatistics and E-Learning and [3]General and Clinical Pathology, Medical University of Plovdiv, [1]Clinic of Obstetrics and Gynecology, University Hospital "St. George," Plovdiv, Bulgaria

Abstract

We present an autopsied fetus with Turner syndrome (TS), obtained after a therapeutic abortion at the Clinic of Obstetrics and Gynecology at the University Hospital, Plovdiv, Bulgaria. It was a female fetus weighing 75 g. The chorionic villus sampling followed by karyotyping established monosomy XO. The fetal autopsy confirmed agenesis of the cerebellar vermis and cerebellar hypoplasia. The immunohistochemical study of the brain with S100 protein (S100), glial fibrillary acidic protein (GFAP), neuron-specific enolase (NSE), and cluster of differentiation 68 was taken into consideration. The presence of extensive gliosis reaction is proved in the cerebellar structures of TS by the positivity of glial markers: (GFAP) and S100 protein. The quantity of neurons proved by NSE marker is probably associated with the deficiency of differentiation and cell migration caused by inhibition in the development of young cells. The presented case of TS found a new phenotype with cerebellar abnormalities described for the first time.

Keywords: *Agenesis of the cerebellar vermis, brain, fetal autopsy, glial marker, immunohistochemical study, Turner syndrome*

Introduction

The purpose of this study is to present a unique case of Turner syndrome (TS) associated with cerebellar abnormalities, utilizing modern investigation methods (ultrasound, amniocentesis, karyotype studies, and immunohistochemistry) in additionn to fetopathological autopsy as a final stage of diagnosis, as well as prognosis for future pregnancies

Case Report

The fetus was acquired from the therapeutic abortion of the first pregnancy of a 19-year-old female, at the Clinic of Obstetrics and Gynecology at the University Hospital "St. George," Plovdiv, Bulgaria. The control prenatal ultrasound of the fetus found a defect in the posterior cranial fossa [Figure 1], following which a chorionic villus sampling and a karyotype examination were performed. The karyotype was found to be monosomy XO. Informed consent was obtained from both parents. A classical autopsy of the fetus immediately followed by the abortion and histological and immunohistochemical examinations of the brain structures were performed. All specimens were routinely fixed in 10% buffered formaldehyde and embedded in paraffin, and 3.5-µm-thick sections were stained with H and E [Figure 2]. After a longitudinal section of the cerebellum, the slides were selected for an immunohistochemical study by immunoperoxidase staining for S100 protein (S100), glial fibrillary acidic protein (GFAP), neuron-specific enolase (NSE), and cluster of differentiation 68 (CD 68) markers using the DAKO immunostainer "Link 48" standard procedure [Table 1].

As a control specimen, a cerebellum was used without anomalies of a miscarried fetus at the 16th gestational week. Microphotographs were performed using the Nikon Microphoto-SA microscope (Japan), combined with Camedia-5050Z digital camera (Olympus, Japan). The measurements were performed with the help of the software"DP– Soft" 3.2 (Olympus, Japan). The microscopic field of study is divided by a rectangular grid with a X-horizontal and Y-vertical span. The parameters for this type of measurement and grid size of 20/20 pixels were set. Numerically, cellular densities in each square field (30 grids) of the same 300 mm^2 area were counted for each of the three markers for TS [Figure 3].

How to cite this article: Kitova TT, Uchikova EH, Kilova KP, Belovejdov VT. Turner syndrome associated with cerebellar abnormalities. J Anat Soc India 2020;69:XX-XX.

Article Info

Received: 10 May 2020
Revised: 17 May 2020
Accepted: 22 May 2020
Available online: ***

Address for correspondence:
Dr. Tanya T. Kitova, Department of Anatomy, Histology and Embryology, Medical University of Plovdiv, Vasil Aprilov" Street 15A, Plovdiv 4002, Bulgaria.
E-mail: tanyakitova@yahoo.com

Access this article online

Website: www.jasi.org.in
DOI: 10.4103/JASI.JASI_50_19
Quick Response Code:

The autopsy found biometric indicators confirming a fetal age of 16 gestational weeks and intrauterine growth retardation (fetal weight – 75 g). Facial dysmorphia (oblique eye slit, low-set and poorly formed auricles, long philtrum, and microretrognathia) and flat feet were present [Figure 4a and b]. Macrocephaly, pterygium, cystic hygroma of the neck , and horseshoe kidney malformations were also observed [Figure 4b and c]. The autopsy of the brain diagnosed cerebellar hypoplasia (weight of cerebellum – 1 g) and agenesis of the cerebellar vermis [Figure 4d].

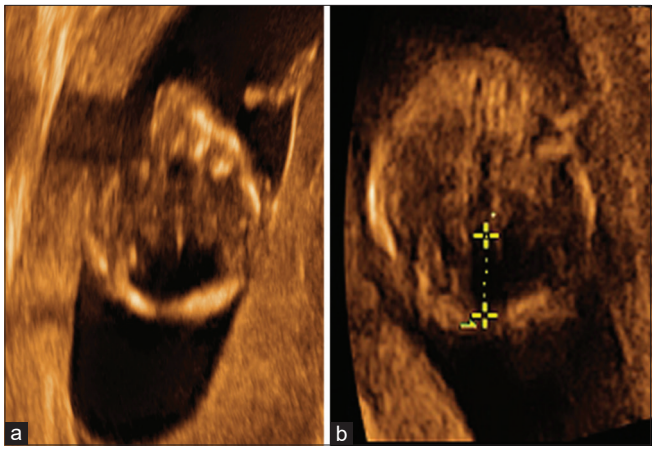

Figure 1: (a) Ultrasound of the skull and brain structures. (b) Cystic dilatation of posterior cranial fossa

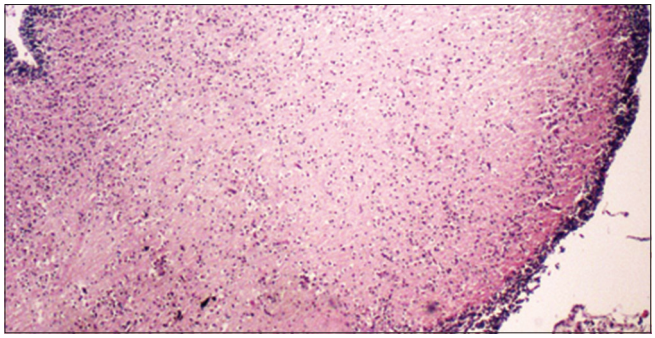

Figure 2: Cerebellum of Turner syndrome (H and E, 10 × 0, 25)

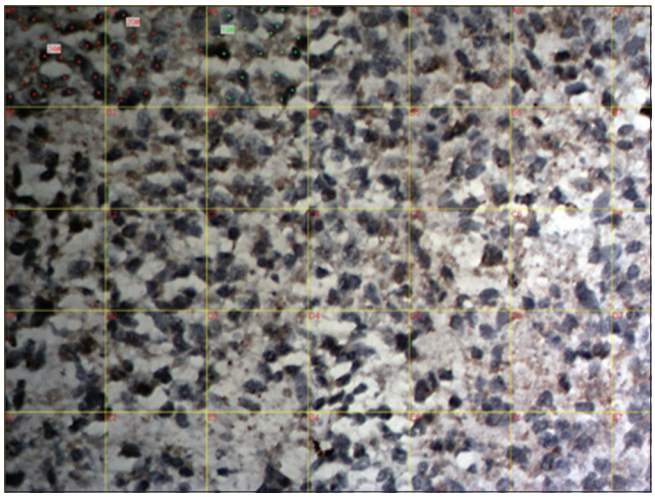

Figure 3: Method of morphometry

Glial fibrillary acidic protein marker

The immunohistochemical study of the cerebellar structures with GFAP marker revealed increased gliosis in the case compared to the control [Figure 5a and b]. The morphometry established an increased cell expression in TS. Student's *t*-test revealed a statistically significant difference of expression of the GFAP marker in the case compared to the control [Figure 6 and Table 2].

S100 marker

The expression of the S100 marker in the cerebellum revealed an increased gliosis in the case with TS compared to the control [Figure 5c and d]. The morphometry established a weaker cell expression in the TS case compared to the control [Figure 6]. Student's *t*-test did not detect a statistically significant difference for the S100 marker in the case compared to the control [Table 2].

Neuron-specific enolase marker

NSE marker showed higher expression in the control specimen when compared to the case of TS [Figure 7a and b]. The morphometry established a weaker expression of NSE marker in TS [Figure 6 and Table 2].

Cluster of differentiation 68 marker

The lysosomal marker CD68 is negative in the control specimen, but in the case of TS, its expression is focal. Infiltration of mononuclear inflammatory cells in the fetal cerebellum with TS is increased [Figure 7c and d].

Discussion

Monosomy X is a chromosomal anomaly which represents about 65% of all aneuploidies.[1]

In the present study, the fetal autopsy confirmed agenesis of the cerebellar vermis and hypoplasia. The presence of extensive gliosis reaction is proved in the cerebellar structures of TS by the positivity of both glial markers GFAP and S100. Although only GFAF reaches statistical significance this is important, this is important because

Table 1: Distribution of the used products

Used antibodies	Specific	Primary
Anti-GFAP	Polyclonal rabbit anti-glial fibrillary acidic protein	Ready to use
Anti-S100	Poly Rb a S100, RTU	Ready to use
Anti-NSE	Mab a Hu NSE, cl BBS/ NC/VI-H14, RTU	Ready to use
Anti-CD68	Monoclonal mouse anti-human, clone PG-M1	Ready to use

NSE: Neuron-specific enolase, GFAP: Glial fibrillary acidic protein, RTU: Ready to use

Table 2: *t*-test statistical significance for morphometry of glial fibrillary acidic protein, S100, and neuron-specific enolase markers

Types	Variable	Control (*n*=14)	Turner syndrome (*n*=13)	*t*	*P*
GFAP	Mean (SD)	12.93 (12.07)	182.31 (49.54)	12.419	0.000
S100	Mean (SD)	102.4 (54.6)	103.8 (20.2)	0.093	0.927
NSE	Mean (SD)	91.6 (51.2)	86.0 (26.4)	0.376	0.710

SD: Standard deviation, NSE: Neuron-specific enolase, GFAP: Glial fibrillary acidic protein

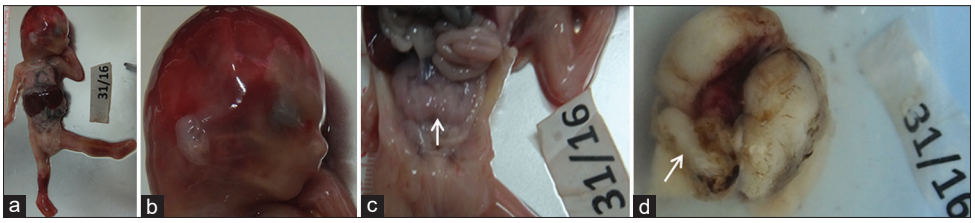

Figure 4: (a) Fetus with Turner syndrome. (b) Facial dysmorphia – oblique eye slit, low-set and poorly formed auricle, and microretrognathia. Cystic hygroma of the neck. (c) Horseshoe kidney malformation. (d) Hypoplasia of the cerebellum, agenesis of the cerebellar vermis

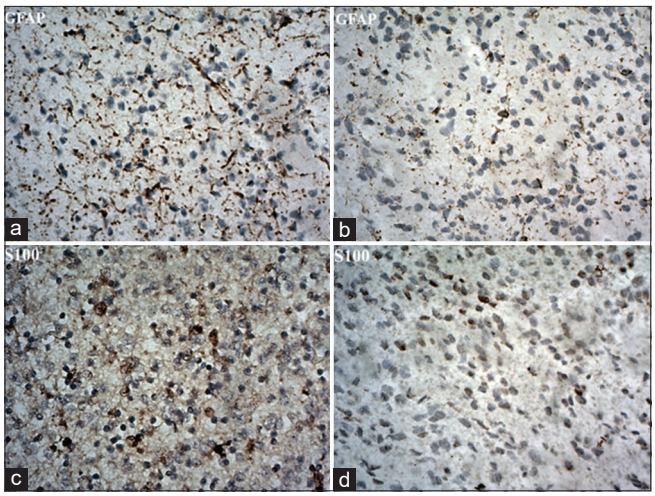

Figure 5: Immunohistochemistry with glial fibrillary acidic protein and S100 markers. (a) Glial fibrillary acidic protein: Turner syndrome. (b) Glial fibrillary acidic protein: control. (c) S100: Turner syndrome. (d) S100: control. The expression of both markers in the cerebellum reveals cellular architecture with increased gliosis in the case with Turner syndrome compared to the control (10 × 40)

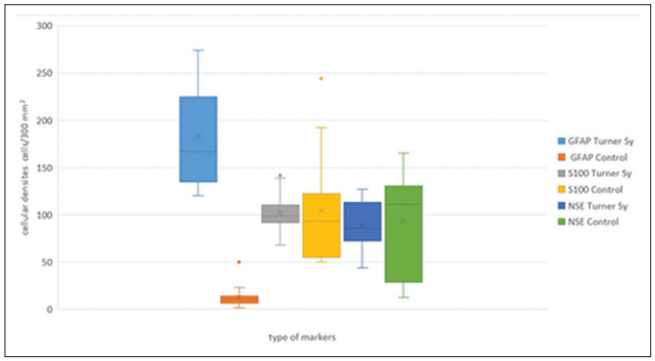

Figure 6: Graphic representation of the morphometric results with markers such as glial fibrillary acidic protein, S100, and neuron-specific enolase

GFAP is a predicative molecular signal for the degree of early developmental disturbances of fetal cerebellum.

The NSE marker does not show a statistically significant variation in the quantity of neurons, however, this does not deny the differences in cellular neuro-morphology. It is probably associated with deficiency of differentiation and cell migration, caused by inhibition in the development of young cells.

Cerebellar hypoplasia with glial proliferation suggests a disturbance in brain function, which does not correlate with the statement that there is no mental retardation in TS.[2]

Some authors explain the disturbance in the cerebellar development with intrauterine oxidative stress, while others with the absence of the X chromosome, which leads to a disturbance in the migration of neurons, but only once neuronal migration has been completed in the cortex of the cerebral hemispheres.[3] This explains the inefficiency of neuronal migration in the cerebellum and olive, which means that the process of neuronal migration is affected around the 4th month.[4] The morphogenesis of the cerebellum is impaired by the disturbances in neuronal migration and cell architectonics, long after the closure of the neural tube.[5]

According to the most recent studies, an increased immune reactivity of interleukin 1 and S100 markers is found in degenerative processes, such as Down syndrome and Alzheimer's disease.[6,7] Similar disturbances are found in Zellweger syndrome and trisomy 21. The association of TS with cerebellar hypoplasia is an additional evidence of a disturbance in the embryonic development of the brain. Although the prognosis for its clinical presentation in the postnatal period is difficult, the questions regarding the necessity of a prenatal genetic study and abortion due to medical reasons in cases of a positive result remain.

Conclusion

The presented case of TS found new phenotype with cerebellar abnormalities. This phenotype is a result of

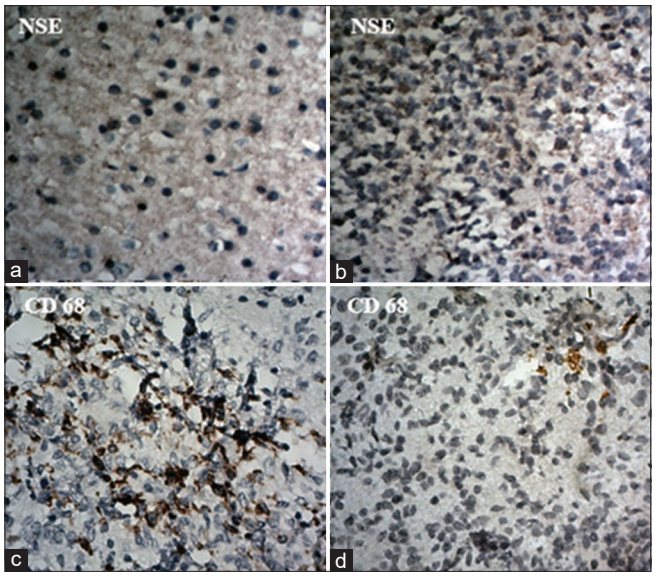

Figure 7: Immunohistochemistry with neuron-specific enolase and cluster of differentiation 68 markers. (a) Neuron-specific enolase: Turner syndrome. (b) Neuron-specific enolase: control. Neuron-specific enolase marker shows higher expression in the control specimen than in the case of Turner syndrome/CD68 Turner syndrome. (d) Cluster of differentiation 68: control. The lysosomal marker cluster of differentiation 68 is negative in the control specimen, but in the case of Turner syndrome, its expression is focal (10 × 40)

disturbances in the morphogenesis up to the 16th gestational week of embryonic development, due to impaired neuronal migration and cell architectonics. The most crucial aspect of the prenatal diagnosis remains the karyotype examination, even though chorionic biopsy is associated with an increased risk for the pregnancy.

Declaration of patient consent

The authors certify that they have obtained all appropriate patient consent forms. In the form the patient(s) has/have given his/her/their consent for his/her/their images and other clinical information to be reported in the journal. The patients understand that their names and initials will not be published and due efforts will be made to conceal their identity, but anonymity cannot be guaranteed.

Financial support and sponsorship

Nil.

Conflicts of interest

There are no conflicts of interest.

References

1. Baena N, de Vigan C, Cariati E, Clementi M, Stoll C, Caballín MR, *et al*. Turner syndrome: Evaluation of prenatal diagnosis in 19 European registries. Am J Med Genet A 2004;129A: 16-20.
2. Basson MA, Wingate RJ. Congenital hypoplasia of the cerebellum: Developmental causes and behavioral consequences. Front Neuroanat 2013;7:29.
3. Ross ME, Walsh CA. Human brain malformations and their lessons for neuronal migration. Annu Rev Neurosci 2001;24:1041-70.
4. Giustina ED, Forabosco A, Botticelli AR, Pace P. Neuropathology of the turner syndrome. Pediatr Med Chir 1985;7:49-55.
5. Kitov B, Zhelyazkov H, Dimitrova D, Milkov D. Meningocele associated with diastematomyelia (split cord malformation) and butterfly vertebra. Compt Rend Acad Bulg Sci 2017;70:563-70.
6. Griffin WS, Stanley LC, Ling C, White L, MacLeod V, Perrot LJ, *et al*. Brain interleukin 1 and S-100 immunoreactivity are elevated in down syndrome and Alzheimer disease. Proc Natl Acad Sci (USA) 1989;86:7611-5.
7. Hartley D, Blumenthal T, Carrillo M, DiPaolo G, Esralew L, Gardiner K, *et al*. Down syndrome and Alzheimer's disease: Common pathways, common goals. Alzheimers Dement 2015;11:700-9.

The Editorial Process

A manuscript will be reviewed for possible publication with the understanding that it is being submitted to Journal of the Anatomical Society of India alone at that point in time and has not been published anywhere, simultaneously submitted, or already accepted for publication elsewhere. The journal expects that authors would authorize one of them to correspond with the Journal for all matters related to the manuscript. All manuscripts received are duly acknowledged. On submission, editors review all submitted manuscripts initially for suitability for formal review. Manuscripts with insufficient originality, serious scientific or technical flaws, or lack of a significant message are rejected before proceeding for formal peer-review. Manuscripts that are unlikely to be of interest to the Journal of the Anatomical Society of India readers are also liable to be rejected at this stage itself.

Manuscripts that are found suitable for publication in Journal of the Anatomical Society of India are sent to two or more expert reviewers. During submission, the contributor is requested to provide names of two or three qualified reviewers who have had experience in the subject of the submitted manuscript, but this is not mandatory. The reviewers should not be affiliated with the same institutes as the contributor/s. However, the selection of these reviewers is at the sole discretion of the editor. The journal follows a double-blind review process, wherein the reviewers and authors are unaware of each other's identity. Every manuscript is also assigned to a member of the editorial team, who based on the comments from the reviewers takes a final decision on the manuscript. The comments and suggestions (acceptance/ rejection/ amendments in manuscript) received from reviewers are conveyed to the corresponding author. If required, the author is requested to provide a point by point response to reviewers' comments and submit a revised version of the manuscript. This process is repeated till reviewers and editors are satisfied with the manuscript.

Manuscripts accepted for publication are copy edited for grammar, punctuation, print style, and format. Page proofs are sent to the corresponding author. The corresponding author is expected to return the corrected proofs within three days. It may not be possible to incorporate corrections received after that period. The whole process of submission of the manuscript to final decision and sending and receiving proofs is completed online. To achieve faster and greater dissemination of knowledge and information, the journal publishes articles online as 'Ahead of Print' immediately on acceptance.

Clinical trial registry

Journal of the Anatomical Society of India favors registration of clinical trials and is a signatory to the Statement on publishing clinical trials in Indian biomedical journals. Journal of the Anatomical Society of India would publish clinical trials that have been registered with a clinical trial registry that allows free online access to public. Registration in the following trial registers is acceptable: http://www.ctri.in/; http://www.actr.org.au/; http://www.clinicaltrials.gov/; http://isrctn.org/; http://www.trialregister.nl/trialreg/index.asp; and http://www.umin.ac.jp/ctr. This is applicable to clinical trials that have begun enrollment of subjects in or after June 2008. Clinical trials that have commenced enrollment of subjects prior to June 2008 would be considered for publication in Journal of the Anatomical Society of India only if they have been registered retrospectively with clinical trial registry that allows unhindered online access to public without charging any fees.

Authorship Criteria

Authorship credit should be based only on substantial contributions to each of the three components mentioned below:

1. Concept and design of study or acquisition of data or analysis and interpretation of data;
2. Drafting the article or revising it critically for important intellectual content; and
3. Final approval of the version to be published.

Participation solely in the acquisition of funding or the collection of data does not justify authorship. General supervision of the research group is not sufficient for authorship. Each contributor should have participated sufficiently in the work to take public responsibility for appropriate portions of the content of the manuscript. The order of naming the contributors should be based on the relative contribution of the contributor towards the study and writing the manuscript. Once submitted the order cannot be changed without written consent of all the contributors. The journal prescribes a maximum number of authors for manuscripts depending upon the type of manuscript, its scope and number of institutions involved (vide infra). The authors should provide a justification, if the number of authors exceeds these limits.

Contribution Details

Contributors should provide a description of contributions made by each of them towards the manuscript. Description should be divided in following categories, as applicable: concept, design, definition of intellectual content, literature search, clinical studies, experimental studies, data acquisition, data analysis, statistical analysis, manuscript preparation, manuscript editing and manuscript review. Authors' contributions will be printed along with the article. One or more author should take responsibility for the integrity of the work as a whole from inception to published article and should be designated as 'guarantor'.

Conflicts of Interest/ Competing Interests

All authors of must disclose any and all conflicts of interest they may have with publication of the manuscript or an institution or product that is mentioned in the manuscript and/or is important to the outcome of the study presented. Authors should also disclose conflict of interest with products that compete with those mentioned in their manuscript.

Submission of Manuscripts

All manuscripts must be submitted on-line through the website http://www.journalonweb.com/jasi. First time users will have to register at this site. Registration is free but mandatory. Registered authors can keep track of their articles after logging into the site using their user name and password.

- If you experience any problems, please contact the editorial office by e-mail at editor@jasi.org.in

The submitted manuscripts that are not as per the "Instructions to Authors" would be returned to the authors for technical correction, before they undergo editorial/ peer-review. Generally, the manuscript should be submitted in the form of two separate files:

[1] Title Page/First Page File/covering letter:

This file should provide

1. The type of manuscript (original article, case report, review article, Letter to editor, Images, etc.) title of the manuscript, running title, names of all authors/ contributors (with their highest academic degrees, designation and affiliations) and name(s) of department(s) and/ or institution(s) to which the work should be credited, . All information which can reveal your identity should be here. Use text/rtf/doc files. Do not zip the files.
2. The total number of pages, total number of photographs and word counts separately for abstract and for the text (excluding the references, tables and abstract), word counts for introduction + discussion in case of an original article;
3. Source(s) of support in the form of grants, equipment, drugs, or all of these;
4. Acknowledgement, if any. One or more statements should specify 1) contributions that need acknowledging but do not justify authorship, such as general support by a departmental chair; 2) acknowledgments of technical help; and 3) acknowledgments of financial and material support, which should specify the nature of the support. This should be included in the title page of the manuscript and not in the main article file.
5. If the manuscript was presented as part at a meeting, the organization, place, and exact date on which it was read. A full statement to the editor about all submissions and previous reports that might be regarded as redundant publication of the same or very similar work. Any such work should be referred to specifically, and referenced in the new paper. Copies of such material should be included with the submitted paper, to help the editor decide how to handle the matter.
6. Registration number in case of a clinical trial and where it is registered (name of the registry and its URL)
7. Conflicts of Interest of each author/ contributor. A statement of financial or other relationships that might lead to a conflict of interest, if that information is not included in the manuscript itself or in an authors' form
8. Criteria for inclusion in the authors'/ contributors' list
9. A statement that the manuscript has been read and approved by all the authors, that the requirements for authorship as stated earlier in this document have been met, and that each author believes that the manuscript represents honest work, if that information is not provided in another form (see below); and
10. The name, address, e-mail, and telephone number of the corresponding author, who is responsible for communicating with the other authors about revisions and final approval of the proofs, if that information is not included on the manuscript itself.

[2] Blinded Article file: The main text of the article, beginning from Abstract till References (including tables) should be in this file. The file must not contain any mention of the authors' names or initials or the institution at which the study was done or acknowledgements. Page headers/ running title can include the title but not the authors' names. Manuscripts not in compliance with the Journal's blinding policy will be returned to the corresponding author. Use rtf/doc files. Do not zip the files. **Limit the file size to 1 MB.** Do not incorporate images in the file. If file size is large, graphs can be submitted as images separately without incorporating them in the article file to reduce the size of the file. The pages should be numbered consecutively, beginning with the first page of the blinded article file.

[3] Images: Submit good quality color images. **Each image should be less than 2 MB in size.** Size of the image can be reduced by decreasing the actual height and width of the images (keep up to 1600 x 1200 pixels or 5-6 inches). Images can be submitted as jpeg files. Do not zip the files. Legends for the figures/images should be included at the end of the article file.

[4] The contributors' / copyright transfer form (template provided below) has to be submitted in original with the signatures of all the contributors within two weeks of submission via courier, fax or email as a scanned image. Print ready hard copies of the images (one set) or digital images should be sent to the journal office at the time of submitting revised manuscript. High resolution images (up to 5 MB each) can be sent by email.

Contributors' form / copyright transfer form can be submitted online from the authors' area on http://www.journalonweb.com/jasi.

Preparation of Manuscripts

Manuscripts must be prepared in accordance with "Uniform requirements for Manuscripts submitted to Biomedical Journals" developed by the International Committee of Medical Journal Editors (October 2008). The uniform requirements and specific requirement of Journal of the Anatomical Society of India are summarized below. Before submitting a manuscript, contributors are requested to check for the latest instructions available. Instructions are also available from the website of the journal (www.jasi.org.in) and from the manuscript submission site http://www.journalonweb.com/jasi).

Journal of the Anatomical Society of India accepts manuscripts written in American English.

Copies of any permission(s)

It is the responsibility of authors/ contributors to obtain permissions for reproducing any copyrighted material. A copy of the permission obtained must accompany the manuscript. Copies of any and all published articles or other manuscripts in preparation or submitted elsewhere that are related to the manuscript must also accompany the manuscript.

Types of Manuscripts

Original articles:

These include randomized controlled trials, intervention studies, studies of screening and diagnostic test, outcome studies, cost effectiveness analyses, case-control series, and surveys with high response rate. The text of original articles amounting to up to 3000 words (excluding Abstract, references and Tables) should be divided into sections with the headings Abstract, Key-words, Introduction, Material and Methods, Results, Discussion and Conclusion, References, Tables and Figure legends.

An abstract should be in a structured format under following heads: **Introduction, Material and Methods, Results,** and **Discussion and Conclusion.**

Introduction: State the purpose and summarize the rationale for the study or observation.

Material and Methods: It should include and describe the following aspects:

Ethics: When reporting studies on human beings, indicate whether the procedures followed were in accordance with the ethical standards of the responsible committee on human experimentation (institutional or regional) and with the Helsinki Declaration of 1975, as revised in 2000 (available at http://www.wma.net/e/policy/17-c_e.html). For prospective studies involving human participants, authors are expected to mention about approval of (regional/ national/ institutional or independent Ethics Committee or Review Board, obtaining informed consent from adult research participants and obtaining assent for children aged over 7 years participating in the trial. The age beyond which assent would be required could vary as per regional and/ or national guidelines. Ensure confidentiality of subjects by desisting from mentioning participants' names, initials or hospital numbers, especially in illustrative material. When reporting experiments on animals, indicate whether the institution's or a national research council's guide for, or any national law on the care and use of laboratory animals was followed. Evidence for approval by a local Ethics Committee (for both human as well as animal studies) must be supplied by the authors on demand. Animal experimental procedures should be as humane as possible and the details of anesthetics and analgesics used should be clearly stated. The ethical standards of experiments must be in accordance with the guidelines provided by the CPCSEA and World Medical Association Declaration of Helsinki on Ethical Principles for Medical Research Involving Humans for studies involving experimental animals and human beings, respectively). The journal will not consider any paper which is ethically unacceptable. A statement on ethics committee permission and ethical practices must be included in all research articles under the 'Materials and Methods' section.

Study design:

Selection and Description of Participants: Describe your selection of the observational or experimental participants (patients or laboratory animals, including controls) clearly, including eligibility and exclusion criteria and a description of the source population. *Technical information*: Identify the methods, apparatus (give the manufacturer›s name and address in parentheses), and procedures in sufficient detail to allow other workers to reproduce the results. Give references to established methods, including statistical methods (see below); provide references and brief descriptions for methods that have been published but are not well known; describe new or substantially modified methods, give reasons for using them, and evaluate their limitations. Identify precisely all drugs and chemicals used, including generic name(s), dose(s), and route(s) of administration.

Reports of randomized clinical trials should present information on all major study elements, including the protocol, assignment of interventions (methods of randomization, concealment of allocation to treatment groups), and the method of masking (blinding), based on the CONSORT Statement (http://www.consort-statement.org).

Reporting Guidelines for Specific Study Designs

Initiative	Type of Study	Source
CONSORT	Randomized controlled trials	http://www.consort-statement.org
STARD	Studies of diagnostic accuracy	http://www.consort-statement.org/stardstatement.htm
QUOROM	Systematic reviews and meta-analyses	http://www.consort- statement.org/Initiatives/MOOSE/moose.pdf statement.org/Initiatives/MOOSE/moose.pdf
STROBE	Observational studies in epidemiology	http://www.strobe-statement.org
MOOSE	Meta-analyses of observational studies in epidemiology	http://www.consort- statement.org/Initiatives/MOOSE/moose.pdf

Statistics: Whenever possible quantify findings and present them with appropriate indicators of measurement error or uncertainty (such as confidence intervals). Authors should report losses to observation (such as, dropouts from a clinical trial). When data are summarized in the Results section, specify the statistical methods used to analyze them. Avoid non-technical uses of technical terms in statistics, such as 'random' (which implies a randomizing device), 'normal', 'significant', 'correlations', and 'sample'. Define statistical terms, abbreviations, and most symbols. Specify the computer software used. Use upper italics (*P* 0.048). For all *P* values include the exact value and not less than 0.05 or 0.001. Mean differences in continuous variables, proportions in categorical variables and relative risks including odds ratios and hazard ratios should be accompanied by their confidence intervals.

Results: Present your results in a logical sequence in the text, tables, and illustrations, giving the main or most important findings first. Do not repeat in the text all the data in the tables or illustrations; emphasize or summarize only important observations. Extra- or supplementary materials and technical detail can be placed in an appendix where it will be accessible but will not interrupt the flow of the text; alternatively, it can be published only in the electronic version of the journal.

When data are summarized in the Results section, give numeric results not only as derivatives (for example, percentages) but also as the absolute numbers from which the derivatives were calculated, and specify the statistical methods used to analyze them. Restrict tables and figures to those needed to explain the argument of the paper and to assess its support. Use graphs as an alternative to tables with many entries; do not duplicate data in graphs and tables. Where scientifically appropriate, analyses of the data by variables such as age and sex should be included.

Discussion: Include summary of *key findings* (primary outcome measures, secondary outcome measures, results as they relate to a prior hypothesis); *Strengths and limitations* of the study (study question, study design, data collection, analysis and interpretation); *Interpretation and implications* in the context of the totality of evidence (is there a systematic review to refer to, if not, could one be reasonably done here and now?, what this study adds to the available evidence, effects on patient care and health policy, possible mechanisms); *Controversies* raised by this study; and *Future research directions* (for this particular research collaboration, underlying mechanisms, clinical research).

Do not repeat in detail data or other material given in the Introduction or the Results section. In particular, contributors should avoid making statements on economic benefits and costs unless their manuscript includes economic data and analyses. Avoid claiming priority and alluding to work that has not been completed. New hypotheses may be stated if needed, however they should be clearly labeled as such. About 30 references can be included. These articles generally should not have more than six authors.

Review Articles:

These are comprehensive review articles on topics related to various fields of Anatomy. The entire manuscript should not exceed 7000 words with no more than 50 references and two authors. Following types of articles can be submitted under this category:

- Newer techniques of dissection and histology
- New methodology in Medical Education
- Review of a current concept

Please note that generally review articles are by invitation only. But unsolicited review articles will be considered for publication on merit basis.

Case reports:

New, interesting and rare cases can be reported. They should be unique, describing a great diagnostic or therapeutic challenge and providing a learning point for the readers. Cases with clinical significance or implications will be given priority. These communications could be of up to 1000 words (excluding Abstract and references) and should have the following headings: Abstract (unstructured), Key-words, Introduction, Case report, Discussion and Conclusion, Reference, Tables and Legends in that order.

The manuscript could be of up to 1000 words (excluding references and abstract) and could be supported with up to 10 references. Case Reports could be authored by up to four authors.

Letter to the Editor:

These should be short and decisive observations. They should preferably be related to articles previously published in the Journal or views expressed in the journal. They

should not be preliminary observations that need a later paper for validation. The letter could have up to 500 words and 5 references. It could be generally authored by not more than four authors.

Book Review: This consists of a critical appraisal of selected books on Anatomy. Potential authors or publishers may submit books, as well as a list of suggested reviewers, to the editorial office. The author/publisher has to pay INR 10,000 per book review.

Other:

Editorial, Guest Editorial, Commentary and Opinion are solicited by the editorial board.

References

References should be *numbered* consecutively in the order in which they are first mentioned in the text (not in alphabetic order). Identify references *in text*, tables, and legends by Arabic numerals in superscript with square bracket after the punctuation *marks. References cited only* in tables or figure legends should be numbered in accordance with the sequence established by the first identification in the text of the particular table or figure. Use the style of the examples below, which are based on the formats used by the NLM *in Index Medicus*. The titles of journals *should be abbreviated* according to the style used in Index Medicus. Use complete name of the journal for non-indexed journals. Avoid using abstracts as references. Information from manuscripts submitted but not accepted should be cited in the text as "unpublished observations" with written permission from the source. Avoid citing a "personal communication" unless it provides essential information not available from a public source, in which case the name of the person and date of communication should be cited in parentheses in the text. The commonly cited types of references are shown here, for other types of references such as newspaper items please refer to ICMJE Guidelines (http://www.icmje.org or http://www.nlm.nih.gov/bsd/uniform_requirements.html).

Articles in Journals

1. Standard journal article (for up to six authors): Parija S C, Ravinder PT, Shariff M. Detection of hydatid antigen in the fluid samples from hydatid cysts by co-agglutination. Trans. R.Soc. Trop. Med. Hyg.1996; 90:255–256.
2. Standard journal article (for more than six authors): List the first six contributors followed by *et al*.

Roddy P, Goiri J, Flevaud L, Palma PP, Morote S, Lima N. *et al*., Field Evaluation of a Rapid Immunochromatographic Assay for Detection of Trypanosoma cruzi Infection by Use of Whole Blood. J. Clin. Microbiol. 2008; 46: 2022-2027.

3. Volume with supplement: Otranto D, Capelli G, Genchi C: Changing distribution patterns of canine vector borne diseases in Italy: leishmaniosis vs. dirofilariosis. Parasites & Vectors 2009; Suppl 1:S2.

Books and Other Monographs

1. Personal author(s): Parija SC. Textbook of Medical Parasitology. 3rd ed. All India Publishers and Distributors. 2008.
2. Editor(s), compiler(s) as author: Garcia LS, Filarial Nematodes In: Garcia LS (editor) Diagnostic Medical Parasitology ASM press Washington DC 2007: pp 319-356.
3. Chapter in a book: Nesheim M C. Ascariasis and human nutrition. In Ascariasis and its prevention and control, D. W. T. Crompton, M. C. Nesbemi, and Z. S. Pawlowski (eds.). Taylor and Francis,London, U.K.1989, pp. 87–100.

Electronic Sources as reference

Journal article on the Internet: Parija SC, Khairnar K. Detection of excretory *Entamoeba histolytica* DNA in the urine, and detection of *E. histolytica* DNA and lectin antigen in the liver abscess pus for the diagnosis of amoebic liver abscess. *BMC Microbiology* 2007, **7**:41. doi:10.1186/1471-2180-7-41. http://www.biomedcentral.com/1471-2180/7/41

Tables

- Tables should be self-explanatory and should not duplicate textual material.
- Tables with more than 10 columns and 25 rows are not acceptable.
- Number tables, in Arabic numerals, consecutively in the order of their first citation in the text and supply a brief title for each.
- Place explanatory matter in footnotes, not in the heading.
- Explain in footnotes all non-standard abbreviations that are used in each table.
- Obtain permission for all fully borrowed, adapted, and modified tables and provide a credit line in the footnote.
- For footnotes use the following symbols, in this sequence: *, †, ‡, §, ‖,¶ , **, ††, ‡‡
- Tables with their legends should be provided at the end of the text after the references. The tables along with their number should be cited at the relevant place in the text

Illustrations (Figures)

- Upload the images in JPEG format. The file size should be within 1024 kb in size while uploading.
- Figures should be numbered consecutively according to the order in which they have been first cited in the text.
- Labels, numbers, and symbols should be clear and of uniform size. The lettering for figures should be large enough to be legible after reduction to fit the width of a printed column.

- Symbols, arrows, or letters used in photomicrographs should contrast with the background and should be marked neatly with transfer type or by tissue overlay and not by pen.
- Titles and detailed explanations belong in the legends for illustrations not on the illustrations themselves.
- When graphs, scatter-grams or histograms are submitted the numerical data on which they are based should also be supplied.
- The photographs and figures should be trimmed to remove all the unwanted areas.
- If photographs of individuals are used, their pictures must be accompanied by written permission to use the photograph.
- If a figure has been published elsewhere, acknowledge the original source and submit written permission from the copyright holder to reproduce the material. A credit line should appear in the legend for such figures.
- Legends for illustrations: Type or print out legends (maximum 40 words, excluding the credit line) for illustrations using double spacing, with Arabic numerals corresponding to the illustrations. When symbols, arrows, numbers, or letters are used to identify parts of the illustrations, identify and explain each one in the legend. Explain the internal scale (magnification) and identify the method of staining in photomicrographs.
- Final figures for print production: Send sharp, glossy, un-mounted, color photographic prints, with height of 4 inches and width of 6 inches at the time of submitting the revised manuscript. Print outs of digital photographs are not acceptable. If digital images are the only source of images, ensure that the image has minimum resolution of 300 dpi or 1800 x 1600 pixels in TIFF format. Send the images on a CD. Each figure should have a label pasted (avoid use of liquid gum for pasting) on its back indicating the number of the figure, the running title, top of the figure and the legends of the figure. Do not write the contributor/s' name/s. Do not write on the back of figures, scratch, or mark them by using paper clips.
- The Journal reserves the right to crop, rotate, reduce, or enlarge the photographs to an acceptable size.

Protection of Patients' Rights to Privacy

Identifying information should not be published in written descriptions, photographs, sonograms, CT scans, etc., and pedigrees unless the information is essential for scientific purposes and the patient (or parent or guardian, wherever applicable) gives informed consent for publication. Authors should remove patients' names from figures unless they have obtained informed consent from the patients. The journal abides by ICMJE guidelines:

1. Authors, not the journals nor the publisher, need to obtain the patient consent form before the publication and have the form properly archived. The consent forms are not to be uploaded with the cover letter or sent through email to editorial or publisher offices.
2. If the manuscript contains patient images that preclude anonymity, or a description that has obvious indication to the identity of the patient, a statement about obtaining informed patient consent should be indicated in the manuscript.

Sending a revised manuscript

The revised version of the manuscript should be submitted online in a manner similar to that used for submission of the manuscript for the first time. However, there is no need to submit the "First Page" or "Covering Letter" file while submitting a revised version. When submitting a revised manuscript, contributors are requested to include, the 'referees' remarks along with point to point clarification at the beginning in the revised file itself. In addition, they are expected to mark the changes as underlined or colored text in the article.

Reprints and proofs

Journal provides no free printed reprints. Authors can purchase reprints, payment for which should be done at the time of submitting the proofs.

Publication schedule

The journal publishes articles on its website immediately on acceptance and follows a 'continuous publication' schedule. Articles are compiled in issues for 'print on demand' quarterly.

Copyrights

Checklist

Covering letter

- Signed by all contributors
- Previous publication / presentations mentioned
- Source of funding mentioned
- Conflicts of interest disclosed

Authors

- Last name and given name provided along with Middle name initials (where applicable)
- Author for correspondence, with e-mail address provided
- Number of contributors restricted as per the instructions
- Identity not revealed in paper except title page (e.g. name of the institute in Methods, citing previous study as 'our study', names on figure labels, name of institute in photographs, etc.)

Presentation and format

- Double spacing
- Margins 2.5 cm from all four sides
- Page numbers included at bottom
- Title page contains all the desired information
- Running title provided (not more than 50 characters)
- Abstract page contains the full title of the manuscript
- Abstract provided (structured abstract of 250 words for original articles, unstructured abstracts of about 150 words for all other manuscripts excluding letters to the Editor)
- Key words provided (three or more)
- Introduction of 75-100 words
- Headings in title case (not ALL CAPITALS)
- The references cited in the text should be after punctuation marks, in superscript with square bracket.
- References according to the journal's instructions, punctuation marks checked
- Send the article file without 'Track Changes'

Language and grammar

- Uniformly American English
- Write the full term for each abbreviation at its first use in the title, abstract, keywords and text separately unless it is a standard unit of measure. Numerals from 1 to 10 spelt out
- Numerals at the beginning of the sentence spelt out
- Check the manuscript for spelling, grammar and punctuation errors
- If a brand name is cited, supply the manufacturer's name and address (city and state/country).
- Species names should be in italics

Tables and figures

- No repetition of data in tables and graphs and in text
- Actual numbers from which graphs drawn, provided
- Figures necessary and of good quality (colour)
- Table and figure numbers in Arabic letters (not Roman)
- Labels pasted on back of the photographs (no names written)
- Figure legends provided (not more than 40 words)
- Patients' privacy maintained (if not permission taken)
- Credit note for borrowed figures/tables provided
- Write the full term for each abbreviation used in the table as a footnote

Journal of
The Anatomical Society of India

Salient Features:

- Publishes research articles related to all aspects of Anatomy and Allied medical/surgical sciences.
- Pre-Publication Peer Review and Post-Publication Peer Review
- Online Manuscript Submission System
- Selection of articles on the basis of MRS system
- Eminent academicians across the globe as the Editorial board members
- Electronic Table of Contents alerts
- Available in both online and print form.

The journal is registered with the following abstracting partners:
Baidu Scholar, CNKI (China National Knowledge Infrastructure), EBSCO Publishing's Electronic Databases, Ex Libris – Primo Central, Google Scholar, Hinari, Infotrieve, Netherlands ISSN center, ProQuest, TdNet, Wanfang Data

The journal is indexed with, or included in, the following:
SCOPUS, Science Citation Index Expanded, IndMed, MedInd, Scimago Journal Ranking, Emerging Sources Citation Index.

Impact Factor® as reported in the 2018 Journal Citation Reports® (Clarivate Analytics, 2019): 0.168

Editorial Office:
Dr. Vishram Singh, Editor-in-Chief, JASI
OC-5/103, 1st floor, Orange County Society,
Ahinsa Khand-I, Indirapuram, Ghaziabad,
Delhi, NCR- 201014.
Email: editorjasi@gmail.com
(O) | Website: www.asiindia.in

The journal is owned and run by The Anatomical Society of India